Contemporary Mathematics
https://ojs.wiserpub.com/index.php/CM/

Research Article

# Double Valued Neutrosophic Soft Topologies with Cotangent Similarity Analytics for Real Time Target Identification

**Maha Mohammed Saeed[1], Raed Hatamleh[2], Mohammed Mamoun Ahmed Abubakr[3], Hamza Ali Abujabal[4], Aliazer H. Jinang[5], Arif Mehmood[6], Zeeshan Ali[7], Jamil J. Hamja[8], Cris L. Armada[9,10], Dragan Pamucar[11]***

[1] Department of Mathematics, Faculty of Sciences, King Abdulaziz University, P. O. Box 80203, Jeddah, 21589, Saudi Arabia
[2] Department of Mathematics, Faculty of Science, Jadara University, P.O. Box 733, Irbid, 21110, Jordan
[3] College of Business Administration, Northern Border University, Arar, Saudi Arabia
[4] Department of mathematics, King Abdulaziz University, P.O. Box 80003, Jeddah, 21589, Saudi Arabia
[5] MSU-TCTO Sitangkai Junior High School, Secondary Education Department, Mindanao State University-Tawi-Tawi College of Technology and Oceanography, Bongao, 7500, Philippines
[6] Department of Mathematics, Institute of Numerical Sciences, Gomal University, Dera Ismail Khan, KPK, 29050, Pakistan
[7] Department of information Management, National Yunlin University of Science and Technology, 123 University Road, Section 3, Douliou, Yunlin, 64002, Taiwan, R.O.C.
[8] Department of Mathematics, College of Mathematical Sciences, Mindanao State University-Tawi-Tawi College of Technology and Oceanography, Bongao, 7500, Philippines
[9] Vietnam National University Ho Chi Minh City, Linh Trung Ward, Thu Duc City, Ho Chi Minh City, Vietnam
[10] Department of Applied Mathematics, Faculty of Applied Science, Ho Chi Minh City University of Technology (HCMUT), 268 Ly Thuong Kiet, Ward 14, District 10, Ho Chi Minh City, Vietnam
[11] School of Engineering and Technology, Sunway University, Selangor, Malaysia
E-mail: pamucar.dragan@sze.hu

**Received:** 8 September 2025; **Revised:** 24 November 2025; **Accepted:** 2 December 2025

**Abstract:** In this study, Double Valued Neutrosophic Soft Sets (DNSSs) are examined. Basic operations are provided with examples. Based on this set, Double-Valued Neutrosophic Soft Topological Spaces (DNSTSs) are introduced. Basic operations are studied, and theorems are presented. For better understanding, examples are provided. Additionally, this study examines the analysis of Cotangent Similarity Measure (Cot SM) scores between signal samples $(S_1 - S_4)$ and class templates $(T_1 - T_4)$, focusing on their effectiveness in real-time military target identification. The Cot SM values quantify the alignment between signals and predefined templates, facilitating target classification by indicating the strength of the match. Higher Cot SM values (e.g., $> 0.85$) suggest a high degree of similarity, implying an immediate engagement decision, while lower values indicate weaker matches, requiring further verification. Various visualization techniques, including Heatmaps, Principal Component Analysis (PCA), t-Distributed Stochastic Neighbor Embedding (t-SNE), and 3D plots, are used to represent the correlations and patterns within the data. These methods visually showcase the strength and direction of signal-template relationships, with a specific emphasis on identifying strong matches and distinguishing weak correlations. PCA and t-SNE are employed to reduce dimensionality, enabling the clear identification of clusters and outliers. The Elbow Method optimizes clustering, ensuring effective partitioning of the data. The analysis identifies the strongest matches, such as template $T_1$ with class $C_4$, and provides a comprehensive view of the data's structure. This framework improves target classification and decision-making by providing a quantitative, visual, and efficient method for prioritizing actions in military contexts. The techniques and tools presented also offer broader applications


DOI: https://doi.org/10.37256/cm.7220268563

in fields such as biomedical diagnostics and disaster management.

***Keywords*:** neutrosophic soft set, Double Valued Neutrosophic Soft Sets (DNSSs), Double-Valued Neutrosophic Soft Topological Spaces (DNSTSs), interior, closure, cotangent similarity measure, machine learning techniques

**MSC:** 03E72, 54A40, 68T37

## Abbreviation

| | |
|---|---|
| DNSSs | Double Valued Neutrosophic Soft Sets |
| DNSTSs | Double Valued Neutrosophic Soft Topological Spaces |

## 1. Introduction

One of the most important aspects of the information and decision-making processes is the handling of uncertainty, imprecise, and insufficient information. Many real-world scenarios involving uncertainty are typically not explicable by the traditional subset theory, which holds that components are either members of a set or not. To address this, Fuzzy Sets (FSs) [1] were developed, in which partial truth is reflected by assigning a membership degree with a value between 0 and 1. This was a significant advancement, but only in terms of degree of determinacy. More complicated uncertainty than FSs is modeled by Intuitionistic Fuzzy Sets (IFSs) [2], which are expanded by adding a non-membership degree to represent indeterminacy. This concept was further generalized by Interval-Valued IFSs (IVIFSs) [3], where membership and non-membership degrees are now interval numbers rather than points. A extremely powerful parameterized framework for handling uncertainty that was unencumbered by probability or membership functions was provided by Molodtsov's creation of soft set theory [4]. Maji et al. [5] extended this paradigm in great detail later and demonstrated its true value in decision-making. Since then, several hybrids have been established. Although these developments had occurred, there still existed the circumstance when neither of the membership and non-membership degrees was sufficient to correctly characterize all cases of incomplete knowledge, especially indeterminacy/neutrality. This spurred the proposal of Neutrosophic Sets (NSs) [6]. A subfield of philosophy called neutrosophy formalizes the idea of neutralities and their relationship to ideational spectrum. To get around this, certain simpler models, such as the Simpler Neutrosophic Set (SNS), were put forth [7]. The Single-Valued Neutrosophic Set (SVNS) [8], in which the three degrees of membership are single and specified values of the standard segment [0, 1], remains the most well-known and practical of these. Because of this, SVNSs are a useful and controllable tool for solving problems in the real world. Many other set theories, such as IFSs, Picture Fuzzy Sets, Pythagorean Fuzzy Sets (PFSs), $q$-Rung Orthopair Fuzzy Sets ($q$-ROFSs), and Spherical Fuzzy Sets (SFSs), are generalized by Vague Sets (VSs) [9]. They have been widely used in engineering, medical diagnosis, and Multi-Attribute Decision-Making (MADM) [10–12]. A significant step toward the creation of the intuitionistic neutrosophic soft set was the introduction of the neutrosophic soft set by [13, 14]. Since the parameterizations of soft sets is never so forcefully applied to this expressivity, these hybrid structures are well adapted to the profound expressiveness requirements of neutrosophic sets.

### 1.1 *Literature review*

There has been extensive research on SVNSs, both theoretically and practically. Since then, Ye [15–18] has been the first to investigate this field utilizing cluster analysis, MADM, aggregation operators, and similarity metrics. Ali et al. [19] extended this to complex neutrosophic sets, and Liu et al. [20] added new aggregation operators. Saqlain et al. [21] successfully combined new techniques like SVNSs with pre-existing techniques like Technique for Order of Preference by Similarity to Ideal Solution (TOPSIS). Additionally, industrial evaluation [22] have been special areas of research focus.

Additional research have expanded the theoretical frameworks by focusing on aggregation operators [23–25] using combination models.

Compared to its predecessors, such as IFSs and PyFSs, whose similarity metrics were also thoroughly examined, the scope and flexibility of SVNSs have consistently been determined to be more general and wider [26–32]. Sarfraz et al. [33] proposed similarity measurements on the spherical fuzzy sets. This work was expanded by Bui et al. [34], who developed new similarity metrics for Neutrosophic Sets (NS). In order to solve MADM problems, Thao et al. [35] presented a theoretical framework of SVNSs and employed similarity metrics. In line with this, Ali et al. [36] offered fresh examples of SVNS commonalities in a MADM context. A hybrid approach by Ozlu et al. [37] that combined some SVNSs and type-2 fuzzy sets and applied the TOPSIS is closely related to the earlier study. Bakro and others used SVNSs in another example of this type of digital image processing [38]. Industrial inspection was the subject of Tang Yu et al. [39], who presented a novel intelligent detection technique for forging flaws. Thong et al. [40] have attempted to make further theoretical advances by creating a Probabilistic Neutrosophic (PN) semi-supervised fuzzy clustering technique to handle noisy data. The theory of SVNSs was expanded by Mandour et al. [41] and Dey et al. [42] through the examination of additional graph operations and associated Simple Walks (SW) characteristics. Regarding the energy system, Yan et al. [12, 43–45] modeled and optimized a rope cell hybrid micro-grid system using a bio-inspired algorithm. The theory of Schweizer Sklar operations on fuzzy sets was introduced and developed in a series of publications by Sarfraz [25, 46–50]. Interval-valued SVNSs were first proposed by Chou et al. [51] and used to energy selection issues with a dissimilarity measure. Finally, similarity metrics of PFS over fundamental operations and MADM techniques using a convex combination of weighted vector similarity measures of neutrosophic sets were introduced by [52, 53]. Recent research has established complex tangent trigonometric methods for advanced fuzzy sets [54] and extended complex cubic intuitionistic fuzzy sets to algebraic structures [55]. Additionally, the analysis of minimal units in fuzzy neutrosophic rings [56] and the foundational work on topological spaces using symbolic n-plithogenic intervals [57] show the growing frontier of this field, offering a solid mathematical foundation for addressing problems with inherent ambiguity and multifaceted information. For future work, neutrosophic soft sets could model the indeterminacy in non-Hermitian topological phase transitions and the robustness of Majorana modes [58].

## 1.2 *Motivation for research*

Medical diagnosis is a challenging field in and of itself, involving uncertainty, vague symptoms, and insufficient information. A popular paradigm for handling these challenges is SVNS, which model the data using three independent memberships: truth, indeterminacy, and falsity. The similarity measure, which compares a patient's symptom profile to a known disease profile, is the key component of SVNSs used in diagnosis. As seen in Table 1, researchers have developed unique SVNS similarity metrics in this regard. The methodology of Chai et al. uses a tangent function to magnify the critical differences, which results in high accuracy; the scale in the measure proposed by Sahin and Karabacak is highly sensitive to changes in all three neutrosophic components; and the model designed by Ye takes a geometric approach to comprehensive matching. The neutrosophic framework is transforming medical data preparation in addition to direct diagnosis.

Table 2 lists its applications in image processing, including hybrid models that combine NS with metaheuristics to generate automatic picture enhancements, clustering models like Neutrosophic Set-Fuzzy C-Means (NS-FCM) to segment medical images (e.g., identifying malignancies), and a generic architecture to handle uncertainty. Furthermore, as shown in Table 3, the field is making strides by combining multi-criteria decision-making techniques like VIKOR with measures that further extend the neutrosophic concept to deal with even more complex types of data, such as Interval-Valued Neutrosophic Sets (IVNS) and information with some basis of reliability (Neutrosophic Z-Number Sets (NZNS)). However, there is a serious flaw in how these sophisticated models are used to interpret and validate the data. Despite the measures' ability to produce numerical similarity scores, the field lacks a reliable visual approach to interpret the results. The pattern and correlations in the data are not adequately displayed using other powerful visualization tools like Heat Map, Principal Component Analysis (PCA), t-Distributed Stochastic Neighbor Embedding (t-SNE), 3D plots, PAC, and Elbow techniques. The methods are required to clearly illustrate the strength and direction of signal-template relationships, with particular focus on highlighting strong matches and separating weak correlations.

**Table 1.** Applications of SVNS similarity measures in medical diagnosis

| Model/Approach | Key components | Primary handling mechanism | Best application domain |
|---|---|---|---|
| Improved Cosine Similarity [18] | Cosine of angle & magnitude of SVNS vectors | Measures geometric proximity and vector size for a comprehensive similarity score | Medical diagnosis (Matching patient symptoms to diseases) |
| Tangent Function-Based Similarity [59] | Tangent of a normalized Hamming distance | Amplifies small differences between SVNS elements for high precision | Pattern recognition and complex medical diagnosis problems |
| Novel Multi-component Similarity [60] | Integrated differences of T, I, F and a truth-membership function | Highly sensitive to variations in all three membership domains | Medical diagnosis, taxonomy, and clustering analysis |

**Table 2.** Neutrosophic sets based image processing techniques

| Model/Approach | Key components | Primary handling mechanism | Best application domain |
|---|---|---|---|
| General NS Framework [61] | Pixels as T, I, F sets | Converting uncertainty into indeterminacy (I) | A universal framework for all image processing tasks (e.g., segmentation, denoising, enhancement) |
| NS-Clustering (e.g., NS-FCM) [62] | Clustering in NS domain (T, I, F features) | Using I to weight data points and manage uncertainty | Medical image segmentation (e.g., tumor detection in mammograms) |
| Metaheuristic-NS Enhancement [63] | NS domain + optimization algorithms (e.g., PSO, GA) | Optimizing parameters to maximize enhancement of T and minimize I | Automated, parameter-free image contrast and detail enhancement |
| Saliency-NS Segmentation [64] | Saliency map + NS domain + K-Means | Using saliency to guide clustering and reduce search space | Fast segmentation of natural images with prominent objects |

**Table 3.** Analysis of advanced similarity measures based on neutrosophic sets

| Model/Approach | Key components | Primary handling mechanism | Best application domain |
|---|---|---|---|
| Distance & Entropy for Interval-Valued Neutrosophic Sets (IVNS) [65] | Distances, similarities, and entropy for IVNS | Extends measures to handle interval-based uncertainty, with proven relationships between them | Data analysis involving highly imprecise and interval-valued information |
| Similarity for NZNS [66] | Generalized distance measure for NZNS | Captures the reliability of information alongside its uncertain value in a unified measure | MADM under complex uncertainty and partial reliability |
| Tangent Similarity [67] | Tangent function applied to neutrosophic distances | Magnifies small differences between alternatives, providing high sensitivity | MADM for ranking and selection problems |
| Improved VIKOR Method [68] | Improved distance measure and score function integrated with the VIKOR method | Normalization of decision matrix | Improved distance measures and score function integrated with VIKOR method |

## 1.3 *Existing of research gap*

Conceptually, the neutrosophic and soft set theory has advanced considerably, despite several research gaps. However, the majority of DNSS models now in use place more emphasis on algebraic qualities and decision rules than they do on topological properties like the properties of closure, interiority, or continuity. Particularly for spatial or signal-associated data, these methods may have made it easier to describe uncertainty boundaries and transitions with more robustness. Second, the existing neutrosophic soft set framework does not fully encompass even sophisticated visual

aids like as heat maps, PCA, t-SNE, 3D plots, PAC, and the Elbow approach. This gap motivates the study of double-valued neutrosophic soft topological structures, double-valued neutrosophic soft set theory, and decision-making issues like military threat identification with sophisticated machine learning algorithms and cotangent similarity measures. Heat maps, PCA, t-SNE, 3D plots, PAC, and the Elbow approach are some of these sophisticated machine learning algorithms.

### 1.4 *Novelty of the research*

Regardless of the truth and false factors, a comprehensive approach of the indeterminacy element of neutrosophic sets is described in this work. Illustrative examples are used to discuss simple operations on this collection. This serves as the foundation for defining the idea of double-valued neutrosophic soft topological spaces and presenting its key operations and related theorems with the aid of real-world examples. Additionally, the paper analyzes Cotangent Similarity (Cot SM) scores using class templates $(T_1 - T_4)$ and signal samples $(S_1 - S_4)$, focusing on their potential applications in real-time military target recognition. By indicating the strength of the match, the Cot SM values are utilized to determine the target by measuring the alignment of signals with their predefined templates. While lower values indicate poorer matches that need more validation, a high SM value (e.g., above 0.85) indicates high similarity and suggests early interaction. To gain a deeper understanding of the correlations and patterns in the data, a range of visualization techniques are employed, such as Heatmaps, PCA, t-SNE, and 3D plots.

These techniques distinguish between strong matches and weak correlations, giving an indication of the direction and strength of signal-template relationships. To find clusters and outliers, PCA and t-SNE reduce the dimensionality of the data. The data partitioning method is effective because the Elbow Method maximizes clustering. By distinguishing between strong and weak correlations, these techniques give an indication of the direction and intensity of signal-template relationships. PCA and t-SNE are used to diminish the dimensionality of data in order to find outliers and clusters. Effective data partitioning is achieved by maximizing clustering through the application of the Elbow Method.

## 2. Preliminaries

The prerequisites that are crucial for the other sections are covered in the first section.

**Definition 1** [69] On the universe of discourse $\mathbf{X}$, a neutrosophic set $\mathscr{A}$ is defined as follows:

$$A = \{\langle x,\ \mathrm{T}_{\mathscr{A}}(x),\ \mathrm{I}_{\mathscr{A}}(x),\ \mathrm{F}_A(x)\rangle : x \in \mathbf{X}\},$$

where, $\mathrm{T}, \mathrm{I}, \mathrm{F} : \mathbf{X} \longrightarrow ]^{-}0,\ 1^{+}[$ and ${}^{-}0 \leq \mathrm{T}_A(x) + \mathrm{I}_A(x) + \mathrm{F}_A(x) \leq 3^{+}$.

According to philosophy, the values of the neutrosophic set are derived from the actual non-standard or standard subsets of $]^{-}0,\ 1^{+}[$. However, it is difficult to use a neutrosophic set with values from a real standard or non-standard subset of $]^{-}0,\ 1^{+}[$ when applying this idea to real scientific and engineering problems.

**Definition 2** [4] Let $P(\mathbf{X})$ be the powerset of $\mathbf{X}$, $\check{E}$ be a set of all parameters, and let $\mathbf{X}$ be an starting universe. When $F$ is a mapping with the formula $F : \check{E} \longrightarrow P(X)$, the pair $(F,\ \check{E})$ referred to as a soft set over $\mathbf{X}$. Stated otherwise, the set is the set of $e$-approximate elements of the soft sets, or

$$(F,\ \check{E}) = \{(\grave{e},\ F(\grave{e})) : \grave{e} \in \check{E},\ F : \check{E} \longrightarrow P(\mathbf{X})\},$$

or parameterized family of subsets of the set $\mathbf{X}$ for $e$-elements of the soft set $(F,\ \check{E})$.

**Definition 3** [13] Let $\check{E}$ be a set of all parameters, and $\mathbf{X}$ be a set of beginning universes. Let $P(\mathbf{X})$ the set of all possible sets of $\mathbf{X}$ that are neutrosophic. Then, a set defined by a set valued function $\mathscr{F}$ that represents a mapping $\mathscr{F} : \check{E} \longrightarrow P(\mathbf{X})$ is referred to as an approximate function of neutrosophic soft set $(\mathscr{F},\ \check{E})$ over $\mathbf{X}$. $\mathscr{F}$ is also known as the

approximate function of the neutrosophic soft set $(\mathscr{F},\ \check{E})$. Stated differently, the neutrosophic soft set can be expressed as a set of order pairs

$$(\mathscr{F},\ \check{E}) = \{(\grave{e},\ \langle x,\ \mathrm{T}_{\mathscr{F}(\grave{e})}(x),\ \mathrm{I}_{\mathscr{F}(\grave{e})}(x),\ \mathrm{F}_{\mathscr{F}(\grave{e})}(x)\rangle : x \in \mathbf{X}) : \grave{e} \in \check{E}\}.$$

We refer to the truth-membership, indeterminacy-membership, and falsity-membership functions of $\mathscr{F}(\grave{e})$ as $\mathrm{T}_{\mathscr{F}(\grave{e})}(x),\ \mathrm{T}_{\mathscr{F}(\grave{e})}(x),\ \mathrm{F}_{\mathscr{F}(\grave{e})}(x) \in [0,\ 1]$, respectively. Since supremum of each T, I, F is 1. It follows that the inequality $0 \leq \mathrm{T}_{\mathscr{F}(\grave{e})}(x) + \mathrm{I}_{\mathscr{F}(\grave{e})}(x) + \mathrm{F}_{\mathscr{F}(\grave{e})}(x) \leq 3$ is obvious.

**Definition 4** [70] If $(\mathscr{F},\ \check{E})$ is Neutrosophic Soft Sets (NSS) over universe set $\mathbf{X}$, then $(\mathscr{F},\ \check{E})^c$ is a complement of $(\mathscr{F},\ \check{E})$, and is defined as:

$$(\mathscr{F},\ \check{E})^c = \{(\grave{e},\ \langle x,\ \mathrm{F}_{\mathscr{F}(\grave{e})}(x),\ 1 - \mathrm{I}_{\mathscr{F}(\grave{e})}(x),\ \mathrm{T}_{\mathscr{F}(\grave{e})}(x)\rangle : x \in \mathbf{X}) : \grave{e} \in \check{E}\}.$$

It should be clear that, $((\mathscr{F},\ \check{E})^c)^c = (\mathscr{F},\ \check{E})$.

**Definition 5** [13] If $(\mathscr{F},\ \check{E})$ and $(\mathscr{G},\ \check{E})$ be NSSs over set $\mathbf{X}$. We state that $(\mathscr{F},\ \check{E}) \subseteq (\mathscr{G},\ \check{E})$ if and only if $\grave{e} \in \check{E}$ and $\forall\ x \in \mathbf{X}$, and the following conditions hold.

$$\mathrm{T}_{\mathscr{F}(\grave{e})}(x) \leq \mathrm{T}_{\mathscr{G}(\grave{e})}(x), \quad \mathrm{I}_{\mathscr{F}(\grave{e})}(x) \leq \mathrm{I}_{\mathscr{G}(\grave{e})}(x), \quad \mathrm{F}_{\mathscr{F}(\grave{e})}(x) \geq \mathrm{F}_{\mathscr{G}(\grave{e})}(x).$$

**Definition 6** [71] Given two NSSs $(\mathscr{F}_1,\ \check{E})$ and $(\mathscr{F}_2,\ \check{E})$ over the universe $\mathbf{X}$, then their union is represented by $(\mathscr{F}_1,\ \check{E}) \cup (\mathscr{F}_2,\ \check{E}) = (\mathscr{F}_3,\ \check{E})$, which is defined as follows:

$$(\mathscr{F}_3,\ \check{E}) = \left\{ \left(\grave{e},\ \langle x,\ \mathrm{T}_{\mathscr{F}_3(\grave{e})}(x),\ \mathrm{I}_{\mathscr{F}_3(\grave{e})}(x),\ \mathrm{F}_{\mathscr{F}_3(\grave{e})}(x)\rangle\right) : x \in \mathbf{X},\ \grave{e} \in \check{E} \right\},$$

where

$$\mathrm{T}_{\mathscr{F}_3(\grave{e})}(x) = \max\left\{\mathrm{T}_{\mathscr{F}_1(\grave{e})}(x),\ \mathrm{T}_{\mathscr{F}_2(\grave{e})}(x)\right\},$$

$$\mathrm{I}_{\mathscr{F}_3(\grave{e})}(x) = \max\left\{\mathrm{I}_{\mathscr{F}_1(\grave{e})}(x),\ \mathrm{I}_{\mathscr{F}_2(\grave{e})}(x)\right\},$$

$$\mathrm{F}_{\mathscr{F}_3(\grave{e})}(x) = \min\left\{\mathrm{F}_{\mathscr{F}_1(\grave{e})}(x),\ \mathrm{F}_{\mathscr{F}_2(\grave{e})}(x)\right\}.$$

**Definition 7** [71] Given two NSSs $(\mathscr{F}_1,\ \check{E})$ and $(\mathscr{F}_2,\ \check{E})$ over the universe $\mathbf{X}$, then their intersection is represented by $(\mathscr{F}_1,\ \check{E}) \cap (\mathscr{F}_2,\ \check{E}) = (\mathscr{F}_3,\ \check{E})$, which is defined as follows:

$$(\mathscr{F}_3,\ \check{E}) = \left\{ \left(\grave{e},\ \langle x,\ \mathrm{T}_{\mathscr{F}_3(\grave{e})}(x),\ \mathrm{I}_{\mathscr{F}_3(\grave{e})}(x),\ \mathrm{F}_{\mathscr{F}_3(\grave{e})}(x)\rangle\right) : x \in \mathbf{X},\ \grave{e} \in \check{E} \right\},$$

where

$$\mathrm{T}_{\mathscr{F}_3(\grave{e})}(x) = \min\left\{\mathrm{T}_{\mathscr{F}_1(\grave{e})}(x),\ \mathrm{T}_{\mathscr{F}_2(\grave{e})}(x)\right\},$$

$$\mathrm{I}_{\mathscr{F}_3(\grave{e})}(x) = \min\left\{\mathrm{I}_{\mathscr{F}_1(\grave{e})}(x),\ \mathrm{I}_{\mathscr{F}_2(\grave{e})}(x)\right\},$$

$$\mathrm{F}_{\mathscr{F}_3(\grave{e})}(x) = \max\left\{\mathrm{F}_{\mathscr{F}_1(\grave{e})}(x),\ \mathrm{F}_{\mathscr{F}_2(\grave{e})}(x)\right\}.$$

**Definition 8** [71] Given a family of NSSs over set $\mathbf{X}$, $\{(\mathscr{F}_{\mathfrak{i}},\ \breve{E}) : \mathfrak{i} \in \mathrm{I}\}$ then:

$$\bigcup_{\mathfrak{i}\in\mathrm{I}}(\mathscr{F}_{\mathfrak{i}},\ \breve{E}) = \left\{\left(\grave{e},\ \langle x,\ \sup_{\mathfrak{i}\in\mathrm{I}}\mathrm{T}_{\mathscr{F}_{\mathfrak{i}(\grave{e})}}(x),\ \sup_{\mathfrak{i}\in\mathrm{I}}\mathrm{I}_{\mathscr{F}_{\mathfrak{i}(\grave{e})}}(x),\ \inf_{\mathfrak{i}\in\mathrm{I}}\mathrm{F}_{\mathscr{F}_{\mathfrak{i}(\grave{e})}}(x)\rangle\right) : x \in \mathbf{X},\ \grave{e} \in \breve{E}\right\}.$$

$$\bigcap_{\mathfrak{i}\in\mathrm{I}}(\mathscr{F}_{\mathfrak{i}},\ \breve{E}) = \left\{\left(\grave{e},\ \langle x,\ \inf_{\mathfrak{i}\in\mathrm{I}}\mathrm{T}_{\mathscr{F}_{\mathfrak{i}(\grave{e})}}(x),\ \inf_{\mathfrak{i}\in\mathrm{I}}\mathrm{I}_{\mathscr{F}_{\mathfrak{i}(\grave{e})}}(x),\ \sup_{\mathfrak{i}\in\mathrm{I}}\mathrm{F}_{\mathscr{F}_{\mathfrak{i}(\grave{e})}}(x)\rangle\right) : x \in \mathbf{X},\ \grave{e} \in \breve{E}\right\}.$$

**Definition 9** [71] Consider two NSSs over sets $\mathbf{X}$, $(\tilde{\mathscr{F}}_1,\ \acute{\mathscr{E}})$ and $(\tilde{\mathscr{F}}_2,\ \acute{\mathscr{E}})$. Then AND operation on them is expressed as: $(\mathscr{F}_1,\ \mathscr{E}) \wedge (\mathscr{F}_2,\ \breve{E}) = (\mathscr{F}_3,\ \breve{E} \times \breve{E})$

$$(\mathscr{F}_3,\ \breve{E} \times \breve{E}) = \left\{\left((\grave{e}_1,\ \grave{e}_2),\ \langle x,\ \mathrm{T}_{\mathscr{F}_3(\grave{e}_1,\ \grave{e}_2)}(x),\ \mathrm{I}_{\mathscr{F}_3(\grave{e}_1,\ \grave{e}_2)}(x),\ \mathrm{F}_{\mathscr{F}_3(\grave{e}_1,\ \grave{e}_2)}(x)\rangle : x \in \mathbb{X}\right) : (\grave{e}_1,\ \grave{e}_2) \in \breve{E} \times \breve{E}\right\},$$

where

$$\mathrm{T}_{\mathscr{F}_3(\grave{e}_1,\ \grave{e}_2)}(x) = \min\left\{\mathrm{T}_{\mathscr{F}_1(\grave{e}_1)}(x),\ \mathrm{T}_{\mathscr{F}_2(\grave{e}_2)}(x)\right\},$$

$$\mathrm{I}_{\mathscr{F}_3(\grave{e}_1,\ \grave{e}_2)}(x) = \min\left\{\mathrm{I}_{\mathscr{F}_1(\grave{e}_1)}(x),\ \mathrm{I}_{\mathscr{F}_2(\grave{e}_2)}(x)\right\},$$

$$\mathrm{F}_{\mathscr{F}_3(\grave{e}_1,\ \grave{e}_2)}(x) = \max\left\{\mathrm{F}_{\mathscr{F}_1(\grave{e}_1)}(x),\ \mathrm{F}_{\mathscr{F}_2(\grave{e}_2)}(x)\right\}.$$

**Definition 10** [71] Consider two NSSs over sets $\mathbf{X}$, $(\tilde{\mathscr{F}}_1,\ \acute{\mathscr{E}})$ and $(\tilde{\mathscr{F}}_2,\ \acute{\mathscr{E}})$. Then OR operation on them is expressed as: $(\mathscr{F}_1,\ \mathscr{E}) \vee (\mathscr{F}_2,\ \breve{E}) = (\mathscr{F}_3,\ \breve{E} \times \breve{E})$

$$(\mathscr{F}_3,\ \breve{E} \times \breve{E}) = \left\{\left((\grave{e}_1,\ \grave{e}_2),\ \langle x,\ \mathrm{T}_{\mathscr{F}_3(\grave{e}_1,\ \grave{e}_2)}(x),\ \mathrm{I}_{\mathscr{F}_3(\grave{e}_1,\ \grave{e}_2)}(x),\ \mathrm{F}_{\mathscr{F}_3(\grave{e}_1,\ \grave{e}_2)}(x)\rangle : x \in \mathbb{X}\right) : (\grave{e}_1,\ \grave{e}_2) \in \breve{E} \times \breve{E}\right\},$$

where

$$\mathrm{T}_{\mathscr{F}_3(\grave{e}_1,\,\grave{e}_2)}(x) = \max\left\{\mathrm{T}_{\mathscr{F}_1(\grave{e}_1)}(x),\ \mathrm{T}_{\mathscr{F}_2(\grave{e}_2)}(x)\right\},$$

$$\mathrm{I}_{\mathscr{F}_3(\grave{e}_1,\,\grave{e}_2)}(x) = \max\left\{\mathrm{I}_{\mathscr{F}_1(\grave{e}_1)}(x),\ \mathrm{I}_{\mathscr{F}_2(\grave{e}_2)}(x)\right\},$$

$$\mathrm{F}_{\mathscr{F}_3(\grave{e}_1,\,\grave{e}_2)}(x) = \min\left\{\mathrm{F}_{\mathscr{F}_1(\grave{e}_1)}(x),\ \mathrm{F}_{\mathscr{F}_2(\grave{e}_2)}(x)\right\}.$$

**Definition 11** [71] The following criteria must be met for a NSS $(\mathscr{F},\ \check{E})$ on $\mathbf{X}$ to be considered null neutrosophic soft set:

$$\mathrm{T}_{\mathscr{F}(\grave{e})}(x) = 0, \quad \mathrm{I}_{\mathscr{F}(\grave{e})}(x) = 0, \quad \mathrm{F}_{\mathscr{F}(\grave{e})}(x) = 1, \quad \forall\, \mathfrak{e} \in \check{E},\ \forall\, x \in \mathbf{X},$$

$0_{(\mathbf{X},\,\check{E})}$ is the symbol for it.

**Definition 12** [71] The following criteria must be met for a NSS $(\mathscr{F},\ \check{E})$ on $\mathbf{X}$ to be considered absolute neutrosophic soft set:

$$\mathrm{T}_{\mathscr{F}(\grave{e})}(x) = 1, \quad \mathrm{I}_{\mathscr{F}(\grave{e})}(x) = 1, \quad \mathrm{F}_{\mathscr{F}(\grave{e})}(x) = 0, \quad \forall \grave{e} \in \check{E},\ \forall x \in \mathbf{X},$$

$1_{(\mathbf{X},\,\check{E})}$ is the symbol for it.

## 3. Operations on Dual Neutrosophic Soft Sets (DNSSs)

This section presents the fundamental theory of DNSSs, defining their structure through truth, contradiction-based indeterminacy, hesitation-based indeterminacy, and falsity membership functions. Basic operations including complement, union, intersection, difference, AND, and OR are formally developed (Definitions 13-24), along with key algebraic properties.

An illustrative example involving military target evaluation under uncertain and conflicting intelligence information demonstrates the practical application of DNSS. The results of union (Figure 1), intersection (Figure 2), complements (Figures 3-4), differences (Figures 5-6), and logical OR/AND operations (Figures 7-8) highlight the effectiveness of DNSS in handling uncertainty in decision-making contexts.

**Definition 13** Let $\check{E}$ be a set of all parameters, and $\mathbf{X}$ be a set of initial universes. Let $P(\mathbf{X})$ denotes the set of all DNSSs of $\mathbf{X}$. A DNSS $(\mathscr{F},\ \check{E})$ is defined as a set valued function $\mathscr{F} : \check{E} \longrightarrow P(\mathbf{X})$, where $\mathscr{F}$ is called as an approximate function of DNSS $(\mathscr{F},\ \check{E})$. In other words, a DNSS is a parameterized family of some elements of the set $P(\mathbf{X})$ and can be written as a set of ordered pairs:

$$(\mathscr{F},\ \check{E}) = \{(\grave{e},\ \langle x,\ \mathrm{T}_{\mathscr{F}(\grave{e})}(x),\ \mathrm{I}_{C_{\mathscr{F}(\grave{e})}}(x),\ \mathrm{I}_{H_{\mathscr{F}(\grave{e})}}(x),\ \mathrm{F}_{\mathscr{F}(\grave{e})}(x)\rangle : x \in \mathbf{X}) : \grave{e} \in \check{E}\}.$$

Where $\mathrm{T}_{\mathscr{F}(\grave{e})}(x),\ \mathrm{I}_{C_{\mathscr{F}(\grave{e})}}(x),\ \mathrm{I}_{H_{\mathscr{F}(\grave{e})}}(x),\ \mathrm{F}_{\mathscr{F}(\grave{e})}(x) \in [0,\ 1]$ refer to the truth-membership, indeterminacy leans toward contradiction-membership, and falsity leans toward hesitation-membership functions of $\mathscr{F}(\grave{e})$respectively. Since supremum of each $\mathrm{T},\ \mathrm{I}_C,\ \mathrm{I}_H,\ \mathrm{F}$ is 1. It follows that the inequality $0 \leq \mathrm{T}_{\mathscr{F}(\grave{e})}(x) + \mathrm{I}_{C_{\mathscr{F}(\grave{e})}}(x) + \mathrm{I}_{H_{\mathscr{F}(\grave{e})}}(x) + \mathrm{F}_{\mathscr{F}(\grave{e})}(x) \leq 3$ is obvious.

**Definition 14** [70] Let $(\mathscr{F},\ \check{E})$ be DNSS over set $\mathbf{X}$, then $(\mathscr{F},\ \check{E})^c$ is a complement of $(\mathscr{F},\ \check{E})$, and is defined as:

$$(\mathscr{F},\ \check{E})^c = \{(\grave{e},\ \langle x,\ \mathrm{F}_{\mathscr{F}(\grave{e})}(x),\ 1-\mathrm{I}_{C_{\mathscr{F}(\grave{e})}}(x),\ 1-\mathrm{I}_{H_{\mathscr{F}(\grave{e})}}(x),\ \mathrm{T}_{\mathscr{F}(\grave{e})}(x)\rangle : x \in \mathbf{X}) : \grave{e} \in \check{E}\},$$

clearly, $((\mathscr{F},\ \check{E})^c)^c = (\mathscr{F},\ \check{E})$.

**Definition 15** [13] Let $(\mathscr{F},\ \check{E})$ and $(\mathscr{G},\ \check{E})$ be two DNSSs over set $\mathbf{X}$. Then $(\mathscr{F},\ \check{E}) \subseteq (\mathscr{G},\ \check{E})$ if and only if $\grave{e} \in \check{E}$ and $\forall\ x \in \mathbf{X}$, and the following conditions hold.

$$\mathrm{T}_{\mathscr{F}(\grave{e})}(x) \leq \mathrm{T}_{\mathscr{G}(\grave{e})}(x), \quad \mathrm{I}_{C_{\mathscr{F}(\grave{e})}}(x) \leq \mathrm{I}_{C_{\mathscr{G}(\grave{e})}}(x), \quad \mathrm{I}_{H_{\mathscr{F}(\grave{e})}}(x) \leq \mathrm{I}_{H_{\mathscr{G}(\grave{e})}}(x), \quad \mathrm{F}_{\mathscr{F}(\grave{e})}(x) \geq \mathrm{F}_{\mathscr{G}(\grave{e})}(x).$$

**Definition 16** [13] Let $(\mathscr{F},\ \check{E})$ and $(\mathscr{G},\ \check{E})$ be two DNSSs over set $\mathbf{X}$. Then $(\mathscr{F},\ \check{E}) = (\mathscr{G},\ \check{E})$ if and only if $\grave{e} \in \check{E}$ and $\forall\ x \in \mathbf{X}$, and the following conditions hold. From $(\mathscr{F},\ \check{E}) \subseteq (\mathscr{G},\ \check{E})$

$$\mathrm{T}_{\mathscr{F}(\grave{e})}(x) \leq \mathrm{T}_{\mathscr{G}(\grave{e})}(x), \quad \mathrm{I}_{C_{\mathscr{F}(\grave{e})}}(x) \leq \mathrm{I}_{C_{\mathscr{G}(\grave{e})}}(x), \quad \mathrm{I}_{H_{\mathscr{F}(\grave{e})}}(x) \leq \mathrm{I}_{H_{\mathscr{G}(\grave{e})}}(x), \quad \mathrm{F}_{\mathscr{F}(\grave{e})}(x) \geq \mathrm{F}_{\mathscr{G}(\grave{e})}(x).$$

And from $(\mathscr{G},\ \check{E}) \subseteq (\mathscr{F},\ \check{E})$

$$\mathrm{T}_{\mathscr{G}(\grave{e})}(x) \leq \mathrm{F}_{\mathscr{G}(\grave{e})}(x), \quad \mathrm{I}_{C_{\mathscr{G}(\grave{e})}}(x) \leq \mathrm{I}_{C_{\mathscr{F}(\grave{e})}}(x), \quad \mathrm{I}_{H_{\mathscr{G}(\grave{e})}}(x) \leq \mathrm{I}_{H_{\mathscr{F}(\grave{e})}}(x), \quad \mathrm{F}_{\mathscr{G}(\grave{e})}(x) \geq \mathrm{F}_{\mathscr{F}(\grave{e})}(x).$$

**Definition 17** Let $(\mathscr{F}_1,\ \check{E})$ and $(\mathscr{F}_2,\ \check{E})$ be two DNSSs over the $\mathbf{X}$. Then, their union is represented by $(\mathscr{F}_1,\ \check{E}) \cup (\mathscr{F}_2,\ \check{E}) = (\mathscr{F}_3,\ \check{E})$. Is defined as:

$$(\mathscr{F}_3,\ \check{E}) = \left\{\left(\grave{e},\ \langle x,\ \mathrm{T}_{\mathscr{F}_3(\grave{e})}(x),\ \mathrm{I}_{C_{\mathscr{F}_3(\grave{e})}}(x),\ \mathrm{I}_{H_{\mathscr{F}_3(\grave{e})}}(x),\ \mathrm{F}_{\mathscr{F}_3(\grave{e})}(x)\rangle : x \in \mathbf{X}\right) : \grave{e} \in \check{E}\right\}.$$

Where

$$\mathrm{T}_{\mathscr{F}_3(\grave{e})}(x) = \max\{\mathrm{T}_{\mathscr{F}_1(\grave{e})}(x),\ \mathrm{T}_{\mathscr{F}_2(\grave{e})}(x)\}$$

$$\mathrm{I}_{C_{\mathscr{F}_3(\grave{e})}}(x) = \max\{\mathrm{I}_{C_{\mathscr{F}_1(\grave{e})}}(x),\ \mathrm{I}_{C_{\mathscr{F}_2(\grave{e})}}(x)\}$$

$$\mathrm{I}_{H_{\mathscr{F}_3(\grave{e})}}(x) = \max\{\mathrm{I}_{H_{\mathscr{F}_1(\grave{e})}}(x),\ \mathrm{I}_{H_{\mathscr{F}_2(\grave{e})}}(x)\}$$

$$\mathrm{F}_{\mathscr{F}_3(\grave{e})}(x) = \min\{\mathrm{F}_{\mathscr{F}_1(\grave{e})}(x),\ \mathrm{F}_{\mathscr{F}_2(\grave{e})}(x)\}.$$

**Definition 18** Let $(\mathscr{F}_1,\ \check{E})$ and $(\mathscr{F}_2,\ \check{E})$ be two Double Valued Neutrosophic Soft (DNS) sets over the $\mathbf{X}$ universe set. Then, $(\mathscr{F}_1,\ \check{E}) \cap (\mathscr{F}_2,\ \check{E}) = (\mathscr{F}_3,\ \check{E})$ represents their intersection. Then definition is:

$$(\mathscr{F}_3,\ \check{E}) = \left\{\left(\grave{e},\ \langle x,\ \mathrm{T}_{\mathscr{F}_3(\grave{e})}(x),\ \mathrm{I}_{C_{\mathscr{F}_3(\grave{e})}}(x),\ \mathrm{I}_{H_{\mathscr{F}_3(\grave{e})}}(x),\ \mathrm{F}_{\mathscr{F}_3(\grave{e})}(x)\rangle : x \in \mathbf{X}\right) : \grave{e} \in \check{E}\right\}.$$

Where

$$\mathrm{T}_{\mathscr{F}_3(\grave{e})}(x) = \min\{\mathrm{T}_{\mathscr{F}_1(\grave{e})}(x),\ \mathrm{T}_{\mathscr{F}_2(\grave{e})}(x)\}$$

$$\mathrm{I}_{C_{\mathscr{F}_3(\grave{e})}}(x) = \min\{\mathrm{I}_{C_{\mathscr{F}_1(\grave{e})}}(x),\ \mathrm{I}_{C_{\mathscr{F}_2(\grave{e})}}(x)\}$$

$$\mathrm{I}_{H_{\mathscr{F}_3(\grave{e})}}(x) = \min\{\mathrm{I}_{H_{\mathscr{F}_1(\grave{e})}}(x),\ \mathrm{I}_{H_{\mathscr{F}_2(\grave{e})}}(x)\}$$

$$\mathrm{F}_{\mathscr{F}_3(\grave{e})}(x) = \max\{\mathrm{F}_{\mathscr{F}_1(\grave{e})}(x),\ \mathrm{F}_{\mathscr{F}_2(\grave{e})}(x)\}.$$

**Definition 19** Consider $(\mathscr{F}_1,\ \breve{E})$ and $(\mathscr{F}_2,\ \breve{E})$ be DNS sets over the universe set $\mathbf{X}$. So, $(\mathscr{F}_1,\ \breve{E})$ difference $(\mathscr{F}_2,\ \breve{E})$ operation on them is represented as $(\mathscr{F}_1,\ \breve{E}) \setminus (\mathscr{F}_2,\ \breve{E}) = (\mathscr{F}_3,\ \breve{E})$. It is defined by the intersection of $(\mathscr{F}_1,\ \breve{E})$ with the compliment of $(\mathscr{F}_2,\ \breve{E})$.

$(\mathscr{F}_3,\ \breve{E}) = (\mathscr{F}_1,\ \breve{E}) \cap (\mathscr{F}_2,\ \breve{E})^c$ as follows:

$$(\mathscr{F}_1,\ \breve{E}) = \left\{\left(\grave{e},\ \langle x,\ \mathrm{T}_{\mathscr{F}_1(\grave{e})}(x),\ \mathrm{I}_{C_{\mathscr{F}_1(\grave{e})}}(x),\ \mathrm{I}_{H_{\mathscr{F}_1(\grave{e})}}(x),\ \mathrm{F}_{\mathscr{F}_1(\grave{e})}(x)\rangle : x \in \mathbf{X}\right) : \grave{e} \in \breve{E}\right\},$$

$$(\mathscr{F}_2,\ \breve{E}) = \left\{\left(\grave{e},\ \langle x,\ \mathrm{T}_{\mathscr{F}_2(\grave{e})}(x),\ \mathrm{I}_{C_{\mathscr{F}_2(\grave{e})}}(x),\ \mathrm{I}_{H_{\mathscr{F}_2(\grave{e})}}(x),\ \mathrm{F}_{\mathscr{F}_2(\grave{e})}(x)\rangle : x \in \mathbf{X}\right) : \grave{e} \in \breve{E}\right\},$$

$$(\mathscr{F}_2,\ \breve{E})^c = \left\{\left(\grave{e},\ \langle x,\ \mathrm{T}_{\mathscr{F}_2(\grave{e})}(x),\ 1 - \mathrm{I}_{C_{\mathscr{F}_2(\grave{e})}}(x),\ 1 - \mathrm{I}_{H_{\mathscr{F}_2(\grave{e})}}(x),\ \mathrm{F}_{\mathscr{F}_2(\grave{e})}(x)\rangle : x \in \mathbf{X}\right) : \grave{e} \in \breve{E}\right\}.$$

Therefore, the resulting DNSS is

$$(\mathscr{F}_3,\ \breve{E}) = \left\{\left(\grave{e},\ \langle x,\ \mathrm{T}_{\mathscr{F}_3(\grave{e})}(x),\ \mathrm{I}_{C_{\mathscr{F}_3(\grave{e})}}(x),\ \mathrm{I}_{H_{\mathscr{F}_3(\grave{e})}}(x),\ \mathrm{F}_{\mathscr{F}_3(\grave{e})}(x)\rangle : x \in \mathbf{X}\right) : \grave{e} \in \breve{E}\right\},$$

where

$$\mathrm{T}_{\mathscr{F}_3(\grave{e})}(x) = \min\{\mathrm{T}_{\mathscr{F}_1(\grave{e})}(x),\ \mathrm{F}_{\mathscr{F}_2(\grave{e})}(x)\}$$

$$\mathrm{I}_{C_{\mathscr{F}_3(\grave{e})}}(x) = \min\{\mathrm{I}_{C_{\mathscr{F}_1(\grave{e})}}(x),\ 1 - \mathrm{I}_{C_{\mathscr{F}_2(\grave{e})}}(x)\}$$

$$\mathrm{I}_{H_{\mathscr{F}_3(\grave{e})}}(x) = \min\{\mathrm{I}_{H_{\mathscr{F}_1(\grave{e})}}(x),\ 1 - \mathrm{I}_{H_{\mathscr{F}_2(\grave{e})}}(x)\}$$

$$\mathrm{F}_{\mathscr{F}_3(\grave{e})}(x) = \max\{\mathrm{F}_{\mathscr{F}_1(\grave{e})}(x),\ \mathrm{T}_{\mathscr{F}_2(\grave{e})}(x)\}.$$

**Definition 20** Let $\{(\mathscr{F}_{\mathrm{i}},\ \breve{E}) : \mathrm{i} \in \mathrm{I}\}$ be a family of DNS sets over $\mathbf{X}$, then

$$\bigcup_{\mathfrak{i}\in\mathrm{I}}(\mathscr{F}_{\mathfrak{i}},\,\breve{E})=\left\{\left(\grave{e},\,\langle x,\,\sup_{\mathfrak{i}\in\mathrm{I}}\mathrm{T}_{\mathscr{F}_{\mathfrak{i}(\grave{e})}}(x),\,\sup_{\mathfrak{i}\in\mathrm{I}}\mathrm{I}_{C_{\mathscr{F}_{\mathfrak{i}(\grave{e})}}}(x),\,\sup_{\mathfrak{i}\in\mathrm{I}}\mathrm{I}_{H_{\mathscr{F}_{\mathfrak{i}(\grave{e})}}}(x),\,\inf_{\mathfrak{i}\in\mathrm{I}}\mathrm{F}_{\mathscr{F}_{\mathfrak{i}(\grave{e})}}(x)\rangle:x\in\mathbf{X}\right):\grave{e}\in\breve{E}\right\}.$$

$$\bigcap_{\mathfrak{i}\in\mathrm{I}}(\mathscr{F}_{\mathfrak{i}},\,\breve{E})=\left\{\left(\grave{e},\,\langle x,\,\inf_{\mathfrak{i}\in\mathrm{I}}\mathrm{T}_{\mathscr{F}_{\mathfrak{i}(\grave{e})}}(x),\,\inf_{\mathfrak{i}\in\mathrm{I}}\mathrm{I}_{C_{\mathscr{F}_{\mathfrak{i}(\grave{e})}}}(x),\,\inf_{\mathfrak{i}\in\mathrm{I}}\mathrm{I}_{H_{\mathscr{F}_{\mathfrak{i}(\grave{e})}}}(x),\,\sup_{\mathfrak{i}\in\mathrm{I}}\mathrm{F}_{\mathscr{F}_{\mathfrak{i}(\grave{e})}}(x)\rangle:x\in\mathbf{X}\right):\grave{e}\in\breve{E}\right\}.$$

**Definition 21** Let $(\mathscr{F}_1,\,\breve{E})$ and $(\mathscr{F}_2,\,\breve{E})$ be two DNS sets over the universe set $\mathbf{X}$. Then, the AND operation on them is symbolized by $(\mathscr{F}_1,\,\breve{E})\wedge(\mathscr{F}_2,\,\breve{E})=(\mathscr{F}_3,\,\breve{E}\times\breve{E})$ and is described as follows:

$$(\mathscr{F}_3,\,\breve{E}\times\breve{E})=\left\{\left((\grave{e}_1,\,\grave{e}_2),\,\langle x,\,\mathrm{T}_{\mathscr{F}_3(\grave{e}_1,\,\grave{e}_2)}(x),\,\mathrm{I}_{C_{\mathscr{F}_3(\grave{e}_1,\,\grave{e}_2)}}(x),\right.\right.$$

$$\left.\left.\mathrm{I}_{H_{\mathscr{F}_3(\grave{e}_1,\,\grave{e}_2)}}(x),\,\mathrm{F}_{\mathscr{F}_3(\grave{e}_1,\,\grave{e}_2)}(x)\rangle:x\in\mathbf{X}\right):(\grave{e}_1,\,\grave{e}_2)\in\breve{E}\times\breve{E}\right\},$$

where

$$\mathrm{T}_{\mathscr{F}_3(\grave{e}_1,\,\grave{e}_2)}(x)=\min\left\{\mathrm{T}_{\mathscr{F}_1(\grave{e}_1,\,\grave{e}_2)}(x),\,\mathrm{T}_{\mathscr{F}_2(\grave{e}_1,\,\grave{e}_2)}(x)\right\},$$

$$\mathrm{I}_{C_{\mathscr{F}_3(\grave{e}_1,\,\grave{e}_2)}}(x)=\min\left\{\mathrm{I}_{C_{\mathscr{F}_1(\grave{e}_1,\,\grave{e}_2)}}(x),\,\mathrm{I}_{C_{\mathscr{F}_2(\grave{e}_1,\,\grave{e}_2)}}(x)\right\},$$

$$\mathrm{I}_{H_{\mathscr{F}_3(\grave{e}_1,\,\grave{e}_2)}}(x)=\min\left\{\mathrm{I}_{H_{\mathscr{F}_1(\grave{e}_1,\,\grave{e}_2)}}(x),\,\mathrm{I}_{H_{\mathscr{F}_2(\grave{e}_1,\,\grave{e}_2)}}(x)\right\},$$

$$\mathrm{F}_{\mathscr{F}_3(\grave{e}_1,\,\grave{e}_2)}(x)=\max\left\{\mathrm{F}_{\mathscr{F}_1(\grave{e}_1,\,\grave{e}_2)}(x),\,\mathrm{F}_{\mathscr{F}_2(\grave{e}_1,\,\grave{e}_2)}(x)\right\}.$$

**Definition 22** Consider $(\mathscr{F}_1,\,\breve{E})$ and $(\mathscr{F}_2,\,\breve{E})$ be DNS sets over the universe $\mathbf{X}$. Then, the OR operation on them is represented by $(\mathscr{F}_1,\,\breve{E})\vee(\mathscr{F}_2,\,\breve{E})=(\mathscr{F}_3,\,\breve{E}\times\breve{E})$ and is given as:

$$(\mathscr{F},\,\breve{E}\times\breve{E})=\left\{\left((\grave{e}_1,\,\grave{e}_2),\,\langle x,\,\mathrm{T}_{\mathscr{F}_3(\grave{e}_1,\,\grave{e}_2)}(x),\,\mathrm{I}_{C_{\mathscr{F}_3(\grave{e}_1,\,\grave{e}_2)}}(x),\right.\right.$$

$$\left.\left.\mathrm{I}_{H_{\mathscr{F}_3(\grave{e}_1,\,\grave{e}_2)}}(x),\,\mathrm{F}_{\mathscr{F}_3(\grave{e}_1,\,\grave{e}_2)}(x)\rangle:x\in\mathbf{X}\right):(\grave{e}_1,\,\grave{e}_2)\in\breve{E}\times\breve{E}\right\},$$

where

$$\mathrm{T}_{\mathscr{F}_3(\grave{e}_1,\,\grave{e}_2)}(x)=\max\left\{\mathrm{T}_{\mathscr{F}_1(\grave{e}_1,\,\grave{e}_2)}(x),\,\mathrm{T}_{\mathscr{F}_2(\grave{e}_1,\,\grave{e}_2)}(x)\right\},$$

$$\mathrm{I}_{C_{\mathscr{F}_3(\grave{e}_1,\,\grave{e}_2)}}(x)=\max\left\{\mathrm{I}_{C_{\mathscr{F}_1(\grave{e}_1,\,\grave{e}_2)}}(x),\,\mathrm{I}_{C_{\mathscr{F}_2(\grave{e}_1,\,\grave{e}_2)}}(x)\right\},$$

$$\mathrm{I}_{H_{\mathscr{F}_3(\grave{e}_1,\,\grave{e}_2)}}(x)=\max\left\{\mathrm{I}_{H_{\mathscr{F}_1(\grave{e}_1,\,\grave{e}_2)}}(x),\,\mathrm{I}_{H_{\mathscr{F}_2(\grave{e}_1,\,\grave{e}_2)}}(x)\right\},$$

$$\mathrm{F}_{\mathscr{F}_3(\grave{e}_1,\,\grave{e}_2)}(x)=\min\left\{\mathrm{F}_{\mathscr{F}_1(\grave{e}_1,\,\grave{e}_2)}(x),\,\mathrm{F}_{\mathscr{F}_2(\grave{e}_1,\,\grave{e}_2)}(x)\right\}.$$

**Definition 23** Set $(\mathscr{F},\,\breve{E})$ for a DNS across the universe set $\mathbf{X}$ is a *null DNS set* by definition if

$$\mathrm{T}_{\mathscr{F}(\grave{e})}(x)=0,\quad \mathrm{I}_{C_{\mathscr{F}(\grave{e})}}(x)=0,\quad \forall \grave{e}\in\breve{E},\,\forall x\in\mathbf{X},$$

$$\mathrm{I}_{H_{\mathscr{F}(\grave{e})}}(x)=0,\quad \mathrm{F}_{\mathscr{F}(\grave{e})}(x)=1,\quad \forall \grave{e}\in\breve{E},\,\forall x\in\mathbf{X}.$$

It is indicated by $0_{(\mathbf{X},\,\breve{E})}$.

**Definition 24** An $(\mathscr{F},\,\breve{E})$ DNS set is *absolute DNS set* over the universe set $\mathbf{X}$ if

$$\mathrm{T}_{\mathscr{F}(\grave{e})}(x)=1,\quad \mathrm{I}_{C_{\mathscr{F}(\grave{e})}}(x)=1,\quad \forall \grave{e}\in\breve{E},\,\forall x\in\mathbf{X},$$

$$\mathrm{I}_{H_{\mathscr{F}(\grave{e})}}(x)=1,\quad \mathrm{F}_{\mathscr{F}(\grave{e})}(x)=0,\quad \forall \grave{e}\in\breve{E},\,\forall x\in\mathbf{X}.$$

Evidently,

$$0^c_{(\mathbf{X},\,\breve{E})}=1_{(\mathbf{X},\,\breve{E})},\quad 1^c_{(\mathbf{X},\,\breve{E})}=0_{(\mathbf{X},\,\breve{E})}.$$

**Proposition 1** Let $(\mathscr{F}_1,\,\breve{E})$ and $(\mathscr{F}_2,\,\breve{E})$ be two DNS sets over the $\mathbf{X}$ universe set. Next,
1. $[(\mathscr{F}_1,\,\breve{E})\cup(\mathscr{F}_2,\,\breve{E})]^c=(\mathscr{F}_1,\,\breve{E})^c\cap(\mathscr{F}_2,\,\breve{E})^c$.
2. $[(\mathscr{F}_1,\,\breve{E})\cap(\mathscr{F}_2,\,\breve{E})]^c=(\mathscr{F}_1,\,\breve{E})^c\cup(\mathscr{F}_2,\,\breve{E})^c$.

**Proof.** (i) For all $\grave{e}\in\breve{E}$ and $x\in\mathbf{X}$,

$$(\mathscr{F}_1,\,\breve{E})=\left\{\left(\grave{e},\,\langle x,\,\mathrm{T}_{\mathscr{F}_1(\grave{e})}(x),\,\mathrm{I}_{C_{\mathscr{F}_1(\grave{e})}}(x),\,\mathrm{I}_{H_{\mathscr{F}_1(\grave{e})}}(x),\,\mathrm{F}_{\mathscr{F}_1(\grave{e})}(x)\rangle : x\in\mathbf{X}\right) : \grave{e}\in\breve{E}\right\},$$

$$(\mathscr{F}_2,\,\breve{E})=\left\{\left(\grave{e},\,\langle x,\,\mathrm{T}_{\mathscr{F}_2(\grave{e})}(x),\,\mathrm{I}_{C_{\mathscr{F}_2(\grave{e})}}(x),\,\mathrm{I}_{H_{\mathscr{F}_2(\grave{e})}}(x),\,\mathrm{F}_{\mathscr{F}_2(\grave{e})}(x)\rangle : x\in\mathbf{X}\right) : \grave{e}\in\breve{E}\right\},$$

$$(\mathscr{F}_1,\, \check{E}) \cup (\mathscr{F}_2,\, \check{E}) = \{\langle x,\, \max\{\mathrm{T}_{\mathscr{F}_1(\grave{e})}(x),\, \mathrm{T}_{\mathscr{F}_2(\grave{e})}(x)\},\, \max\{\mathrm{I}_{C_{\mathscr{F}_1(\grave{e})}}(x),\, \mathrm{I}_{C_{\mathscr{F}_2(\grave{e})}}(x)\},$$

$$\max\{\mathrm{I}_{H_{\mathscr{F}_1(\grave{e})}}(x),\, \mathrm{I}_{H_{\mathscr{F}_2(\grave{e})}}(x)\},\, \min\{\mathrm{F}_{\mathscr{F}_1(\grave{e})}(x),\, \mathrm{F}_{\mathscr{F}_2(\grave{e})}(x)\}\rangle\},$$

$$[(\mathscr{F}_1,\, \check{E}) \cup (\mathscr{F}_2,\, \check{E})]^c = \{\langle x,\, \min\{\mathrm{F}_{\mathscr{F}_1(\grave{e})}(x),\, \mathrm{F}_{\mathscr{F}_2(\grave{e})}(x)\},\, 1 - \max\{\mathrm{I}_{C_{\mathscr{F}_1(\grave{e})}}(x),\, \mathrm{I}_{C_{\mathscr{F}_2(\grave{e})}}(x)\},$$

$$1 - \max\{\mathrm{I}_{H_{\mathscr{F}_1(\grave{e})}}(x),\, \mathrm{I}_{H_{\mathscr{F}_2(\grave{e})}}(x)\},\, \max\{\mathrm{T}_{\mathscr{F}_1(\grave{e})}(x),\, \mathrm{T}_{\mathscr{F}_2(\grave{e})}(x)\}\rangle\}.$$

Now,

$$(\mathscr{F}_1,\, \check{E})^c = \{\langle x,\, \mathrm{F}_{\mathscr{F}_1(\grave{e})}(x),\, 1 - \mathrm{I}_{C_{\mathscr{F}_1(\grave{e})}}(x),\, 1 - \mathrm{I}_{H_{\mathscr{F}_1(\grave{e})}}(x),\, \mathrm{T}_{\mathscr{F}_1(\grave{e})}(x)\rangle\}$$

$$(\mathscr{F}_2,\, \check{E})^c = \{\langle x,\, \mathrm{F}_{\mathscr{F}_2(\grave{e})}(x),\, 1 - \mathrm{I}_{C_{\mathscr{F}_2(\grave{e})}}(x),\, 1 - \mathrm{I}_{H_{\mathscr{F}_2(\grave{e})}}(x),\, \mathrm{T}_{\mathscr{F}_2(\grave{e})}(x)\rangle\}.$$

After that,

$$(\mathscr{F}_1,\, \check{E})^c \cap (\mathscr{F}_2,\, \check{E})^c = \{\langle x,\, \min\{\mathrm{F}_{\mathscr{F}_1(\grave{e})}(x),\, \mathrm{F}_{\mathscr{F}_2(\grave{e})}(x)\},\, \min\{1 - \mathrm{I}_{C_{\mathscr{F}_1(\grave{e})}}(x),\, 1 - \mathrm{I}_{C_{\mathscr{F}_2(\grave{e})}}(x)\},$$

$$\min\{1 - \mathrm{I}_{H_{\mathscr{F}_1(\grave{e})}}(x),\, 1 - \mathrm{I}_{H_{\mathscr{F}_2(\grave{e})}}(x)\},\, \max\{\mathrm{T}_{\mathscr{F}_1(\grave{e})}(x),\, \mathrm{T}_{\mathscr{F}_2(\grave{e})}(x)\}\rangle\}$$

$$(\mathscr{F}_1,\, \check{E})^c \cap (\mathscr{F}_2,\, \check{E})^c = \{\langle x,\, \min\{\mathrm{F}_{\mathscr{F}_1(\grave{e})}(x),\, \mathrm{F}_{\mathscr{F}_2(\grave{e})}(x)\},\, 1 - \max\{\mathrm{I}_{C_{\mathscr{F}_1(\grave{e})}}(x),\, \mathrm{I}_{C_{\mathscr{F}_2(\grave{e})}}(x)\},$$

$$1 - \max\{\mathrm{I}_{H_{\mathscr{F}_1(\grave{e})}}(x),\, \mathrm{I}_{H_{\mathscr{F}_2(\grave{e})}}(x)\},\, \max\{\mathrm{T}_{\mathscr{F}_1(\grave{e})}(x),\, \mathrm{T}_{\mathscr{F}_2(\grave{e})}(x)\}\rangle\}.$$

Hence, $[(\mathscr{F}_1,\, \check{E}) \cup (\mathscr{F}_2,\, \check{E})]^c = (\mathscr{F}_1,\, \check{E})^c \cap (\mathscr{F}_2,\, \check{E})^c$.
(ii) In the same way, $\forall\ \grave{e} \in \check{E}$ and $x \in \mathbf{X}$,

$$(\mathscr{F}_1,\, \check{E}) \cap (\mathscr{F}_2,\, \check{E}) = \{\langle x,\, \min\{\mathrm{T}_{\mathscr{F}_1(\grave{e})}(x),\, \mathrm{T}_{\mathscr{F}_2(\grave{e})}(x)\},\, \min\{\mathrm{I}_{C_{\mathscr{F}_1(\grave{e})}}(x),\, \mathrm{I}_{C_{\mathscr{F}_2(\grave{e})}}(x)\},$$

$$\min\{\mathrm{I}_{H_{\mathscr{F}_1(\grave{e})}}(x),\, \mathrm{I}_{H_{\mathscr{F}_2(\grave{e})}}(x)\},\, \max\{\mathrm{F}_{\mathscr{F}_1(\grave{e})}(x),\, \mathrm{F}_{\mathscr{F}_2(\grave{e})}(x)\}\rangle\},$$

$$[(\mathscr{F}_1,\, \check{E}) \cap (\mathscr{F}_2,\, \check{E})]^c = \{\langle x,\, \max\{\mathrm{F}_{\mathscr{F}_1(\grave{e})}(x),\, \mathrm{F}_{\mathscr{F}_2(\grave{e})}(x)\},\, 1 - \min\{\mathrm{I}_{C_{\mathscr{F}_1(\grave{e})}}(x),\, \mathrm{I}_{C_{\mathscr{F}_2(\grave{e})}}(x)\},$$

$$1 - \min\{\mathrm{I}_{H_{\mathscr{F}_1(\grave{e})}}(x),\, \mathrm{I}_{H_{\mathscr{F}_2(\grave{e})}}(x)\},\, \min\{\mathrm{T}_{\mathscr{F}_1(\grave{e})}(x),\, \mathrm{T}_{\mathscr{F}_2(\grave{e})}(x)\}\rangle\}.$$

Now,

$$(\mathscr{F}_1,\, \breve{E})^c = \{\langle x,\, \mathrm{F}_{\mathscr{F}_1(\grave{e})}(x),\, \mathrm{I}_{C_{\mathscr{F}_1(\grave{e})}}(x),\, \mathrm{I}_{H_{\mathscr{F}_1(\grave{e})}}(x),\, \mathrm{T}_{\mathscr{F}_1(\grave{e})}(x)\rangle\}$$

$$(\mathscr{F}_2,\, \breve{E})^c = \{\langle x,\, \mathrm{F}_{\mathscr{F}_2(\grave{e})}(x),\, \mathrm{I}_{C_{\mathscr{F}_2(\grave{e})}}(x),\, \mathrm{I}_{H_{\mathscr{F}_2(\grave{e})}}(x),\, \mathrm{T}_{\mathscr{F}_2(\grave{e})}(x)\rangle\}.$$

So,

$$(\mathscr{F}_1,\, \breve{E})^c \cup (\mathscr{F}_2,\, \breve{E})^c = \{\langle x,\, \max\{\mathrm{F}_{\mathscr{F}_1(\grave{e})}(x),\, \mathrm{F}_{\mathscr{F}_2(\grave{e})}(x)\},\, \max\{1-\mathrm{I}_{C_{\mathscr{F}_1(\grave{e})}}(x),\, 1-\mathrm{I}_{C_{\mathscr{F}_2(\grave{e})}}(x)\},$$

$$\max\{1-\mathrm{I}_{H_{\mathscr{F}_1(\grave{e})}}(x),\, 1-\mathrm{I}_{H_{\mathscr{F}_2(\grave{e})}}(x)\},\, \min\{\mathrm{T}_{\mathscr{F}_1(\grave{e})}(x),\, \mathrm{T}_{\mathscr{F}_2(\grave{e})}(x)\}\rangle\}$$

$$(\mathscr{F}_1,\, \breve{E})^c \cup (\mathscr{F}_2,\, \breve{E})^c = \{\langle x,\, \max\{\mathrm{F}_{\mathscr{F}_1(\grave{e})}(x),\, \mathrm{F}_{\mathscr{F}_2(\grave{e})}(x)\},\, 1-\min\{\mathrm{I}_{C_{\mathscr{F}_1(\grave{e})}}(x),\, \mathrm{I}_{C_{\mathscr{F}_2(\grave{e})}}(x)\},$$

$$1-\min\{\mathrm{I}_{H_{\mathscr{F}_1(\grave{e})}}(x),\, \mathrm{I}_{H_{\mathscr{F}_2(\grave{e})}}(x)\},\, \min\{\mathrm{T}_{\mathscr{F}_1(\grave{e})}(x),\, \mathrm{T}_{\mathscr{F}_2(\grave{e})}(x)\}\rangle\}.$$

Hence, $[(\mathscr{F}_1,\, \breve{E}) \cap (\mathscr{F}_2,\, \breve{E})]^c = (\mathscr{F}_1,\, \breve{E})^c \cup (\mathscr{F}_2,\, \breve{E})^c$. □

**Proposition 2** Consider $(\mathscr{F}_1,\, \breve{E})$ and $(\mathscr{F}_2,\, \breve{E})$ be two DNS sets over the universe set $\mathbf{X}$. So,
1. $[(\mathscr{F}_1,\, \breve{E}) \vee (\mathscr{F}_2,\, \breve{E})]^c = (\mathscr{F}_1,\, \breve{E})^c \wedge (\mathscr{F}_2,\, \breve{E})^c$.
2. $[(\mathscr{F}_1,\, \breve{E}) \wedge (\mathscr{F}_2,\, \breve{E})]^c = (\mathscr{F}_1,\, \breve{E})^c \vee (\mathscr{F}_2,\, \breve{E})^c$.

**Proof.** (i) $\forall\ \grave{e} \in \breve{E}$ and $x \in \mathbf{X}$,

$$(\mathscr{F}_1,\, \breve{E}) = \left\{\left(\grave{e},\, \langle x,\, \mathrm{T}_{\mathscr{F}_1(\grave{e})}(x),\, \mathrm{I}_{C_{\mathscr{F}_1(\grave{e})}}(x),\, \mathrm{I}_{H_{\mathscr{F}_1(\grave{e})}}(x),\, \mathrm{F}_{\mathscr{F}_1(\grave{e})}(x)\rangle : x \in \mathbf{X}\right) : \grave{e} \in \breve{E}\right\},$$

$$(\mathscr{F}_2,\, \breve{E}) = \left\{\left(\grave{e},\, \langle x,\, \mathrm{T}_{\mathscr{F}_2(\grave{e})}(x),\, \mathrm{I}_{C_{\mathscr{F}_2(\grave{e})}}(x),\, \mathrm{I}_{H_{\mathscr{F}_2(\grave{e})}}(x),\, \mathrm{F}_{\mathscr{F}_2(\grave{e})}(x)\rangle : x \in \mathbf{X}\right) : \grave{e} \in \breve{E}\right\},$$

$$(\mathscr{F}_1,\, \breve{E}) \vee (\mathscr{F}_2,\, \breve{E}) = \{\langle x,\, \max\{\mathrm{T}_{\mathscr{F}_1(\grave{e})}(x),\, \mathrm{T}_{\mathscr{F}_2(\grave{e})}(x)\},\, \max\{\mathrm{I}_{C_{\mathscr{F}_1(\grave{e})}}(x),\, \mathrm{I}_{C_{\mathscr{F}_2(\grave{e})}}(x)\},$$

$$\max\{\mathrm{I}_{H_{\mathscr{F}_1(\grave{e})}}(x),\, \mathrm{I}_{H_{\mathscr{F}_2(\grave{e})}}(x)\},\, \min\{\mathrm{F}_{\mathscr{F}_1(\grave{e})}(x),\, \mathrm{F}_{\mathscr{F}_2(\grave{e})}(x)\}\rangle\},$$

$$[(\mathscr{F}_1,\, \breve{E}) \vee (\mathscr{F}_2,\, \breve{E})]^c = \{\langle x,\, \min\{\mathrm{F}_{\mathscr{F}_1(\grave{e})}(x),\, \mathrm{F}_{\mathscr{F}_2(\grave{e})}(x)\},\, 1-\min\{\mathrm{I}_{H_{\mathscr{F}_1(\grave{e})}}(x),\, \mathrm{I}_{H_{\mathscr{F}_2(\grave{e})}}(x)\},$$

$$1-\min\{\mathrm{I}_{C_{\mathscr{F}_1(\grave{e})}}(x),\, \mathrm{I}_{C_{\mathscr{F}_2(\grave{e})}}(x)\},\, \max\{\mathrm{T}_{\mathscr{F}_1(\grave{e})}(x),\, \mathrm{T}_{\mathscr{F}_2(\grave{e})}(x)\}\rangle\}.$$

Presently,

$$(\mathscr{F}_1,\, \check{E})^c = \{\langle x,\, \mathrm{F}_{\mathscr{F}_1(\grave{e})}(x),\, 1-\mathrm{I}_{C_{\mathscr{F}_1(\grave{e})}}(x),\, 1-\mathrm{I}_{H_{\mathscr{F}_1(\grave{e})}}(x),\, \mathrm{T}_{\mathscr{F}_1(\grave{e})}(x)\rangle\}$$

$$(\mathscr{F}_2,\, \check{E})^c = \{\langle x,\, \mathrm{F}_{\mathscr{F}_2(\grave{e})}(x),\, 1-\mathrm{I}_{C_{\mathscr{F}_2(\grave{e})}}(x),\, 1-\mathrm{I}_{H_{\mathscr{F}_2(\grave{e})}}(x),\, \mathrm{T}_{\mathscr{F}_2(\grave{e})}(x)\rangle\}.$$

So,

$$(\mathscr{F}_1,\, \check{E})^c \wedge (\mathscr{F}_2,\, \check{E})^c = \{\langle x,\, \min\{\mathrm{F}_{\mathscr{F}_1(\grave{e})}(x),\, \mathrm{F}_{\mathscr{F}_2(\grave{e})}(x)\},\, \min\{1-\mathrm{I}_{C_{\mathscr{F}_1(\grave{e})}}(x),\, 1-\mathrm{I}_{C_{\mathscr{F}_2(\grave{e})}}(x)\},$$

$$\min\{1-\mathrm{I}_{H_{\mathscr{F}_1(\grave{e})}}(x),\, 1-\mathrm{I}_{H_{\mathscr{F}_2(\grave{e})}}(x)\},\, \max\{\mathrm{T}_{\mathscr{F}_1(\grave{e})}(x),\, \mathrm{T}_{\mathscr{F}_2(\grave{e})}(x)\}\rangle\}$$

$$(\mathscr{F}_1,\, \check{E})^c \wedge (\mathscr{F}_2,\, \check{E})^c = \{\langle x,\, \min\{\mathrm{F}_{\mathscr{F}_1(\grave{e})}(x),\, \mathrm{F}_{\mathscr{F}_2(\grave{e})}(x)\},\, 1-\max\{\mathrm{I}_{C_{\mathscr{F}_1(\grave{e})}}(x),\, \mathrm{I}_{C_{\mathscr{F}_2(\grave{e})}}(x)\},$$

$$1-\max\{\mathrm{I}_{H_{\mathscr{F}_1(\grave{e})}}(x),\, \mathrm{I}_{H_{\mathscr{F}_2(\grave{e})}}(x)\},\, \max\{\mathrm{T}_{\mathscr{F}_1(\grave{e})}(x),\, \mathrm{T}_{\mathscr{F}_2(\grave{e})}(x)\}\rangle\}.$$

Hence, $[(\mathscr{F}_1,\, \check{E}) \vee (\mathscr{F}_2,\, \check{E})]^c = (\mathscr{F}_1,\, \check{E})^c \wedge (\mathscr{F}_2,\, \check{E})^c$.
(ii) In a similar way, $\forall\, \grave{e} \in \check{E}$ and $x \in \mathbf{X}$,

$$(\mathscr{F}_1,\, \check{E}) \wedge (\mathscr{F}_2,\, \check{E}) = \{\langle x,\, \min\{\mathrm{T}_{\mathscr{F}_1(\grave{e})}(x),\, \mathrm{T}_{\mathscr{F}_2(\grave{e})}(x)\},\, \min\{\mathrm{I}_{C_{\mathscr{F}_1(\grave{e})}}(x),\, \mathrm{I}_{C_{\mathscr{F}_2(\grave{e})}}(x)\},$$

$$\min\{\mathrm{I}_{H_{\mathscr{F}_1(\grave{e})}}(x),\, \mathrm{I}_{H_{\mathscr{F}_2(\grave{e})}}(x)\},\, \max\{\mathrm{F}_{\mathscr{F}_1(\grave{e})}(x),\, \mathrm{F}_{\mathscr{F}_2(\grave{e})}(x)\}\rangle\},$$

$$[(\mathscr{F}_1,\, \check{E}) \wedge (\mathscr{F}_2,\, \check{E})]^c = \{\langle x,\, \max\{\mathrm{F}_{\mathscr{F}_1(\grave{e})}(x),\, \mathrm{F}_{\mathscr{F}_2(\grave{e})}(x)\},\, 1-\min\{\mathrm{I}_{C_{\mathscr{F}_1(\grave{e})}}(x),\, \mathrm{I}_{C_{\mathscr{F}_2(\grave{e})}}(x)\},$$

$$1-\min\{\mathrm{I}_{H_{\mathscr{F}_1(\grave{e})}}(x),\, \mathrm{I}_{H_{\mathscr{F}_2(\grave{e})}}(x)\},\, \min\{\mathrm{T}_{\mathscr{F}_1(\grave{e})}(x),\, \mathrm{T}_{\mathscr{F}_2(\grave{e})}(x)\}\rangle\}.$$

Now,

$$(\mathscr{F}_1,\, \check{E})^c = \{\langle x,\, \mathrm{F}_{\mathscr{F}_1(\grave{e})}(x),\, 1-\mathrm{I}_{C_{\mathscr{F}_1(\grave{e})}}(x),\, 1-\mathrm{I}_{H_{\mathscr{F}_1(\grave{e})}}(x),\, \mathrm{T}_{\mathscr{F}_1(\grave{e})}(x)\rangle\}$$

$$(\mathscr{F}_2,\, \check{E})^c = \{\langle x,\, \mathrm{F}_{\mathscr{F}_2(\grave{e})}(x),\, 1-\mathrm{I}_{C_{\mathscr{F}_2(\grave{e})}}(x),\, 1-\mathrm{I}_{H_{\mathscr{F}_2(\grave{e})}}(x),\, \mathrm{T}_{\mathscr{F}_2(\grave{e})}(x)\rangle\}$$

So,

$$(\mathscr{F}_1,\, \check{E})^c \vee (\mathscr{F}_2,\, \check{E})^c = \{\langle x,\, \max\{\mathrm{F}_{\mathscr{F}_1(\grave{e})}(x),\, \mathrm{F}_{\mathscr{F}_2(\grave{e})}(x)\},\, \max\{1-\mathrm{I}_{C_{\mathscr{F}_1(\grave{e})}}(x),\, 1-\mathrm{I}_{C_{\mathscr{F}_2(\grave{e})}}(x)\},$$

$$\max\{1-\mathrm{I}_{H_{\mathscr{F}_1(\grave{e})}}(x),\, 1-\mathrm{I}_{H_{\mathscr{F}_2(\grave{e})}}(x)\},\, \min\{\mathrm{T}_{\mathscr{F}_1(\grave{e})}(x),\, \mathrm{T}_{\mathscr{F}_2(\grave{e})}(x)\}\rangle\}$$

$$(\mathscr{F}_1,\, \breve{E})^c \vee (\mathscr{F}_2,\, \breve{E})^c = \{\langle x,\, \max\{\mathrm{F}_{\mathscr{F}_1(\grave{e})}(x),\, \mathrm{F}_{\mathscr{F}_2(\grave{e})}(x)\},\, 1-\min\{\mathrm{I}_{C_{\mathscr{F}_1(\grave{e})}}(x),\, \mathrm{I}_{C_{\mathscr{F}_2(\grave{e})}}(x)\},$$

$$1-\min\{\mathrm{I}_{H_{\mathscr{F}_1(\grave{e})}}(x),\, \mathrm{I}_{H_{\mathscr{F}_2(\grave{e})}}(x)\},\, \min\{\mathrm{T}_{\mathscr{F}_1(\grave{e})}(x),\, \mathrm{T}_{\mathscr{F}_2(\grave{e})}(x)\}\rangle\}.$$

Hence, $[(\mathscr{F}_1,\, \breve{E}) \wedge (\mathscr{F}_2,\, \breve{E})]^c = (\mathscr{F}_1,\, \breve{E})^c \vee (\mathscr{F}_2,\, \breve{E})^c$. □

**Example 1** Assume that $\mathbf{X}$ is the universe set, which is $\mathbf{X} = \{x_1,\, x_2,\, x_3,\, x_4\}$, where each $x_i$ is potential target such that $x_1$: Potential Target 1 (e.g., high-ranking enemy commander), $x_2$: Potential target 2 (e.g., armored vehicle unit), $x_3$: potential target 3 (e.g., enemy communication center) and $x_3$: potential target 4 (e.g., Ammunition depot or supply line). This setup makes it clear that each element in $\mathbf{X}$ corresponds to a specific target of interest in a strategic or military context. Set of Parameters $\breve{E} = \{\grave{e}_1,\, \grave{e}_2\}$ represents target evaluation criteria, such as: $\grave{e}_1$: threat level and $\grave{e}_1$: strategic importance. Each evaluation under a parameter is represented using:

$\mathrm{T}_{\mathscr{F}(\grave{e})}(x)$: Truth-membership (confidence target satisfies the parameter).

$\mathrm{I}_{C_{\mathscr{F}(\grave{e})}}(x)$: Contradiction-membership (disagree in the assessment).

$\mathrm{I}_{H_{\mathscr{F}(\grave{e})}}(x)$: Hesitation-membership (hesitation or delay in decision).

$\mathrm{F}_{\mathscr{F}(\grave{e})}(x)$: Falsity-membership (confidence the target does not satisfy the parameter).

All values are in [0, 1], and: $0 \leq \mathrm{T}_{\mathscr{F}(\grave{e})}(x) + \mathrm{I}_{C_{\mathscr{F}(\grave{e})}}(x) + \mathrm{I}_{H_{\mathscr{F}(\grave{e})}}(x) + \mathrm{F}_{\mathscr{F}(\grave{e})}(x) \leq 4$.

Let the two DNSSs $(\mathscr{F}_1,\, \breve{E})$ and $(\mathscr{F}_2,\, \breve{E})$ over $\mathbf{X}$ are as follows.

$$(\mathscr{F}_1,\, \breve{E}) = \begin{bmatrix} \grave{e}_1 = \langle x_1,\, 0.3,\, 0.6,\, 0.4,\, 0.8\rangle,\, \langle x_2,\, 0.4,\, 0.2,\, 0.3,\, 0.5\rangle, \\ \qquad \langle x_3,\, 0.6,\, 0.9,\, 0.7,\, 0.3\rangle,\, \langle x_4,\, 0.3,\, 0.2,\, 0.4,\, 0.6\rangle \\ \grave{e}_2 = \langle x_1,\, 0.5,\, 0.4,\, 0.6,\, 0.2\rangle,\, \langle x_2,\, 0.3,\, 0.5,\, 0.1,\, 0.4\rangle, \\ \qquad \langle x_3,\, 0.3,\, 0.2,\, 0.4,\, 0.9\rangle,\, \langle x_4,\, 0.2,\, 0.8,\, 0.2,\, 0.7\rangle \end{bmatrix}$$

$$(\mathscr{F}_2,\, \breve{E}) = \begin{bmatrix} \grave{e}_1 = \langle x_1,\, 0.2,\, 0.3,\, 0.6,\, 0.8\rangle,\, \langle x_2,\, 0.4,\, 0.6,\, 0.9,\, 0.1\rangle, \\ \qquad \langle x_3,\, 0.6,\, 0.9,\, 0.2,\, 0.3\rangle,\, \langle x_4,\, 0.8,\, 0.9,\, 0.3,\, 0.4\rangle \\ \grave{e}_2 = \langle x_1,\, 0.6,\, 0.8,\, 0.3,\, 0.2\rangle,\, \langle x_2,\, 0.5,\, 0.3,\, 0.4,\, 0.7\rangle, \\ \qquad \langle x_3,\, 0.2,\, 0.4,\, 0.7,\, 0.9\rangle,\, \langle x_4,\, 0.2,\, 0.8,\, 0.9,\, 0.5\rangle \end{bmatrix}.$$

Where $(\mathscr{F}_1,\, \breve{E})$ and $(\mathscr{F}_2,\, \breve{E})$ are two intelligence reports from two different sources. Each one gives four-part scores for each target under each parameter. Each report provides separate evaluations for each target under both criteria.

$$(\mathscr{F}_1, \breve{E}) \cup (\mathscr{F}_2, \breve{E}) = \begin{bmatrix} \grave{e}_1 = \langle x_1, 0.3, 0.6, 0.6, 0.8\rangle, \langle x_2, 0.4, 0.6, 0.9, 0.1\rangle, \\ \langle x_3, 0.6, 0.9, 0.7, 0.3\rangle, \langle x_4, 0.8, 0.9, 0.4, 0.4\rangle \\ \grave{e}_2 = \langle x_1, 0.6, 0.8, 0.6, 0.2\rangle, \langle x_2, 0.5, 0.5, 0.4, 0.4\rangle, \\ \langle x_3, 0.3, 0.4, 0.7, 0.9\rangle, \langle x_4, 0.2, 0.8, 0.9, 0.5\rangle \end{bmatrix}.$$

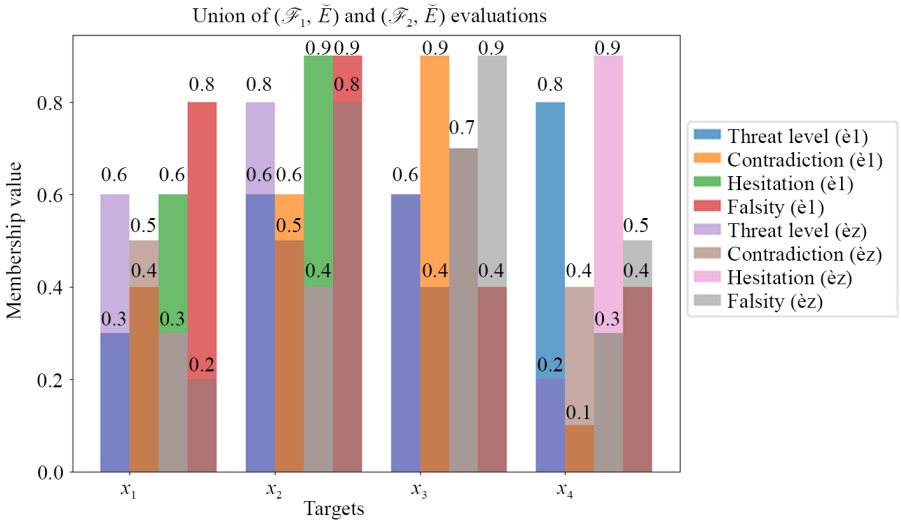


**Figure 1.** The union-based evaluations of $(\mathscr{F}_1, \breve{E})$ and $(\mathscr{F}_2, \breve{E})$ across targets $x_1$-$x_4$ are shown in Figure 1

$$(\mathscr{F}_1, \breve{E}) \cap (\mathscr{F}_2, \breve{E}) = \begin{bmatrix} \grave{e}_1 = \langle x_1, 0.2, 0.3, 0.4, 0.8\rangle, \langle x_2, 0.4, 0.2, 0.3, 0.5\rangle, \\ \langle x_3, 0.6, 0.9, 0.2, 0.3\rangle, \langle x_4, 0.3, 0.2, 0.3, 0.6\rangle \\ \grave{e}_2 = \langle x_1, 0.5, 0.4, 0.3, 0.2\rangle, \langle x_2, 0.3, 0.3, 0.1, 0.7\rangle, \\ \langle x_3, 0.2, 0.2, 0.4, 0.9\rangle, \langle x_4, 0.2, 0.8, 0.2, 0.7\rangle \end{bmatrix}.$$

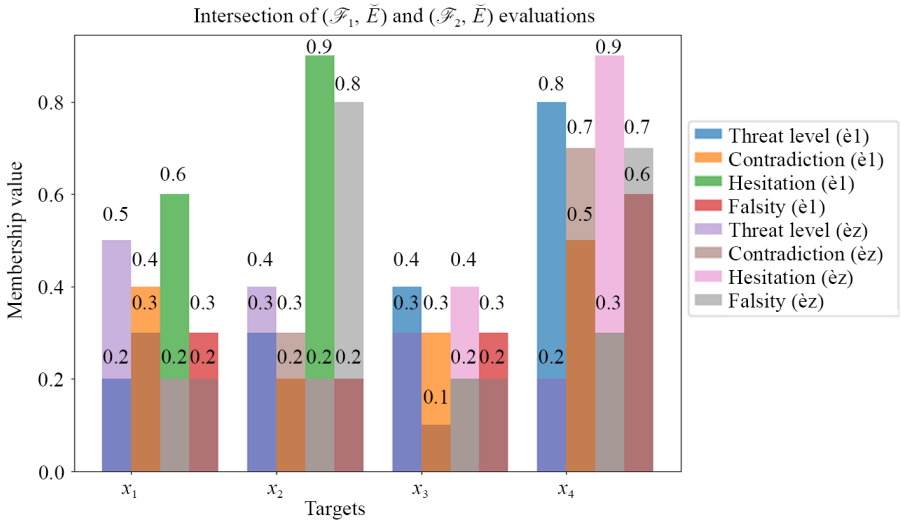


**Figure 2.** The intersection-based evaluations of $(\mathscr{F}_1, \breve{E})$ and $(\mathscr{F}_2, \breve{E})$ across targets $x_1$-$x_4$ are shown in Figure 2

$$(\mathscr{F}_1, \breve{E})^c = \begin{bmatrix} \grave{e}_1 = \langle x_1, 0.8, 0.4, 0.6, 0.3\rangle, \langle x_2, 0.5, 0.8, 0.7, 0.4\rangle, \\ \langle x_3, 0.3, 0.1, 0.3, 0.6\rangle, \langle x_4, 0.6, 0.8, 0.6, 0.3\rangle \\ \grave{e}_2 = \langle x_1, 0.2, 0.6, 0.4, 0.5\rangle, \langle x_2, 0.4, 0.5, 0.9, 0.3\rangle, \\ \langle x_3, 0.9, 0.8, 0.6, 0.3\rangle, \langle x_4, 0.7, 0.2, 0.8, 0.2\rangle \end{bmatrix}.$$

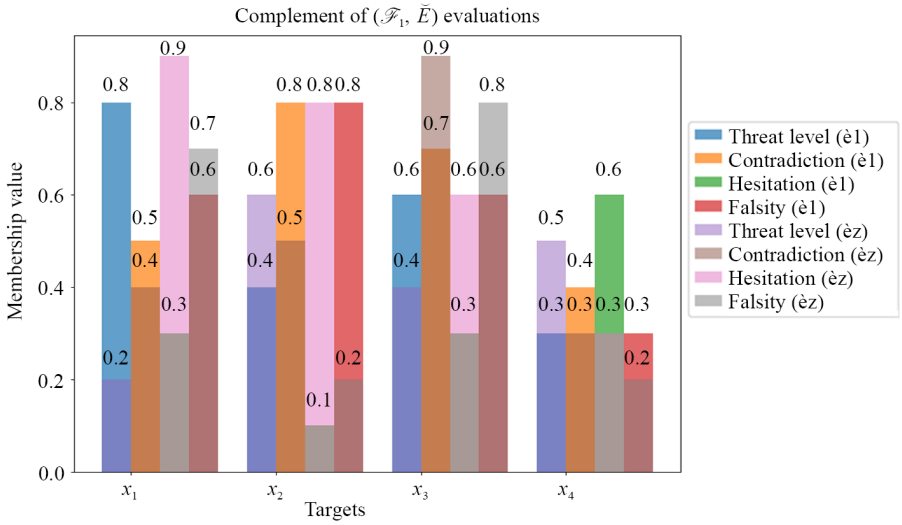


**Figure 3.** The complement-based evaluation of $(\mathscr{F}_1, \breve{E})$ across targets $x_1$-$x_4$ are shown in Figure 3

$$(\mathscr{F}_2, \breve{E})^c = \begin{bmatrix} \grave{e}_1 = \langle x_1, 0.8, 0.7, 0.4, 0.2\rangle, \langle x_2, 0.1, 0.4, 0.1, 0.4\rangle, \\ \langle x_3, 0.3, 0.1, 0.8, 0.6\rangle, \langle x_4, 0.4, 0.1, 0.7, 0.8\rangle \\ \grave{e}_2 = \langle x_1, 0.2, 0.2, 0.7, 0.6\rangle, \langle x_2, 0.7, 0.7, 0.6, 0.5\rangle, \\ \langle x_3, 0.9, 0.6, 0.3, 0.2\rangle, \langle x_4, 0.5, 0.2, 0.1, 0.2\rangle \end{bmatrix}.$$

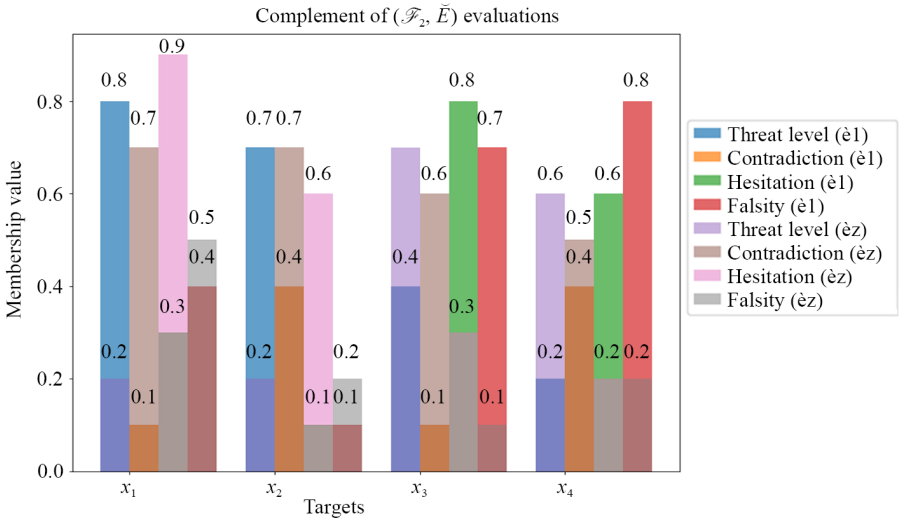


**Figure 4.** The complement-based evaluation of $(\mathscr{F}_2, \breve{E})$ across targets $x_1$-$x_4$ are shown in Figure 4

$$(\mathscr{F}_1, \breve{E}) \setminus (\mathscr{F}_2, \breve{E}) = \begin{bmatrix} \grave{e}_1 = \langle x_1, 0.3, 0.6, 0.4, 0.8\rangle, \langle x_2, 0.1, 0.2, 0.1, 0.5\rangle, \\ \langle x_3, 0.3, 0.1, 0.7, 0.6\rangle, \langle x_4, 0.3, 0.1, 0.4, 0.8\rangle \\ \grave{e}_2 = \langle x_1, 0.2, 0.2, 0.6, 0.6\rangle, \langle x_2, 0.3, 0.5, 0.1, 0.5\rangle, \\ \langle x_3, 0.3, 0.2, 0.3, 0.9\rangle, \langle x_4, 0.2, 0.2, 0.1, 0.7\rangle \end{bmatrix}.$$

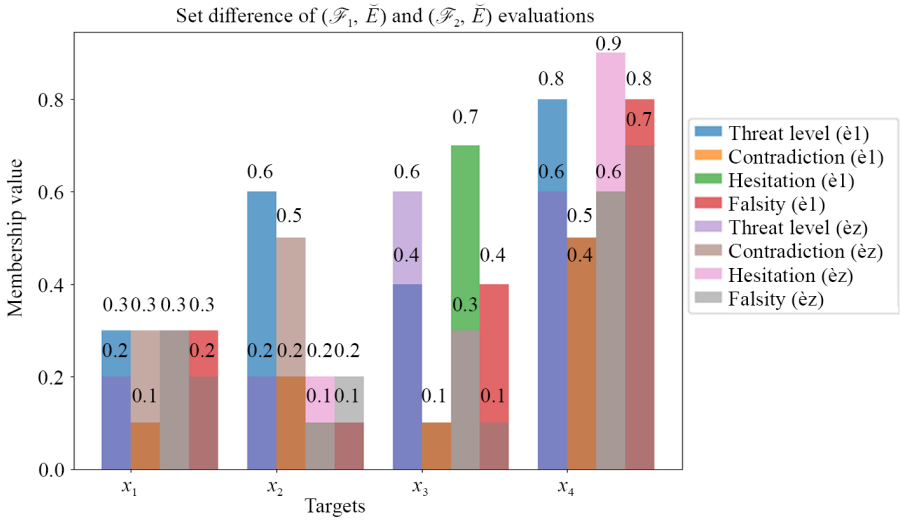


**Figure 5.** The difference-based evaluation of ($\mathscr{F}_1$, $\breve{E}$) and ($\mathscr{F}_2$, $\breve{E}$) across targets $x_1$-$x_4$ are shown in Figure 5

$$(\mathscr{F}_2,\ \breve{E}) \setminus (\mathscr{F}_1,\ \breve{E}) = \begin{bmatrix} \grave{e}_1 = \langle x_1,\ 0.2,\ 0.3,\ 0.6,\ 0.8\rangle,\ \langle x_2,\ 0.4,\ 0.6,\ 0.7,\ 0.4\rangle, \\ \langle x_3,\ 0.3,\ 0.1,\ 0.2,\ 0.6\rangle,\ \langle x_4,\ 0.6,\ 0.8,\ 0.3,\ 0.4\rangle \\ \grave{e}_2 = \langle x_1,\ 0.2,\ 0.6,\ 0.3,\ 0.5\rangle,\ \langle x_2,\ 0.4,\ 0.3,\ 0.4,\ 0.7\rangle, \\ \langle x_3,\ 0.2,\ 0.4,\ 0.6,\ 0.9\rangle,\ \langle x_4,\ 0.2,\ 0.2,\ 0.8,\ 0.5\rangle \end{bmatrix}.$$

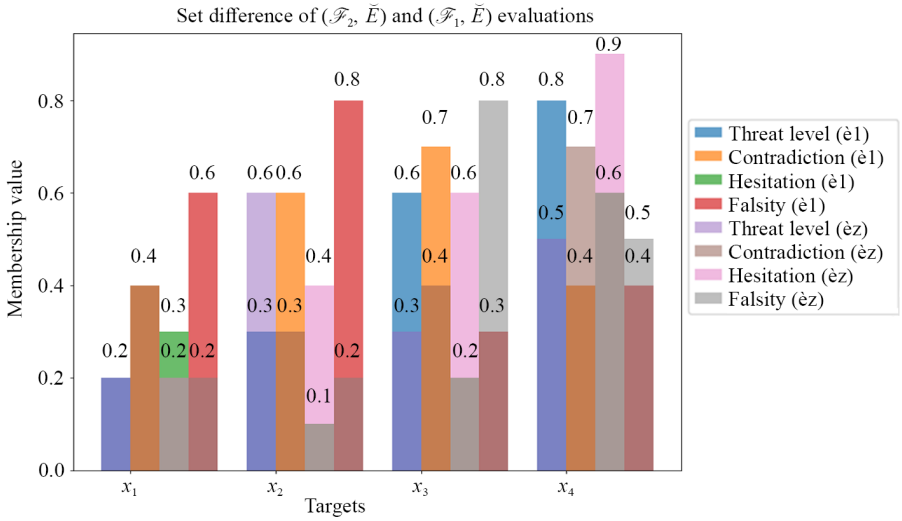


**Figure 6.** The difference-based evaluation of ($\mathscr{F}_2$, $\breve{E}$) and ($\mathscr{F}_1$, $\breve{E}$) across targets $x_1$-$x_4$ are shown in Figure 6

$$(\mathscr{F}_1, \check{E}) \vee (\mathscr{F}_2, \check{E}) = \begin{bmatrix} (\grave{e}_1, \grave{e}_1) = \langle x_1, 0.3, 0.6, 0.6, 0.8\rangle, \langle x_2, 0.4, 0.6, 0.9, 0.1\rangle, \\ \langle x_3, 0.6, 0.9, 0.7, 0.3\rangle, \langle x_4, 0.8, 0.9, 0.4, 0.4\rangle \\ (\grave{e}_1, \grave{e}_2) = \langle x_1, 0.6, 0.8, 0.4, 0.2\rangle, \langle x_2, 0.5, 0.3, 0.4, 0.5\rangle, \\ \langle x_3, 0.6, 0.9, 0.7, 0.3\rangle, \langle x_4, 0.3, 0.8, 0.9, 0.5\rangle \\ (\grave{e}_2, \grave{e}_1) = \langle x_1, 0.5, 0.4, 0.6, 0.2\rangle, \langle x_2, 0.4, 0.6, 0.9, 0.1\rangle, \\ \langle x_3, 0.6, 0.9, 0.4, 0.3\rangle, \langle x_4, 0.8, 0.9, 0.3, 0.4\rangle \\ (\grave{e}_2, \grave{e}_2) = \langle x_1, 0.6, 0.8, 0.6, 0.2\rangle, \langle x_2, 0.5, 0.5, 0.4, 0.4\rangle, \\ \langle x_3, 0.3, 0.4, 0.7, 0.9\rangle, \langle x_4, 0.2, 0.8, 0.9, 0.5\rangle \end{bmatrix}.$$

$$(\mathscr{F}_1, \check{E}) \wedge (\mathscr{F}_2, \check{E}) = \begin{bmatrix} (\grave{e}_1, \grave{e}_1) = \langle x_1, 0.2, 0.3, 0.4, 0.8\rangle, \langle x_2, 0.4, 0.2, 0.3, 0.5\rangle, \\ \langle x_3, 0.6, 0.9, 0.2, 0.3\rangle, \langle x_4, 0.3, 0.2, 0.3, 0.6\rangle \\ (\grave{e}_1, \grave{e}_2) = \langle x_1, 0.3, 0.6, 0.3, 0.8\rangle, \langle x_2, 0.4, 0.2, 0.3, 0.7\rangle, \\ \langle x_3, 0.2, 0.4, 0.7, 0.9\rangle, \langle x_4, 0.2, 0.2, 0.4, 0.6\rangle \\ (\grave{e}_2, \grave{e}_1) = \langle x_1, 0.2, 0.3, 0.6, 0.8\rangle, \langle x_2, 0.3, 0.5, 0.1, 0.4\rangle, \\ \langle x_3, 0.3, 0.2, 0.2, 0.9\rangle, \langle x_4, 0.2, 0.8, 0.2, 0.7\rangle \\ (\grave{e}_2, \grave{e}_2) = \langle x_1, 0.5, 0.4, 0.3, 0.2\rangle, \langle x_2, 0.3, 0.3, 0.1, 0.7\rangle, \\ \langle x_3, 0.2, 0.2, 0.4, 0.9\rangle, \langle x_4, 0.2, 0.8, 0.2, 0.7\rangle \end{bmatrix}.$$

This example demonstrates how DNSSs can be used to evaluate and compare military targets under uncertain, incomplete, or conflicting information from multiple sources.

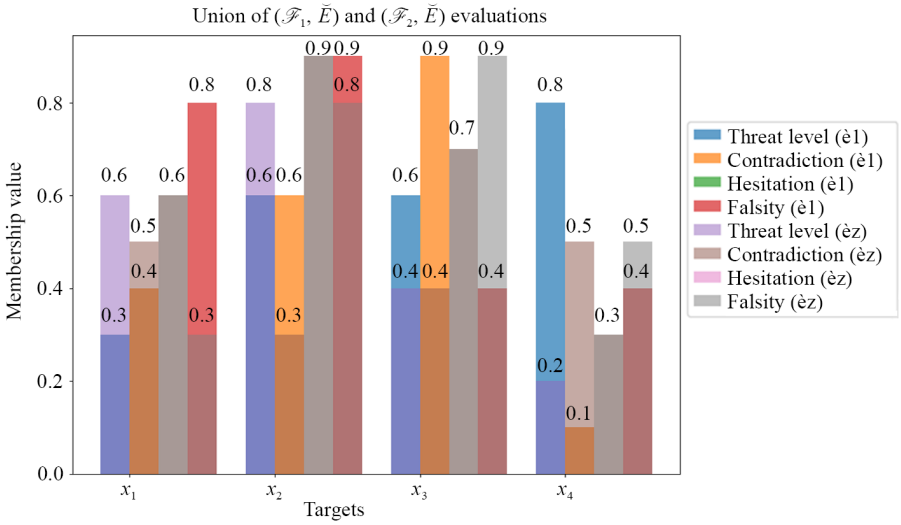


**Figure 7.** The OR-based evaluation of ($\mathscr{F}_1$, $\breve{E}$) and ($\mathscr{F}_2$, $\breve{E}$) across targets $x_1$-$x_4$ are shown in Figure 7

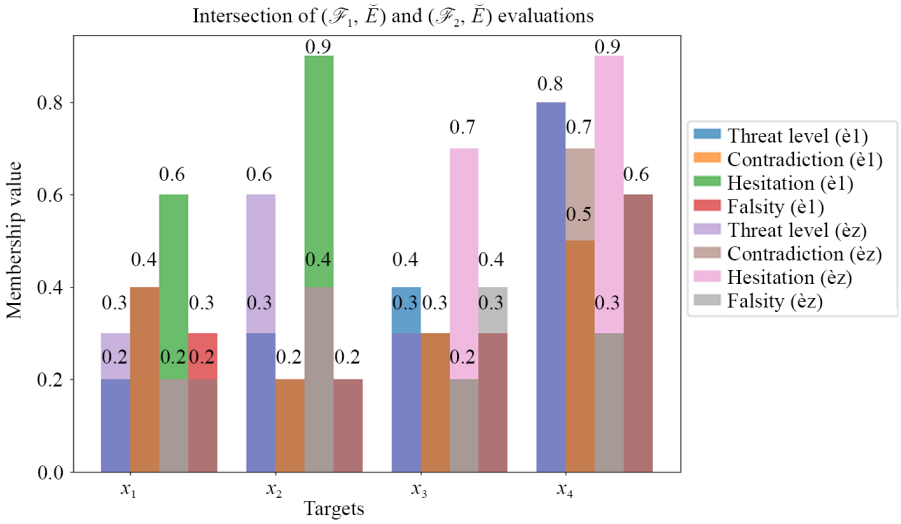


**Figure 8.** The AND-based evaluation of ($\mathscr{F}_1$, $\breve{E}$) and ($\mathscr{F}_2$, $\breve{E}$) across targets $x_1$-$x_4$ are shown in Figure 8

## 4. Operations on DNSTSs

This section develops the topological framework of DNSSs by introducing the family of DNSSs, DNSS topological spaces, closed sets, and discrete and indiscrete topologies. A DNSS topology is defined through axioms involving the null and absolute DNSSs, arbitrary unions, and finite intersections (Definition 25), while DNS closed sets are characterized via complements (Definition 26). The structural concept of a DNS topological space is illustrated in Figure 9. Fundamental properties of closed sets and relationships between different DNSS topologies are established through Propositions 3-4.

An illustrative example based on strategic target evaluation demonstrates the construction of two DNSS topologies and their interactions. The DNSS representations of $(\mathscr{F}_1,\ E), (\mathscr{F}_2,\ E)$ and $(\mathscr{F}_3,\ E)$ are shown in Figures 10-12. The behavior of union and intersection operations within the defined topologies is analyzed in Figures 13-16, highlighting the structural properties of DNSS topological spaces under uncertain and multi-source information.

**Definition 25** Let DNSS$(\mathbf{X}, \breve{E})$ be the family of all DNSSs over the universe set $\mathbf{X}$ and $\tau^{\mathrm{DNSS}} \subset \mathrm{DNSS}(\mathbf{X}, \breve{E})$, then $\tau^{\mathrm{DNSS}}$ is said to be DNSS T on $\mathbf{X}$, if

1. $0_{(\mathbf{X}, \breve{E})}$ and $1_{(\mathbf{X}, \breve{E})} \in \tau^{\mathrm{DNSS}}$,
2. The union of any number of DNS sets in $\tau \in \tau$,
3. The intersection of a finite number of DNS sets in $\tau \in \tau$.

Then $(\mathbf{X}, \tau^{\mathrm{DNSS}}, \breve{E})$ is a DNS Topological Space (DNSTS) over $\mathbf{X}$. Eac Element of $\tau^{\mathrm{DNSS}}$ is a DNS open set.

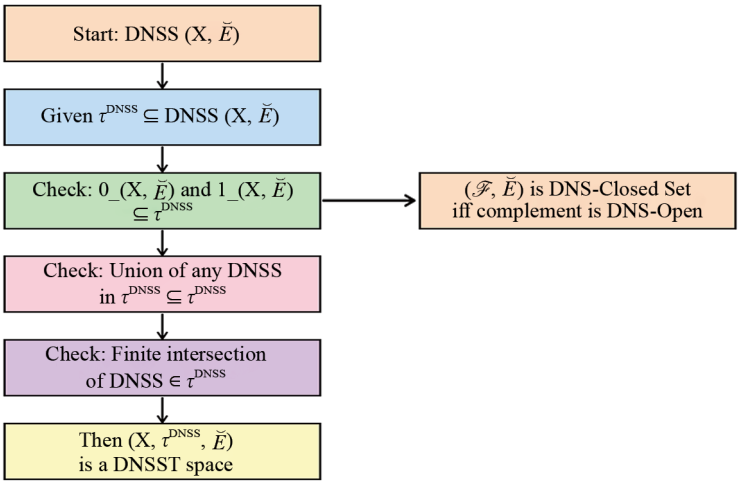


**Figure 9.** Flow chart of DNS topological space is given in Figure 9

**Definition 26** Assume that $(\mathbf{X}, \tau^{\mathrm{DNSS}}, \breve{E})$ be DNST space over $\mathbf{X}$ and the DNS set $(\mathscr{F}, \breve{E})$ over $\mathbf{X}$ are considered. If the complement of $(\mathscr{F}, \breve{E})$ is a DNS open set, then $(\mathscr{F}, \breve{E})$ is a DNS closed set.

**Remark 1** The union of two DNST over $\mathbf{X}$ may or may not be a DNST on $\mathbf{X}$.

**Proposition 3** Consider the DNS topological space $(\mathbf{X}, \tau, \breve{E})$ over the universe set $\mathbf{X}$. Next,

1. $0_{(\mathbf{X}, \breve{E})}$ and $1_{(\mathbf{X}, \breve{E})}$ are DNS closed sets over $\mathbf{X}$,
2. The union of any number of DNS sets is a DNS closed sets over $\mathbf{X}$,
3. The intersection of a finite number of DNS sets is a DNS closed sets over $\mathbf{X}$.

**Definition 27** Suppose that the family of all DNS sets over the universe set $\mathbf{X}$ is DNSS$(\mathbf{X}, \breve{E})$.

1. The DNS indiscrete topology is $\tau$, and the DNS indiscrete topological space over $\mathbf{X}$ is $(\mathbf{X}, \tau, \breve{E})$, if $\tau = \{0_{(\mathbf{X}, \breve{E})}, 1_{(\mathbf{X}, \breve{E})}\}$.
2. $(\mathbf{X}, \tau, \breve{E})$ is a DNS discrete topological space over $\mathbf{X}$, and $\tau = \mathrm{DNSS}(\mathbf{X}, \breve{E})$ is a DNS discrete topology.

**Proposition 4** For the same universe set $\mathbf{X}$, suppose $(\mathbf{X}, \tau_1, \breve{E})$ and $(\mathbf{X}, \tau_2, \breve{E})$ be two DNS topological spaces. The DNS topological space over $\mathbf{X}$ is then $(\mathbf{X}, \tau_1 \cap \tau_2, \breve{E})$.

**Proof.** (i). Given that $0_{(\mathbf{X}, \breve{E})}, 1_{(\mathbf{X}, \breve{E})} \in \tau_1$ and $0_{(\mathbf{X}, \breve{E})}, 1_{(\mathbf{X}, \breve{E})} \in \tau_2$, then $0_{(\mathbf{X}, \breve{E})}, 1_{(\mathbf{X}, \breve{E})} \in \tau_1 \cap \tau_2$.

(ii). Suppose that $\{(\mathscr{F}_{\mathrm{i}}, \breve{E}) | \mathrm{i} \in \mathrm{I}\}$ be a family of DNS sets in $\tau_1 \cap \tau_2$.

Then $(\mathscr{F}_{\mathrm{i}}, \breve{E}) \in \tau_1$ and $(\mathscr{F}_{\mathrm{i}}, \breve{E}) \in \tau_2 \; \forall \, \mathrm{i} \in \mathrm{I}$, so $\cup_{\mathrm{i} \in \mathrm{I}} (\mathscr{F}_{\mathrm{i}}, \breve{E}) \in \tau_1$ and $\cup_{\mathrm{i} \in \mathrm{I}} (\mathscr{F}_{\mathrm{i}}, \breve{E}) \in \tau_2$. Hence $\cup_{\mathrm{i} \in \mathrm{I}} (\mathscr{F}_{\mathrm{i}}, \breve{E}) \in \tau_1 \cap \tau_2$.

(iii). Let $\{(\mathscr{F}_{\mathrm{i}}, \breve{E}) | i = \overline{1, n}\}$ be a family of finite number of DNS sets in $\tau_1 \cap \tau_2$.

So, $(\mathscr{F}_{\mathrm{i}}, \breve{E}) \in \tau_1$ and $(\mathscr{F}_{\mathrm{i}}, \breve{E}) \in \tau_2 \; \forall \; i = \overline{1, n}$, so $\bigcap_{\mathrm{i}=I}^{n} (\mathscr{F}_{\mathrm{i}}, \breve{E}) \in \tau_1$ and $\bigcap_{\mathrm{i}=I}^{n} (\mathscr{F}_{\mathrm{i}}, \breve{E}) \in \tau_2$. Thus $\bigcap_{\mathrm{i}=I}^{n} (\mathscr{F}_{\mathrm{i}}, \breve{E}) \in \tau_1 \cap \tau_2$. □

**Remark 2** A DNS topology over $\mathbf{X}$ might not be the union of two DNS topologies over $\mathbf{X}$.

**Example 2** Assume that $\mathbf{X}$ is the universe set, which is $\mathbf{X} = \{x_1, x_2, x_3, x_4\}$, where each $x_i$ is potential target such that $x_1$: Potential Target 1 (e.g., high-ranking enemy commander), $x_2$: Potential target 2 (e.g., armored vehicle unit), $x_3$: potential target 3 (e.g., enemy communication center) and $x_3$: potential target 4 (e.g., Ammunition depot or supply line).

Such a set up indicates that every component of **X** is related to a definite strategic or military target of interest. Set of Parameters $\breve{E} = \{\grave{e}_1, \grave{e}_2\}$ represents target evaluation criteria, such as: $\grave{e}_1$: threat level and $\grave{e}_1$: strategic importance. Each evaluation under a parameter is represented using:

$T_{\mathscr{F}(\grave{e})}(x)$: Truth-membership (confidence target satisfies the parameter)
$I_{C_{\mathscr{F}(\grave{e})}}(x)$: Contradiction-membership (disagree in the assessment)
$I_{H_{\mathscr{F}(\grave{e})}}(x)$: Hesitation-membership (hesitation or delay in decision)
$F_{\mathscr{F}(\grave{e})}(x)$: Falsity-membership (confidence the target does not satisfy the parameter).
All values are in [0, 1], and: $0 \leq T_{\mathscr{F}(\grave{e})}(x) + I_{C_{\mathscr{F}(\grave{e})}}(x) + I_{H_{\mathscr{F}(\grave{e})}}(x) + F_{\mathscr{F}(\grave{e})}(x) \leq 4$.
Let

$$\tau_1^{\text{DNSS}} = \{0_{(\mathbf{X},\, \breve{E})},\ 1_{(\mathbf{X},\, \breve{E})},\ (\mathscr{F}_1,\, \breve{E}),\ (\mathscr{F}_2,\, \breve{E})\},$$

$$\tau_2^{\text{DNSS}} = \{0_{(\mathbf{X},\, \breve{E})},\ 1_{(\mathbf{X},\, \breve{E})},\ (\mathscr{F}_2,\, \breve{E}),\ (\mathscr{F}_3,\, \breve{E})\},$$

be two DNSTs over **X**, here $(\mathscr{F}_1,\, \breve{E})$, $(\mathscr{F}_2,\, \breve{E})$, $(\mathscr{F}_3,\, \breve{E})$ are defined:

$$(\mathscr{F}_1,\, \breve{E}) = \begin{bmatrix} \grave{e}_1 = \langle x_1,\, 0.6,\, 0.7,\, 0.4,\, 0.2\rangle,\ \langle x_2,\, 0.7,\, 0.9,\, 0.4,\, 0.3\rangle \\ \qquad \langle x_3,\, 0.5,\, 0.8,\, 0.7,\, 0.3\rangle,\ \langle x_4,\, 0.8,\, 0.7,\, 0.5,\, 0.4\rangle \\ \grave{e}_2 = \langle x_1,\, 0.9,\, 0.8,\, 0.5,\, 0.4\rangle,\ \langle x_2,\, 0.7,\, 0.9,\, 0.6,\, 0.4\rangle, \\ \qquad \langle x_3,\, 0.9,\, 0.8,\, 0.5,\, 0.4\rangle,\ \langle x_4,\, 0.7,\, 0.7,\, 0.6,\, 0.3\rangle \end{bmatrix}.$$

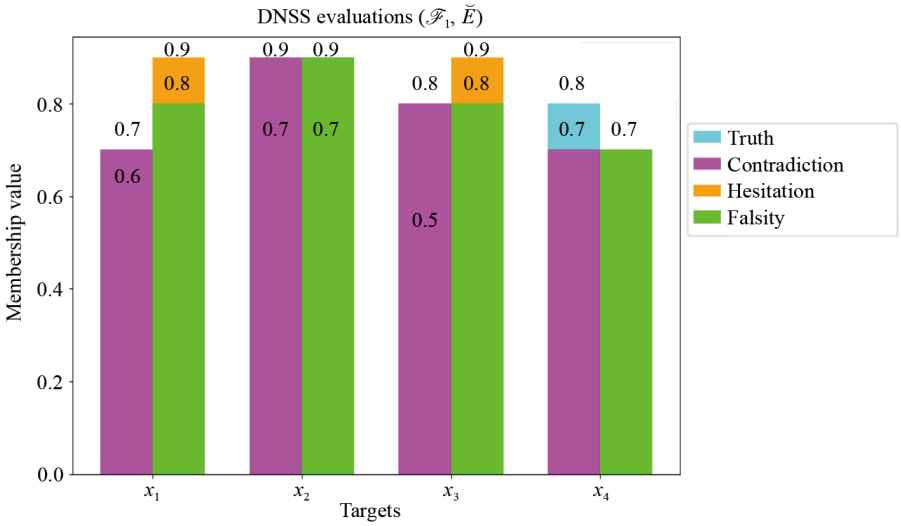


**Figure 10.** The DNSS evaluation of $(\mathscr{F}_1,\, \breve{E})$ across targets $x_1$-$x_4$ are shown in Figure 10

$$(\mathscr{F}_2, \breve{E}) = \begin{bmatrix} \grave{e}_1 = \langle x_1, 0.7, 0.8, 0.4, 0.3\rangle, \langle x_2, 0.3, 0.6, 0.4, 0.6\rangle \\ \langle x_3, 0.6, 0.9, 0.7, 0.2\rangle, \langle x_4, 0.5, 0.2, 0.4, 0.7\rangle \\ \grave{e}_2 = \langle x_1, 0.4, 0.5, 0.8, 0.9\rangle, \langle x_2, 0.4, 0.9, 0.5, 0.4\rangle, \\ \langle x_3, 0.3, 0.4, 0.6, 0.3\rangle, \langle x_4, 0.5, 0.6, 0.7, 0.4\rangle \end{bmatrix}.$$

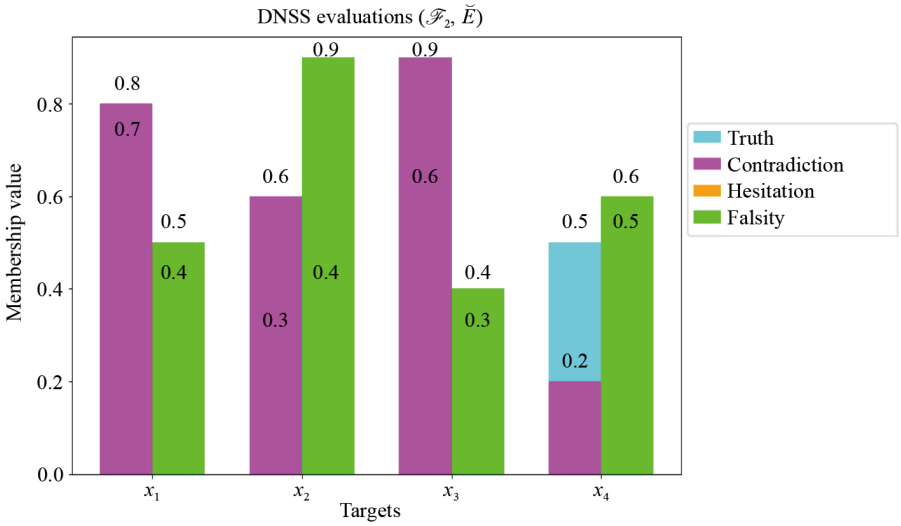


**Figure 11.** The DNSS evaluation of ($\mathscr{F}_2$, $\breve{E}$) across targets $x_1$-$x_4$ are shown in Figure 11

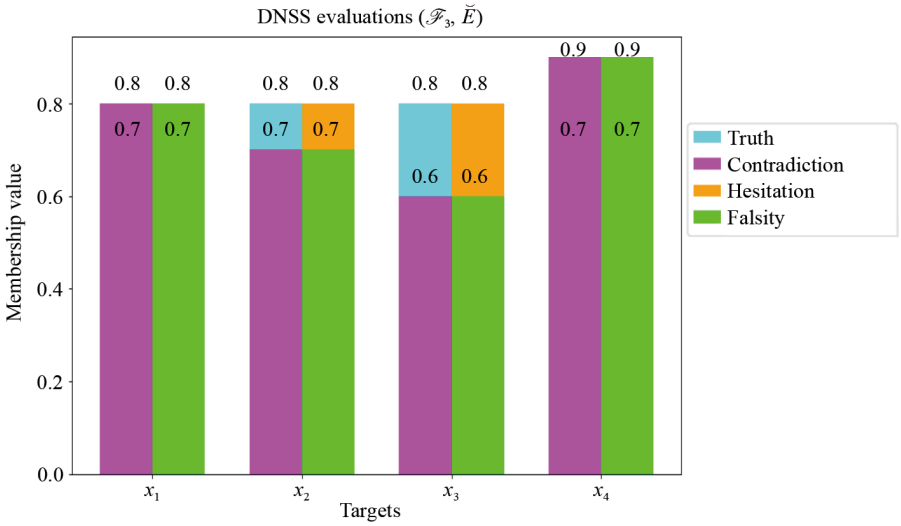


**Figure 12.** The DNSS evaluation of ($\mathscr{F}_3$, $\breve{E}$) across targets $x_1$-$x_4$ are shown in Figure 12

$$(\mathscr{F}_3, \check{E}) = \begin{bmatrix} \grave{e}_1 = \langle x_1, 0.7, 0.8, 0.6, 0.4\rangle, \langle x_2, 0.8, 0.7, 0.9, 0.5\rangle \\ \langle x_3, 0.8, 0.6, 0.4, 0.3\rangle, \langle x_4, 0.7, 0.9, 0.5, 0.4\rangle \\ \grave{e}_2 = \langle x_1, 0.7, 0.8, 0.6, 0.4\rangle, \langle x_2, 0.8, 0.7, 0.9, 0.5\rangle, \\ \langle x_3, 0.8, 0.6, 0.4, 0.3\rangle, \langle x_4, 0.7, 0.9, 0.5, 0.4\rangle \end{bmatrix}.$$

Three intelligence reports from two distinct sources are represented by the letters $(\mathscr{F}_1, \check{E})$ $(\mathscr{F}_2, \check{E})$ and $(\mathscr{F}_3, \check{E})$. For every objective under every criterion, each one provides a four-part score. With distinct evaluations for each target based on both criteria, each report offers a four-part assessment for each target under each parameter.

$$(\mathscr{F}_1, \check{E}) \cup (\mathscr{F}_2, \check{E}) = \begin{bmatrix} \grave{e}_1 = \langle x_1, 0.6, 0.7, 0.4, 0.2\rangle, \langle x_2, 0.7, 0.9, 0.4, 0.3\rangle \\ \langle x_3, 0.5, 0.8, 0.7, 0.3\rangle, \langle x_4, 0.8, 0.7, 0.5, 0.4\rangle \\ \grave{e}_2 = \langle x_1, 0.9, 0.8, 0.5, 0.4\rangle, \langle x_2, 0.7, 0.9, 0.6, 0.4\rangle, \\ \langle x_3, 0.9, 0.8, 0.5, 0.4\rangle, \langle x_4, 0.7, 0.7, 0.6, 0.3\rangle \end{bmatrix} = (\mathscr{F}_1, \check{E}) \in \tau_1.$$

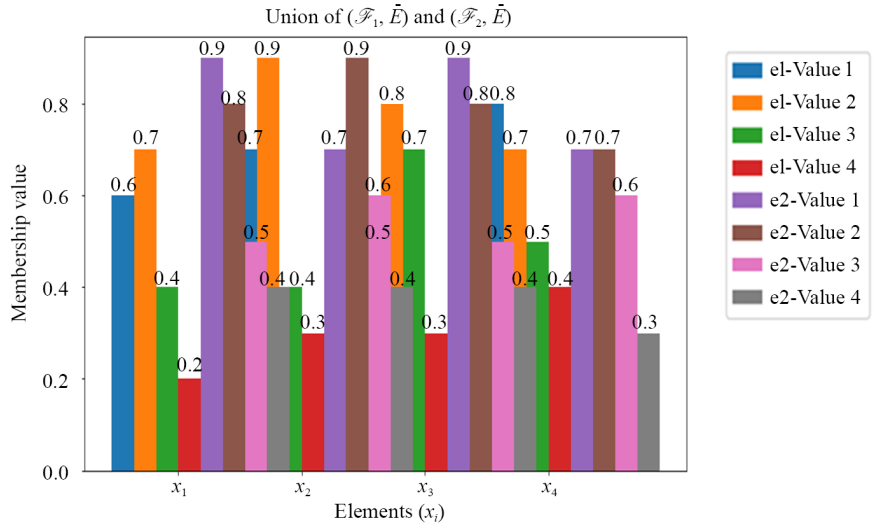


**Figure 13.** The union-based evaluation of $(\mathscr{F}_1, \check{E})$ and $(\mathscr{F}_2, \check{E})$ across targets $x_1$-$x_4$ are shown in Figure 13

$$(\mathscr{F}_2, \check{E}) \cup (\mathscr{F}_3, \check{E}) = \begin{bmatrix} \grave{e}_1 = \langle x_1, 0.7, 0.8, 0.4, 0.3\rangle, \langle x_2, 0.3, 0.6, 0.4, 0.6\rangle \\ \langle x_3, 0.6, 0.9, 0.7, 0.2\rangle, \langle x_4, 0.5, 0.2, 0.4, 0.7\rangle \\ \grave{e}_2 = \langle x_1, 0.4, 0.5, 0.8, 0.9\rangle, \langle x_2, 0.4, 0.9, 0.5, 0.4\rangle, \\ \langle x_3, 0.3, 0.4, 0.6, 0.3\rangle, \langle x_4, 0.5, 0.6, 0.7, 0.4\rangle \end{bmatrix} \neq (\mathscr{F}_2, \check{E}) \notin \tau_1.$$

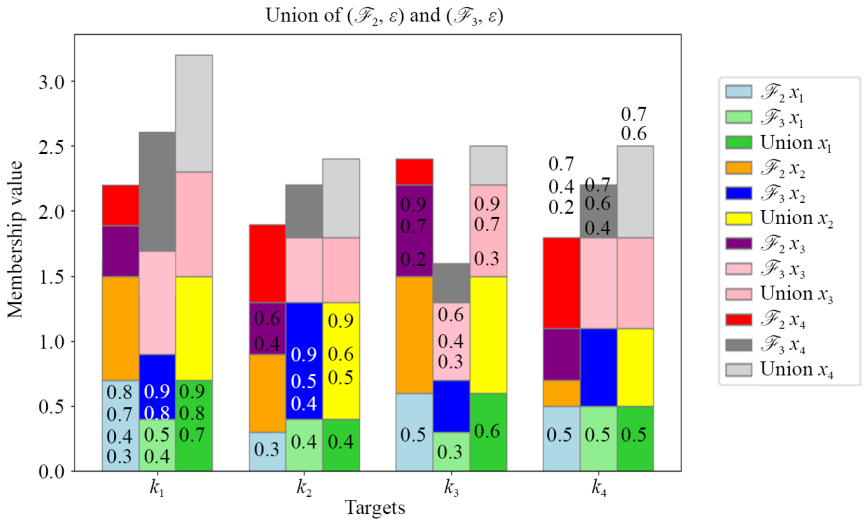


**Figure 14.** The union-based evaluation of $(\mathscr{F}_2, \check{E})$ and $(\mathscr{F}_3, \check{E})$ across targets $k_1$-$k_4$ are shown in Figure 14

$$(\mathscr{F}_1, \check{E}) \cap (\mathscr{F}_2, \check{E}) = \begin{bmatrix} \grave{e}_1 = \langle x_1, 0.7, 0.8, 0.4, 0.3\rangle, \langle x_2, 0.3, 0.6, 0.4, 0.6\rangle \\ \langle x_3, 0.6, 0.9, 0.7, 0.2\rangle, \langle x_4, 0.5, 0.2, 0.4, 0.7\rangle \\ \grave{e}_2 = \langle x_1, 0.4, 0.5, 0.8, 0.9\rangle, \langle x_2, 0.4, 0.9, 0.5, 0.4\rangle, \\ \langle x_3, 0.3, 0.4, 0.6, 0.3\rangle, \langle x_4, 0.5, 0.6, 0.7, 0.4\rangle \end{bmatrix} = (\mathscr{F}_2, \check{E}) \in \tau_1.$$

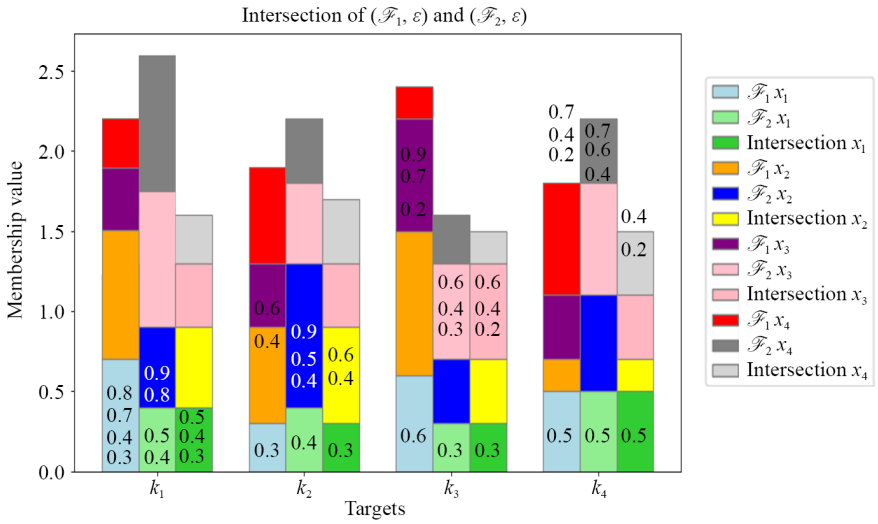


**Figure 15.** The intersection-based evaluation of $(\mathscr{F}_1, \check{E})$ and $(\mathscr{F}_2, \check{E})$ across targets $k_1$-$k_4$ are shown in Figure 15

$$(\mathscr{F}_2, \check{E}) \cap (\mathscr{F}_3, \check{E}) = \begin{bmatrix} \grave{e}_1 = \langle x_1, 0.7, 0.8, 0.6, 0.4\rangle, \langle x_2, 0.8, 0.7, 0.9, 0.5\rangle \\ \langle x_3, 0.8, 0.6, 0.4, 0.3\rangle, \langle x_4, 0.7, 0.9, 0.5, 0.4\rangle \\ \grave{e}_2 = \langle x_1, 0.7, 0.8, 0.6, 0.4\rangle, \langle x_2, 0.8, 0.7, 0.9, 0.5\rangle, \\ \langle x_3, 0.8, 0.6, 0.4, 0.3\rangle, \langle x_4, 0.7, 0.9, 0.5, 0.4\rangle \end{bmatrix} \neq (\mathscr{F}_3, \check{E}) \notin \tau_2.$$

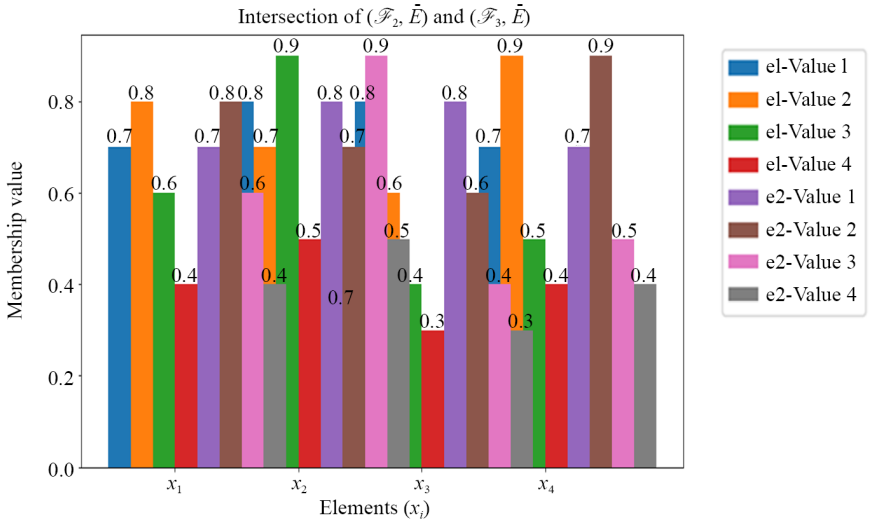


**Figure 16.** The intersection-based evaluation of $(\mathscr{F}_2, \check{E})$ and $(\mathscr{F}_3, \check{E})$ across targets $x_1$-$x_4$ are shown in Figure 16

Hence, $(\mathscr{F}_2, \check{E}) \cup (\mathscr{F}_3, \check{E}) \notin \tau_1^{\text{DNSS}} \cup \tau_2^{\text{DNSS}}$, then $\tau_1^{\text{DNSS}} \cup \tau_2^{\text{DNSS}}$ is not a DNS topology on $\mathbf{X}$.

Uses of DNSS for evaluating military targets with imprecise and unclear intelligence are shown in example 2. While unions, like in the example of $(\mathscr{F}_2, \check{E}) \cup (\mathscr{F}_3, \check{E})$, do not maintain DNST structure, intersections of intelligence reports do. This highlights a significant limitation: merging reports from many sources results in inconsistencies. Therefore, DNSS may only be useful for systematic evaluation in military applications, and great effort should be made to combine intelligence to ensure that decisions are trustworthy.

**Definition 28** If $(\mathscr{F}, \check{E}) \subseteq SS(\mathbf{X})_A$ and let $(\mathbf{X}, \tau^{\mathrm{DNSS}}, \check{E})$ be a DNSTS. If $(\mathscr{F}, \check{E}) \subseteq cl(int(\mathscr{F}, \check{E})) \cup int(cl(\mathscr{F}, \check{E}))$ then, $(\mathscr{F}, \check{E})$ is called a DNS b-open soft sets, and Bopen set $(\mathbf{X}, \tau, \check{E})$ or simply Bopen set $(\mathbf{X})$ represents the set of all Double Valued neutrosophic Set (QNS) b closed sets.

**Definition 29** Let a DNS topological space $(\mathbf{X}, \tau, \check{E})$ over $\mathbf{X}$ and a DNS set $(\mathscr{F}, \check{E}) \in \mathrm{DNSS}(\mathbf{X}, \check{E})$. Next, $(\mathscr{F}, \check{E})$'s DNS interior, represented as $(\mathscr{F}, \check{E})^\circ$ is defined as the DNS union of all of $(\mathscr{F}, \check{E})$'s DNS open subsets. $(\mathscr{F}, \check{E})^\circ$ is evident. $(\mathscr{F}, \check{E})$ contains, the largest DNS open set.

**Theorem 1** If $(\mathbf{X}, \tau, \check{E})$ be a DNS topological space over $\mathbf{X}$ and $(\mathscr{F}, \check{E}) \in \mathrm{DNSS}(\mathbf{X}, \check{E})$. $(\mathscr{F}, \check{E})$ is a DNS b-open set and if and only if $(\mathscr{F}, \check{E}) = (\mathscr{F}, \check{E})^\circ$.

**Proof.** Let the DNS b-open set $(\mathscr{F}, \check{E})$. Then $(\mathscr{F}, \check{E})$ equals $(\mathscr{F}, \check{E})$, which is the largest DNS b-open set contained by $(\mathscr{F}, \check{E})$. It follows that $(\mathscr{F}, \check{E}) = (\mathscr{F}, \check{E})^\circ$.

Conversely, $(\mathscr{F}, \check{E}) = (\mathscr{F}, \check{E})^\circ$, then $(\mathscr{F}, \check{E})$ is a DNS b-open set, then $(\mathscr{F}, \check{E})^\circ$ is a DNS b-open set. □

**Theorem 2** Let DNS topological space $(\mathbf{X}, \tau, \check{E})$ over $\mathbf{X}$. Then $(\mathscr{F}_1, \check{E}), (\mathscr{F}_2, \check{E}) \in \mathrm{DNSS}(\mathbf{X}, \check{E})$. Next,

1. $[(\mathscr{F}, \check{E})^\circ]^\circ = (\mathscr{F}, \check{E})^\circ$,
2. $(0_{(\mathbf{X}, \check{E})})^\circ = 0_{(\mathbf{X}, \check{E})}$ and $(1_{(\mathbf{X}, \check{E})})^\circ = 1_{(\mathbf{X}, \check{E})}$,
3. $(\mathscr{F}_1, \check{E}) \subseteq (\mathscr{F}_2, \check{E}) \Rightarrow (\tilde{F}_1, \check{E})^\circ \subseteq (\mathscr{F}_2, \check{E})^\circ$,
4. $[(\mathscr{F}_1, \check{E}) \cap (\mathscr{F}_2, \check{E})]^\circ = (\mathscr{F}_1, \check{E})^\circ \cap (\mathscr{F}_2, \check{E})^\circ$,
5. $(\mathscr{F}_1, \check{E})^\circ \cup (\mathscr{F}_2, \check{E})^\circ \subseteq [(\mathscr{F}_1, \check{E}) \cup (\mathscr{F}_2, \check{E})]^\circ$.

**Proof.** 1. If $(\mathscr{F}_1, \check{E})$ is DNS b-open, then by definition: $(\mathscr{F}, \check{E})^\circ = (\mathscr{F}, \check{E})$. Suppose $(\mathscr{F}, \check{E}) = (\mathscr{G}, \check{E})$. Since $(\mathscr{F}, \check{E})^\circ$ is the largest DNS b-open subset and $(\mathscr{F}, \check{E})$ and $(\mathscr{G}, \check{E})$ is equal to this interior, it fallow that:

$$(\mathscr{G}, \check{E})^\circ = (\mathscr{G}, \check{E}).$$

That is DNS b-open by definition, hence by construction of $(\mathscr{F}, \check{E})^\circ = (\mathscr{G}, \check{E})$.

So, in particular, we conclude:

$$[(\mathscr{F}_1, \check{E})^\circ]^\circ = (\mathscr{F}_1, \check{E})^\circ.$$

2. Since $0_{(\mathbf{X}, \check{E})}$ and $1_{(\mathbf{X}, \check{E})}$ are always DNS b-open sets, we have:

$$(0_{(\mathbf{X}, \check{E})})^\circ = 0_{(\mathbf{X}, \check{E})}, \quad \text{and} \quad (1_{(\mathbf{X}, \check{E})})^\circ = 1_{(\mathbf{X}, \check{E})}.$$

3. As, $(\mathscr{F}_1, \check{E})^\circ \subseteq (\mathscr{F}_1, \check{E}) \subseteq (\mathscr{F}_2, \check{E})$ and $(\mathscr{F}_2, \check{E})^\circ \subseteq (\mathscr{F}_2, \check{E})$. Since $(\mathscr{F}_2, \check{E})^\circ$ is the largest DNS b-open set contained in $(\mathscr{F}_2, \check{E})$ and so $(\mathscr{F}_1, \check{E})^\circ \subseteq (\mathscr{F}_2, \check{E})^\circ$.

4. Since $(\mathscr{F}_1, \check{E}) \cap (\mathscr{F}_2, \check{E}) \subseteq (\mathscr{F}_1, \check{E})$ and $(\mathscr{F}_1, \check{E}) \cap (\mathscr{F}_2, \check{E}) \subseteq (\mathscr{F}_2, \check{E})$, then $[(\mathscr{F}_1, \check{E}) \cap (\mathscr{F}_2, \check{E})]^\circ \subseteq (\mathscr{F}_1, \check{E})^\circ$ and $[(\mathscr{F}_1, \check{E}) \cap (\mathscr{F}_2, \check{E})]^\circ \subseteq (\mathscr{F}_2, \check{E})^\circ$ and so,

$$[(\mathscr{F}_1, \check{E}) \cap (\mathscr{F}_2, \check{E})]^\circ \subseteq (\mathscr{F}_1, \check{E})^\circ \cap (\mathscr{F}_2, \check{E})^\circ.$$

However, given that $(\mathscr{F}_1, \check{E})^\circ \subseteq (\mathscr{F}_1, \check{E})$ and $(\mathscr{F}_2, \check{E})^\circ \subseteq (\mathscr{F}_2, \check{E})$, then:

$$(\mathscr{F}_1, \check{E})^\circ \cap (\mathscr{F}_2, \check{E})^\circ \subseteq (\mathscr{F}_1, \check{E}) \cap (\mathscr{F}_2, \check{E}).$$

Besides, $[(\mathscr{F}_1, \check{E}) \cap (\mathscr{F}_2, \check{E})]^\circ \subseteq (\mathscr{F}_1, \check{E}) \cap (\mathscr{F}_2, \check{E})$ and is the largest DNS b-open set. Therefore, $(\mathscr{F}_1, \check{E})^\circ \cap (\mathscr{F}_2, \check{E})^\circ \subseteq [(\mathscr{F}_1, \check{E}) \cap (\mathscr{F}_2, \check{E})]^\circ$. Thus, $[(\mathscr{F}_1, \check{E}) \cap (\mathscr{F}_2, \check{E})]^\circ = (\mathscr{F}_1, \check{E})^\circ \cap (\mathscr{F}_2, \check{E})^\circ$.

5. Since $(\mathscr{F}_1, \check{E}) \subseteq (\mathscr{F}_1, \check{E}) \cup (\mathscr{F}_2, \check{E})$ and $(\mathscr{F}_2, \check{E}) \subseteq (\mathscr{F}_1, \check{E}) \cup (\mathscr{F}_2, \check{E})$, then:

$$(\mathscr{F}_1, \check{E})^\circ \subseteq [(\mathscr{F}_1, \check{E}) \cup (\mathscr{F}_2, \check{E})]^\circ, \quad \text{and} \quad (\mathscr{F}_2, \check{E})^\circ \subseteq [(\mathscr{F}_1, \check{E}) \cup (\mathscr{F}_2, \check{E})]^\circ.$$

Therefore,

$$(\mathscr{F}_1, \check{E})^\circ \cup (\mathscr{F}_2, \check{E})^\circ \subseteq [(\mathscr{F}_1, \check{E}) \cup (\mathscr{F}_2, \check{E})]^\circ.$$

□

**Definition 30** Consider a DNS topological space $(\mathbf{X}, \tau^{\text{DNSS}}, \check{E})$ over $\mathbf{X}$ and a DNS set $(\mathscr{F}, \check{E}) \in \text{DNSS}(\mathbf{X}, \check{E})$. The DNS intersection of all the DNS closed supersets of $(\mathscr{F}, \check{E})$ is then the DNS closure of $(\mathscr{F}, \check{E})$, denoted by $\overline{(\mathscr{F}, \check{E})}$. Clearly, the smallest DNS closed set that contains $(\mathscr{F}, \check{E})$ is $\overline{(\mathscr{F}, \check{E})}$.

**Theorem 3** Let $(\mathbf{X}, \tau, \check{E})$ be a DNS topological space over $\mathbf{X}$ and $(\mathscr{F}, \check{E}) \in \text{DNSS}(\mathbf{X}, \check{E})$. $(\mathscr{F}, \check{E})$ is a DNS closed set and if and only if $(\mathscr{F}, \check{E}) = \overline{(\mathscr{F}, \check{E})}$.

**Proof.** Suppose $(\mathscr{F}, \check{E})$ be a DNS closed set. Then the smallest DNS open set that containing $(\mathscr{F}, \check{E})$ is equal to $(\mathscr{F}, \check{E})$. Hence, $(\mathscr{F}, \check{E}) = \overline{(\mathscr{F}, \check{E})}$, it is recognized that $\overline{(\mathscr{F}, \check{E})}$ is a DNS closed set and if $(\mathscr{F}, \check{E}) = \overline{(\mathscr{F}, \check{E})}$, so $(\mathscr{F}, \check{E})$ is a DNS closed set. □

**Theorem 4** Let $(\mathbf{X}, \tau, \check{E})$ is DNS topological space over $\mathbf{X}$. Then $(\mathscr{F}_1, \check{E})$, $(\mathscr{F}_2, \check{E}) \in \text{DNSS}(\mathbf{X}, \check{E})$. So,

1. $\overline{[\overline{(\mathscr{F}, \check{E})}]} = \overline{(\mathscr{F}, \check{E})}$,
2. $\overline{(0_{(\mathbf{X}, \check{E})})} = 0_{(\mathbf{X}, \check{E})}$ and $\overline{(1_{(\mathbf{X}, \check{E})})} = 1_{(\mathbf{X}, \check{E})}$,
3. $(\mathscr{F}_1, \check{E}) \subseteq (\mathscr{F}_2, \check{E}) \Rightarrow \overline{(\mathscr{F}_1, \check{E})} \subseteq \overline{(\mathscr{F}_2, \check{E})}$,
4. $\overline{[(\mathscr{F}_1, \check{E}) \cup (\mathscr{F}_2, \check{E})]} = \overline{(\mathscr{F}_1, \check{E})} \cup \overline{(\mathscr{F}_2, \check{E})}$,
5. $(\mathscr{F}_1, \check{E}) \cap \overline{(\mathscr{F}_2, \check{E})} \subseteq [(\mathscr{F}_1, \check{E}) \cap (\mathscr{F}_2, \check{E})]$.

**Proof.** 1. Let $(\mathscr{F}_1, \check{E}) = (\mathscr{F}_2, \check{E})$ Then $(\mathscr{F}_2, \check{E})$ a DNS closed set. Hence $(\mathscr{F}_2, \check{E})$ and $\overline{(\mathscr{F}_2, \check{E})}$ are equal. Therefore $\overline{[\overline{(\mathscr{F}_1, \check{E})}]} = \overline{(\mathscr{F}_1, \check{E})}$.

2. Since $0_{(\mathbf{X}, \check{E})}$ and $1_{(\mathbf{X}, \check{E})}$ are always DNS closed sets, we have:

$$\overline{(0_{(\mathbf{X}, \check{E})})} = 0_{(\mathbf{X}, \check{E})}, \quad \text{and} \quad \overline{(1_{(\mathbf{X}, \check{E})})} = 1_{(\mathbf{X}, \check{E})}.$$

3. It is known that $(\mathscr{F}_1, \check{E}) \subseteq \overline{(\mathscr{F}_1, \check{E})}$ and $(\mathscr{F}_2, \check{E}) \subseteq \overline{(\mathscr{F}_2, \check{E})}$, so $(\mathscr{F}_1, \check{E}) \subseteq (\mathscr{F}_2, \check{E}) \subseteq \overline{(\mathscr{F}_2, \check{E})}$. Since $\overline{(\mathscr{F}_2, \check{E})}$ is the smallest DNS closed set containing $(\mathscr{F}_1, \check{E})$, then $\overline{(\mathscr{F}_1, \check{E})} \subseteq (\mathscr{F}_2, \check{E})$.

4. Since $(\mathscr{F}_1, \check{E}) \subseteq (\mathscr{F}_1, \check{E}) \cup (\mathscr{F}_2, \check{E})$ and $(\mathscr{F}_2, \check{E}) \subseteq (\mathscr{F}_1, \check{E}) \cup (\mathscr{F}_2, \check{E})$, then $\overline{(\mathscr{F}_1, \check{E})} \subseteq \overline{[(\mathscr{F}_1, \check{E}) \cup (\mathscr{F}_2, \check{E})]}$ and $\overline{(\mathscr{F}_2, \check{E})} \subseteq \overline{[(\mathscr{F}_1, \check{E}) \cup (\mathscr{F}_2, \check{E})]}$ and so,

$$\overline{(\mathscr{F}_1, \check{E})} \cup \overline{(\mathscr{F}_2, \check{E})} \subseteq \overline{[(\mathscr{F}_1, \check{E}) \cup (\mathscr{F}_2, \check{E})]}.$$

Conversely, since $(\mathscr{F}_1,\ \check{E}) \subseteq \overline{(\mathscr{F}_1,\ \check{E})}$ and $(\mathscr{F}_2,\ \check{E}) \subseteq \overline{(\mathscr{F}_2,\ \check{E})}$, then:

$$(\mathscr{F}_1,\ \check{E}) \cup (\mathscr{F}_2,\ \check{E}) \subseteq \overline{(\mathscr{F}_1,\ \check{E})} \cup \overline{(\mathscr{F}_2,\ \check{E})}.$$

Besides, $\overline{[(\mathscr{F}_1,\ \check{E}) \cup (\mathscr{F}_2,\ \check{E})]}$ and is the smallest DNS closed set that containing $(\mathscr{F}_1,\ \check{E}) \cup (\mathscr{F}_2,\ \check{E})$. Therefore, $\overline{[(\mathscr{F}_1,\ \check{E}) \cup (\mathscr{F}_2,\ \check{E})]} \subseteq \overline{(\mathscr{F}_1,\ \check{E})} \cup \overline{(\mathscr{F}_2,\ \check{E})}$. Thus, $\overline{[(\mathscr{F}_1,\ \check{E}) \cup (\mathscr{F}_2,\ \check{E})]} = \overline{(\mathscr{F}_1,\ \check{E})} \cup \overline{(\mathscr{F}_2,\ \check{E})}$.

5. Since

$$(\mathscr{F}_1,\ \check{E}) \cap (\mathscr{F}_2,\ \check{E}) \subseteq \overline{[(\mathscr{F}_1,\ \check{E}) \cap (\mathscr{F}_2,\ \check{E})]}, \quad \text{and} \quad \overline{[(\mathscr{F}_1,\ \check{E}) \cap (\mathscr{F}_2,\ \check{E})]}.$$

is the smallest DNS closed set that containing $(\mathscr{F}_1,\ \check{E}) \cap (\mathscr{F}_2,\ \check{E})$. Then,

$$\overline{[(\mathscr{F}_1,\ \check{E}) \cap (\mathscr{F}_2,\ \check{E})]} \subseteq \overline{(\mathscr{F}_1,\ \check{E})} \cap \overline{(\mathscr{F}_2,\ \check{E})}.$$

□

**Definition 31** Let $(\mathbf{X},\ \tau^{\mathrm{DNSS}},\ \check{E})$ be a DNSTS over $\mathbf{X}$, and let $\mathbf{x}^{\acute{\epsilon}}_{(\hat{s}_1,\ \hat{s}_2,\ \hat{s}_3,\ \hat{s}_4)}$ and $\mathbf{y}^{\acute{\epsilon}}_{(\hat{s}_1,\ \hat{s}_2,\ \hat{s}_3,\ \hat{s}_4)}$ be distinct DNSS points. If there exist DNS b-open sets $(\mathscr{F},\ \check{E})$ and $(\mathscr{G},\ \check{E})$ such that

$$\mathbf{x}^{\acute{\epsilon}}_{(\hat{s}_1,\ \hat{s}_2,\ \hat{s}_3,\ \hat{s}_4)} \in (\mathscr{F},\ \check{E}) \quad \text{and} \quad \mathbf{x}^{\acute{\epsilon}}_{(\hat{s}_1,\ \hat{s}_2,\ \hat{s}_3,\ \hat{s}_4)} \cap (\mathscr{G},\ \check{E}) = 0_{(\mathbf{X},\ \check{E})},$$

or

$$\mathbf{y}^{\acute{\epsilon}}_{(\hat{s}_1,\ \hat{s}_2,\ \hat{s}_3,\ \hat{s}_4)} \in (\mathscr{G},\ \check{E}) \quad \text{and} \quad \mathbf{y}^{\acute{\epsilon}}_{(\hat{s}_1,\ \hat{s}_2,\ \hat{s}_3,\ \hat{s}_4)} \cap (\mathscr{F},\ \check{E}) = 0_{(\mathbf{X},\ \check{E})},$$

then $(\mathbf{X},\ \tau^{\mathrm{DNSS}},\ \check{E})$ is called a DNSS $T_0$-space.

**Definition 32** Let $(\mathbf{X},\ \tau^{\mathrm{DNSS}},\ \check{E})$ be a DNSTS over $\mathbf{X}$, and let $\mathbf{x}^{\acute{\epsilon}}_{(\hat{s}_1,\ \hat{s}_2,\ \hat{s}_3,\ \hat{s}_4)}$ and $\mathbf{y}^{\acute{\epsilon}}_{(\hat{s}_1,\ \hat{s}_2,\ \hat{s}_3,\ \hat{s}_4)}$ be distinct DNSS points. If there exist DNS b-open sets $(\mathscr{F},\ \check{E})$ and $(\mathscr{G},\ \check{E})$ such that

$$\mathbf{x}^{\acute{\epsilon}}_{(\hat{s}_1,\ \hat{s}_2,\ \hat{s}_3,\ \hat{s}_4)} \in (\mathscr{F},\ \check{E}) \quad \text{and} \quad \mathbf{x}^{\acute{\epsilon}}_{(\hat{s}_1,\ \hat{s}_2,\ \hat{s}_3,\ \hat{s}_4)} \cap (\mathscr{G},\ \check{E}) = 0_{(\mathbf{X},\ \check{E})},$$

or

$$\mathbf{y}^{\acute{\epsilon}}_{(\hat{s}_1,\ \hat{s}_2,\ \hat{s}_3,\ \hat{s}_4)} \in (\mathscr{G},\ \check{E}) \quad \text{and} \quad \mathbf{y}^{\acute{\epsilon}}_{(\hat{s}_1,\ \hat{s}_2,\ \hat{s}_3,\ \hat{s}_4)} \cap (\mathscr{F},\ \check{E}) = 0_{(\mathbf{X},\ \check{E})},$$

then $(\mathbf{X},\ \tau^{\mathrm{DNSS}},\ \check{E})$ is called a DNSS $T_1$-space.

**Definition 33** Let $(\mathbf{X},\ \tau^{\mathrm{DNSS}},\ \check{E})$ be a DNSTS over $\mathbf{X}$, and let $\mathbf{x}^{\acute{\epsilon}}_{(\hat{s}_1,\ \hat{s}_2,\ \hat{s}_3,\ \hat{s}_4)}$ and $\mathbf{y}^{\acute{\epsilon}}_{(\hat{s}_1,\ \hat{s}_2,\ \hat{s}_3,\ \hat{s}_4)}$ be distinct DNSS points. If there exist DNS b-open sets $(\mathscr{F},\ \check{E})$ and $(\mathscr{G},\ \check{E})$ such that

$$\mathbf{x}^{\acute{\epsilon}}_{(\hat{s}_1,\ \hat{s}_2,\ \hat{s}_3,\ \hat{s}_4)} \in (\mathscr{F},\ \check{E}),\ \mathbf{y}^{\acute{\epsilon}}_{(\hat{s}_1,\ \hat{s}_2,\ \hat{s}_3,\ \hat{s}_4)} \in (\mathscr{G},\ \check{E}).$$

And

$$(\mathscr{F},\ \check{E}) \cap (\mathscr{G},\ \check{E}) = 0_{(\mathbf{X},\ \check{E})},$$

then $(\mathbf{X},\ \tau^{\mathrm{DNSS}},\ \check{E})$ is called a DNSS $T_2$-space.

**Definition 34** Let $(\mathbf{X},\ \tau^{\mathrm{DNSS}},\ \check{E})$ be a DNSTS over $\mathbf{X}$, $(\mathscr{F},\ \check{E})$ be a DNSS closed set, and

$$\mathbf{x}^{\acute{\acute{e}}}_{(\hat{s}_1,\ \hat{s}_2,\ \hat{s}_3,\ \hat{s}_4)} \cap (\mathscr{F},\ \check{E}) = 0_{(\mathbf{X},\ \check{E})}$$

If there exist DNS b-open sets $(\mathscr{G}_1,\ \check{E})$ and $(\mathscr{G}_2,\ \check{E})$ such that

$$\mathbf{x}^{\acute{\acute{e}}}_{(\hat{s}_1,\ \hat{s}_2,\ \hat{s}_3,\ \hat{s}_4)} \in (\mathscr{G}_1,\ \check{E}),\ (\mathscr{F},\ \check{E}) \subset (\mathscr{G}_2,\ \check{E}),$$

and

$$(\mathscr{G}_1,\ \check{E}) \cap (\mathscr{G}_2,\ \check{E}) = 0_{(\mathbf{X},\ \check{E})}.$$

Then $(\mathbf{X},\ \tau^{\mathrm{DNSS}},\ \check{E})$ is called a DNS regular space. $(\mathbf{X},\ \tau^{\mathrm{DNSS}},\ \check{E})$ is said to be a DNS $T_3$ space if it is both DNS regular and a DNS $T_1$ space.

**Definition 35** A QNSTS $(\mathbf{X},\ \tau^{\mathrm{DNSS}},\ \check{E})$ over $\mathbf{X}$ is called a DNS normal space if for every pair of disjoint DNS closed sets

$$(\mathscr{F}_1,\ \check{E}),\ \ (\mathscr{F}_2,\ \check{E}),$$

there exist disjoint DNS open sets $(\mathscr{G}_1,\ \check{E})$ and $(\mathscr{G}_2,\ \check{E})$ such that

$$(\mathscr{G}_1,\ \check{E}) \subset (\mathscr{G}_2,\ \check{E}) \quad \text{and} \quad (\mathscr{F}_2,\ \check{E}) \subset (\mathscr{G}_2,\ \check{E}).$$

Then $(\mathbf{X},\ \tau^{\mathrm{DNSS}},\ \check{E})$ is said to be a DNS $T_4$ space if it is DNS normal.

**Proposition 5** Let $(\mathbf{Y},\ \tau_{\mathbf{Y}}^{\mathrm{DNSS}},\ \check{E})$ be a soft subspace of a DNSTS $(\mathbf{X},\ \tau^{\mathrm{DNSS}},\ \check{E})$ and $(\mathscr{F},\ \check{E}) \in SS(\mathbf{X})$. Then $(\mathscr{F},\ \check{E})$ satisfies:

1. If $(\mathscr{F},\ \check{E})$ is DNS b-open set in $\mathbf{Y}$ and $\mathbf{Y} \in \tau^{\mathrm{DNSS}}$, then $(\mathscr{F},\ \check{E}) \in \tau^{\mathrm{DNSS}}$.
2. $(\mathscr{F},\ \check{E})$ is DNS b-open set in $\mathbf{Y}$ iff $(\mathscr{F},\ \check{E}) = \mathbf{Y} \cap (\mathscr{G}^{\alpha},\ \check{E})$ for some $(\mathscr{G},\ \check{E}) \in \tau$.
3. $(\mathscr{F},\ \check{E})$ is DNS b close set in $\mathbf{Y}$ iff $(\mathscr{F},\ \check{E}) = \mathbf{Y} \cap (\hat{H},\ \check{E})$ for some $(\hat{H},\ \check{E})$ that is $\tau^{\mathrm{DNSS}}$ soft $b$ close set.

**Proof.** (1) Assume that $(\mathscr{F},\ \check{E})$ is DNS b-open set in $\mathbf{Y}$. Then there exists a DNS b-open set $(\mathscr{G}^{\alpha},\ \check{E})$ in $\mathbf{X}$ such that

$$(\mathscr{F},\ \check{E}) = \mathbf{Y} \cap (\mathscr{G}^{\alpha},\ \check{E}).$$

Now, if $\mathbf{Y} \in \tau^{\mathrm{DNSS}}$, then $\mathbf{Y} \cap (\mathscr{G}^{\alpha},\ \check{E}) \in \tau^{\mathrm{DNSS}}$. Hence $(\mathscr{F},\ \check{E}) \in \tau^{\mathrm{DNSS}}$.

(2) Obvious.

(3) If $(\mathscr{F}, \check{E})$ is DNS b close set in $\mathbf{Y}$, then $(\mathscr{F}, \check{E}) = \mathbf{Y} \setminus (\mathscr{G}^{\alpha}, \check{E})$ for $(\mathscr{G}^{\alpha}, \check{E}) \in \tau_{\mathbf{Y}}^{\mathrm{DNSS}}$. Now, $(\mathscr{G}^{\alpha}, \check{E}) = \mathbf{Y} \cap (\hat{H}, \check{E})$ for QNS b-open set $(\hat{H}, \check{E}) \in \tau^{\mathrm{DNSS}}$. For any $\alpha \in \check{E}$,

$$\mathscr{F}(\alpha) = \mathbf{Y}(\alpha) \setminus \mathscr{G}^{\alpha}(\alpha) = \mathbf{Y}(\alpha) \setminus (\mathbf{Y}(\alpha) \cap \hat{H}(\alpha)) = \mathbf{Y}(\alpha) \cap (\mathbf{X} \setminus \hat{H}(\alpha)) = \mathbf{Y}(\alpha) \cap \left(\hat{H}(\alpha)^{c}\right),$$

$$= \mathbf{Y} \cap (\mathbf{X} \setminus \hat{H}(\alpha)) = \mathbf{Y} \cap \hat{H}(\alpha)^{c} = \mathbf{Y}(\alpha) \cap \left(\hat{H}(\alpha)^{c}\right).$$

Thus $(\mathscr{F}, \check{E}) = \mathbf{Y} \cap (\hat{H}, \check{E})$ is DNS b-close in $\mathbf{X}$ as $(\hat{H}, \check{E}) \in \tau^{\mathrm{DNSS}}$.

Conversely, if $(\mathscr{F}, \check{E}) = \mathbf{Y} \cap (\mathscr{G}^{\alpha}, \check{E})$ for DNS b-close set $(\mathscr{G}^{\alpha}, \check{E})$ in $\mathbf{X} \Rightarrow (\mathscr{G}^{\alpha}, \check{E}) \in \tau^{\mathrm{DNSS}}$. Now if $(\mathscr{G}^{\alpha}, \check{E}) = (\mathbf{X}, \check{E}) \setminus (\hat{H}, \check{E})$ where $(\hat{H}, \check{E})$ is soft b-open set in $\tau$ then for any $\alpha \in \check{E}$

$$\mathscr{F}(\alpha) = \mathbf{Y}(\alpha) \cap \mathscr{G}^{\alpha}(\alpha) = \mathbf{Y} \cap \mathscr{G}^{\alpha}(\alpha) = \mathbf{Y} \cap \left((\mathbf{X}(\alpha) \setminus \hat{H}(\alpha)) = \mathbf{Y} \cap \mathbf{X}(\alpha)\hat{H}(\alpha)^{c}\right)$$

$$= \mathbf{Y} \cap (\mathbf{X}(\alpha) \setminus \hat{H}(\alpha))\mathbf{Y} \setminus \hat{H}(\alpha) = \mathbf{Y} \setminus (\mathbf{Y} \cap \hat{H}(\alpha)) = \mathbf{Y}(\alpha) \setminus \mathbf{Y}(\alpha) \cap \hat{H}(\alpha).$$

Thus $(\mathscr{F}, \check{E}) = \mathbf{Y} \setminus (\mathbf{Y} \cap (\hat{H}, \check{E}))$. Since $(\hat{H}, \check{E}) \in \tau^{\mathrm{DNSS}}$ so, $\mathbf{Y} \cap (\hat{H}, \check{E}) \in \tau^{\mathrm{DNSS}}$.

$\mathbf{Y} \cap (\hat{H}, \check{E}) \in \tau_{\mathbf{Y}}^{\mathrm{DNSS}}$ and hence $(\mathscr{F}, \check{E})$ is DNS b-close set in $\mathbf{Y}$. □

**Proposition 6** Assume that $(\mathbf{X}, \tau_1^{\mathrm{DNSS}}, \tau_2^{\mathrm{DNSS}}, \check{E})$ is Double Valued Neutrosophic Soft Bi-topological Space (DNSBTS). Then, if $(\mathbf{X}, \tau_1^{\mathrm{DNSS}}, \check{E})$ and $(\mathbf{X}, \tau_2^{\mathrm{DNSS}}, \check{E})$ are DNS b $T_3$ then $(\mathbf{X}, \tau_1^{\mathrm{DNSS}}, \tau_2^{\mathrm{DNSS}}, \check{E})$ is a pair wise DNS b $T_2$.

**Proof.** Suppose $(\mathbf{X}, \tau_1^{\mathrm{DNSS}}, \check{E})$ is DNS b $T_3$ with respect to $(\mathbf{X}, \tau_2^{\mathrm{DNSS}}, \check{E})$, then for $x, y \in \mathbf{X}, x \neq y$, $(\mathbf{Y}, \check{E})$ is DNS b close set in $\tau_2$, $x \notin (\mathbf{Y}, \check{E})$, $\exists\, \tau_1^{\mathrm{DNSS}}$ DNS b-open set $(\mathscr{F}, \check{E})$ and $\tau_2^{\mathrm{DNSS}}$ DNS b-open set $(\mathscr{F}, \check{E})$ such that $x \in (\mathscr{F}, \check{E})$, $y \in (\mathbf{Y}, \check{E}) \subseteq (\mathscr{G}^{\alpha}, \check{E})$ and $(\mathscr{F}, \check{E}) \cap (\mathscr{F}, \check{E}) = \phi$. Hence $\tau_1$ is DNS b $T_2$ with respect to $\tau_2^{\mathrm{DNSS}}$. Similarly, if $(\mathbf{X}, \tau_2^{\mathrm{DNSS}}, \check{E})$ is DNS b $T_3$ with respect to $(\mathbf{X}, \tau_1^{\mathrm{DNSS}}, \check{E})$, then for $x, y \in \mathbf{X}, x \neq y$, $(x, \check{E})$ is DNS b close set in $\tau_1^{\mathrm{DNSS}}$ and $y \notin (x, \check{E})$, $\exists\, \tau_2^{\mathrm{DNSS}}$ DNS b-open set $(\mathscr{F}, \check{E})$ and $\tau_1^{\mathrm{DNSS}}$ DNS b-open set $(\mathscr{G}^{\alpha}, \check{E})$ such that $y \in (\mathscr{F}, \check{E})$ and $(\mathscr{F}, \check{E}) \cap (\mathscr{F}, \check{E}) = \phi$. Hence $\tau_2^{\mathrm{DNSS}}$ is DNS b $T_2$, which implies $(\mathbf{X}, \tau_1^{\mathrm{DNSS}}, \tau_2^{\mathrm{DNSS}}, \check{E})$ is pair wise DNS b $T_2$. □

**Proposition 7** Let $(\mathbf{X}, \tau_1^{\mathrm{DNSS}}, \tau_2^{\mathrm{DNSS}}, \check{E})$ be DNSBTS. If $(\mathbf{X}, \tau_1^{\mathrm{DNSS}}, \check{E})$ and $(\mathbf{X}, \tau_2^{\mathrm{DNSS}}, \check{E})$ are DNS b $T_3$, then $(\mathbf{X}, \tau_1^{\mathrm{DNSS}}, \tau_2^{\mathrm{DNSS}}, \check{E})$ is a pair wise QNS b $T_3$.

**Proof.** Suppose $(\mathbf{X}, \tau_1^{\mathrm{DNSS}}, \check{E})$ is DNS b $T_3$ with respect to $(\mathbf{X}, \tau_2^{\mathrm{DNSS}}, \check{E})$; then for $x, y \in \mathbf{X}, x \neq y$, $\exists\, \tau_1$ DNS b-open set $(\mathscr{F}, \check{E})$ and a $\tau_2^{\mathrm{DNSS}}$ DNS b-open set $(\mathscr{G}^{\alpha}, \check{E})$ such that $x \in (\mathscr{F}, \check{E}), y \notin (\mathscr{F}, \check{E})$ or $y \in (\mathscr{G}^{\alpha}, \check{E}), x \notin (\mathscr{G}^{\alpha}, \check{E})$, and $\exists\, \tau_1^{\mathrm{DNSS}}$ DNS b-open set $(\mathscr{G}^{\alpha}, \check{E})$ such that $(\mathscr{F}, \check{E}) \cap (\mathscr{F}, \check{E}) = \phi$. Similarly, $(\mathbf{X}, \tau_2^{\mathrm{DNSS}}, \check{E})$ is DNS b $T_3$ with respect to $(\mathbf{X}, \tau_1^{\mathrm{DNSS}}, \check{E})$, then for $x, y \in \mathbf{X}, x \neq y$, $\exists\, \tau_1$ QNSb-open set $(\mathscr{F}, \check{E})$ and $\tau_2^{\mathrm{DNSS}}$ DNS b-open set $(\mathscr{F}, \check{E})$ such that $x \in (\mathscr{F}, \check{E}), y \notin (\mathscr{F}, \check{E})$ or $y \in (\mathscr{G}^{\alpha}, \check{E}), x \notin (\mathscr{G}^{\alpha}, \check{E})$. Thus for each $x \in \mathbf{X}$, $\tau_2^{\mathrm{DNSS}}$ DNS b close set $(\mathscr{F}, \check{E})$ and $(\mathscr{F}, \check{E}) \cap (\mathscr{F}, \check{E}) = \phi$. Hence, $(\mathbf{X}, \tau_1^{\mathrm{DNSS}}, \tau_2^{\mathrm{DNSS}}, \check{E})$ is pair wise DNS b $T_3$. □

**Proposition 8** If $(\mathbf{X}, \tau_1^{\mathrm{DNSS}}, \tau_2^{\mathrm{DNSS}}, \check{E})$ be DNSBTS; if $(\mathbf{X}, \tau_1^{\mathrm{DNSS}}, \check{E})$ and $(\mathbf{X}, \tau_2^{\mathrm{DNSS}}, \check{E})$ are DNSB $T_4$ spaces then $(\mathbf{X}, \tau_1^{\mathrm{DNSS}}, \tau_2^{\mathrm{DNSS}}, \check{E})$ is pair wise DNSB $T_4$.

**Proof.** Suppose $(\mathbf{X}, \tau_1^{\mathrm{DNSS}}, \check{E})$ is DNSB $T_4$ with respect to $(\mathbf{X}, \tau_2^{\mathrm{DNSS}}, \check{E})$. Then for $x, y \in \mathbf{X}, x \neq y$, $\exists\, \tau_1^{\mathrm{DNSS}}$ DNS b-open set $(\mathscr{F}, \check{E})$ and a $\tau_2^{\mathrm{DNSS}}$ DNS b-open set $(\mathscr{F}, \check{E})$ such that $x \in (\mathscr{F}, \check{E}), y \notin (\mathscr{G}^{\alpha}, \check{E})$ and for each $\tau_1^{\mathrm{DNSS}}$ DNS b close set $(\mathscr{F}, \check{E})$ and $(\mathscr{G}^{\alpha}, \check{E})$, $(\mathscr{F}, \check{E}) \cap (\mathscr{F}, \check{E}) = \varnothing$. There exist $(\mathscr{F}_3, \check{E})$ and $(\mathscr{G}_1^{\alpha}, \check{E})$ such that $(\mathscr{F}_3, \check{E})$ is DNS b $\tau_2^{\mathrm{DNSS}}$ open set, $(\mathscr{F}_1^{\alpha}, \check{E}) \subseteq (\mathscr{F}_3, \check{E})$, $(\mathscr{F}_2^{\alpha}, \check{E}) \subseteq (\mathscr{G}_1^{\alpha}, \check{E})$, $(\mathscr{F}_3, \check{E}) \cap (\mathscr{G}_1^{\alpha}, \check{E}) = \varnothing$. Similarly, $\tau_2^{\mathrm{DNSS}}$ is DNSB $T_4$ with respect to $\tau_1^{\mathrm{DNSS}}$. □

**Proposition 9** Let $(\mathbf{X}, \tau_1^{\mathrm{DNSS}}, \tau_2^{\mathrm{DNSS}}, \check{E})$ be DNSBTS and let $Y \subseteq X$. If $(\mathbf{X}, \tau_{1\mathbf{Y}}, \tau_{2\mathbf{Y}}, \check{E})$ is pair wise DNS $T_3$, then $(\mathbf{Y}, \tau_{1\mathbf{Y}}^{\mathrm{DNSS}}, \tau_{2\mathbf{Y}}^{\mathrm{DNSS}}, \check{E})$ is pair wise DNS $T_3$.

**Proof.** First we prove that $(\mathbf{Y}, \tau_{1\mathbf{Y}}^{\mathrm{DNSS}}, \tau_{2\mathbf{Y}}^{\mathrm{DNSS}}, \breve{E})$ is pairwise DNS $T_1$. Let $x, y \in X, x \neq y$. If $(\mathbf{X}, \tau_1^{\mathrm{DNSS}}, \tau_2^{\mathrm{DNSS}}, \breve{E})$ is pairwise, then $(\mathbf{X}, \tau_1^{\mathrm{DNSS}}, \tau_2^{\mathrm{DNSS}}, \breve{E})$ is pair wise DNS $\tau_1^{\mathrm{DNSS}}$. So $\exists\ \tau_1^{\mathrm{DNSS}}$ DNS b-open set $(\mathscr{F}, \breve{E})$ and $\tau_2^{\mathrm{DNSS}}$ DNS b-open set $(\mathscr{G}^{\alpha}, \breve{E})$ such that $x \in (\mathscr{F}, \breve{E})$ and $y \notin (\mathscr{F}, \breve{E})$, or $y \in (\mathscr{G}^{\alpha}, \breve{E})$ and $x \notin (\mathscr{G}^{\alpha}, \breve{E})$. Now $x \in Y$ and $x \notin (\mathscr{G}^{\alpha}, \breve{E})$ implies $x \in Y \cap (\mathscr{F}, \breve{E}) = (Y_{\mathscr{F}}, \breve{E})$. Since $y \notin Y \cap \alpha$ for $\alpha \in E$, this implies that $y \notin Y \cap \mathscr{F}(\alpha)$ for $\alpha \in E$. Thus $y \notin Y \cap (\mathscr{F}, \breve{E}) = (Y_{\mathscr{F}}, \breve{E})$. Now $y \in \mathbf{Y}$ and $y \in (\mathscr{G}^{\alpha}, \breve{E})$, hence $y \in \mathbf{Y} \cap (\mathscr{G}^{\alpha}, \breve{E}) = (\mathscr{G}_{\mathbf{Y}}^{\alpha}, \breve{E})$, where $(\mathscr{G}^{\alpha}, \breve{E}) \in \tau_2^{\mathrm{DNSS}}$. Consider $x \notin (\mathscr{G}^{\alpha}, \breve{E})$. This means that for $\alpha \in E$, $x \notin Y \cap \mathscr{G}^{\alpha}(\alpha)$, hence $x \notin Y \cap (\mathscr{G}^{\alpha}, \breve{E}) = (\mathscr{G}_{\mathbf{Y}}^{\alpha}, \breve{E}))$. Thus $(\mathbf{Y}, \tau_{1\mathbf{Y}}^{\mathrm{DNSS}}, \tau_{2\mathbf{Y}}^{\mathrm{DNSS}}, \breve{E})$ is pair wise DNS $T_1$. Now we prove that if $(\mathbf{X}, \tau_1^{\mathrm{DNSS}}, \tau_2^{\mathrm{DNSS}}, \breve{E})$ is pair wise DNS $T_3$, then $(\mathbf{X}, \tau_1^{\mathrm{DNSS}}, \tau_2^{\mathrm{DNSS}}, \breve{E})$ is pairwise DNS regular. Let $y \in \mathbf{Y}$ and let $(\mathscr{G}^{\alpha}, \breve{E})$ be a DNS b close set in $\mathbf{Y}$ such that $y \notin (\mathscr{G}^{\alpha}, \breve{E})$ where $(\mathscr{G}^{\alpha}, \breve{E}) \in \tau_1^{\mathrm{DNSS}}$. Then$(\mathscr{G}^{\alpha}, \breve{E}) = (\mathbf{Y}, \breve{E}) \cap (\mathscr{F}, \breve{E})$ for some DNS b close set in $\tau_1^{\mathrm{DNSS}}$. Hence $y \notin (\mathbf{Y}, \breve{E}) \cap (\mathscr{F}, \breve{E})$, but $y \in (\mathbf{Y}, \breve{E})$, so $y \notin (\mathscr{F}, \breve{E})$ since $(\mathbf{X}, \tau_1^{\mathrm{DNSS}}, \tau_2^{\mathrm{DNSS}}, \breve{E})$ is DNS $T_3$.

Since $(\mathbf{X}, \tau_1^{\mathrm{DNSS}}, \tau_2^{\mathrm{DNSS}}, \breve{E})$ is DNS b regular, $\exists\ \tau_1^{\mathrm{DNSS}}$ QNS b-open set $(\mathscr{F}_1, \breve{E})$ and $\tau_2^{\mathrm{DNSS}}$ DNS b-open set $(\mathscr{F}_2, \breve{E})$ such that

$$y \in (\mathscr{F}_1, \breve{E}), \quad (\mathscr{G}^{\alpha}, \breve{E}) \subseteq (\mathscr{F}_2, \breve{E}).$$

Also,

$$(\mathscr{F}_1, \breve{E}) \cap (\mathscr{F}_2, \breve{E}) = \varnothing.$$

Take $(\mathscr{G}_1^{\alpha}, \breve{E}) = (\mathbf{Y}, \breve{E}) \cap (\mathscr{F}_2, \breve{E})$, then $(\mathscr{G}_1^{\alpha}, \breve{E})$ and $(\mathscr{G}_2^{\alpha}, \breve{E})$ are DNS b-open set in $\mathbf{Y}$ such that

$$y \in (\mathscr{G}_1^{\alpha}, \breve{E}),\ (\mathscr{G}^{\alpha}, \breve{E}) \subseteq (\mathbf{Y}, \breve{E}) \cap (\mathscr{F}_2, \breve{E}) = (\mathscr{G}_2^{\alpha}, \breve{E}),$$

$$(\mathscr{G}_1^{\alpha}, \breve{E}) \cap (\mathscr{G}_2^{\alpha}, \breve{E}) \subseteq (\mathscr{F}_1, \breve{E}) \cap (\mathscr{F}_2, \breve{E}) = \varnothing.$$

$$(\mathscr{G}_1^{\alpha}, \breve{E}) \cap (\mathscr{G}_2^{\alpha}, \breve{E}) = \varnothing.$$

Therefore $\tau_{1\mathbf{Y}}^{\mathrm{DNSS}}$ is DNS b regular w.r.t. $\tau_{2\mathbf{Y}}^{\mathrm{DNSS}}$. Similarly, let $y \in \mathbf{Y}$ and $(\mathscr{G}^{\alpha}, \breve{E})$ be a DNS b close set in $\mathbf{Y}$ such that $y \notin (\mathscr{G}^{\alpha}, \breve{E})$ where $(\mathscr{G}^{\alpha}, \breve{E}) \in \tau_2^{\mathrm{DNSS}}$. Then $(\mathscr{G}^{\alpha}, \breve{E}) = (\mathbf{Y}, \breve{E}) \cap (\mathscr{F}, \breve{E})$ for some DNS b close set in $\tau_2^{\mathrm{DNSS}}$. Since $(\mathbf{X}, \tau_1^{\mathrm{DNSS}}, \tau_2^{\mathrm{DNSS}}, \breve{E})$ is b regular, $\exists\ \tau_2^{\mathrm{DNSS}}$ DNS b-open set $(\mathscr{F}_1, \breve{E})$ and $\tau_1^{\mathrm{DNSS}}$ DNS b-open set $(\mathscr{F}_2, \breve{E})$ such that

$$y \in (\mathscr{F}_1, \breve{E}), \qquad (\mathscr{G}^{\alpha}, \breve{E}) \subseteq (\mathscr{F}_2, \breve{E}).$$

And

$$(\mathscr{F}_1, \breve{E}) \cap (\mathscr{F}_2, \breve{E}) = \varnothing.$$

Take $(\mathscr{G}_1^{\alpha}, \breve{E}) = (\mathbf{Y}, \breve{E}) \cap (\mathscr{F}_1, \breve{E})$, then $(\mathscr{G}_1^{\alpha}, \breve{E})$ and $(\mathscr{G}_2^{\alpha}, \breve{E})$ are DNS b-open set in $\mathbf{Y}$ such that

$$y \in (\mathscr{G}_1^{\alpha}, \breve{E}),\ (\mathscr{G}^{\alpha}, \breve{E}) \subseteq (\mathbf{Y}, \breve{E}) \cap (\mathscr{F}_2, \breve{E}) = (\mathscr{G}_2^{\alpha}, \breve{E}).$$

And

$$(\mathscr{G}_1^{\alpha},\ \check{E})\cap(\mathscr{G}_2^{\alpha},\ \check{E})\subseteq(\mathscr{F}_1,\ \check{E})\cap(\mathscr{F}_2,\ \check{E})=\varnothing.$$

Therefore $\tau_{2\mathbf{Y}}^{\mathrm{DNSS}}$ is DNS b regular w.r.t. $\tau_{1\mathbf{Y}}^{\mathrm{DNSS}}$.
Hence

$$(\mathbf{X},\ \tau_1^{\mathrm{DNSS}},\ \tau_2^{\mathrm{DNSS}},\ \check{E}) \text{ is pairwise DNS } T_3.$$

□

**Proposition 10** Let $(\mathbf{X},\ \tau_1^{\mathrm{DNSS}},\ \tau_2^{\mathrm{DNSS}},\ \check{E})$ be a DNSBTS and let $\mathbf{Y}$ be a DNS b C space of $\mathbf{X}$. If $(\mathbf{X},\ \tau_1^{\mathrm{DNSS}},\ \tau_2^{\mathrm{DNSS}},\ \check{E})$ is pairwise DNS b $T_4$ space, then $(\mathbf{Y},\ \tau_{1\mathbf{Y}}^{\mathrm{DNSS}},\ \tau_{2\mathbf{Y}}^{\mathrm{DNSS}},\ \check{E})$ is pairwise DNS b $T_4$ space.

**Proof.** Since $(\mathbf{X},\ \tau_1^{\mathrm{DNSS}},\ \tau_2^{\mathrm{DNSS}},\ \check{E})$ is pairwise DNS b $T_4$, $\Rightarrow(\mathbf{X},\ \tau_1^{\mathrm{DNSS}},\ \tau_2^{\mathrm{DNSS}},\ \check{E})$ is pairwise DNS b $T_1$. We prove that $(\mathbf{X},\ \tau_1^{\mathrm{DNSS}},\ \tau_2^{\mathrm{DNSS}},\ \check{E})$ is pairwise DNS b normal. Let $(\mathscr{G}_1^{\alpha},\ \check{E}),\ (\mathscr{G}_2^{\alpha},\ \check{E})$ be DNS b close sets in $\mathbf{Y}$ such that

$$(\mathscr{G}_1^{\alpha},\ \check{E})\cap(\mathscr{G}_2^{\alpha},\ \check{E})=\varnothing.$$

$$(\mathscr{G}_1^{\alpha},\ \check{E})=(\mathbf{Y},\ \check{E})\cap(\mathscr{F}_1,\ \check{E}),$$

$$(\mathscr{G}_2^{\alpha},\ \check{E})=(\mathbf{Y},\ \check{E})\cap(\mathscr{F}_2,\ \check{E}),$$

where $(\mathscr{F}_1,\ \check{E})$ is a DNS b close set in $\tau_1^{\mathrm{DNSS}}$ and $(\mathscr{F}_2,\ \check{E})$ is a DNS b close set in $\tau_2^{\mathrm{DNSS}}$. Also,

$$(\mathscr{F}_1,\ \check{E})\cap(\mathscr{F}_2,\ \check{E})=\varnothing.$$

Since $\mathbf{Y}$ is a DNS b close subset of $\mathbf{X}$, then $(\mathscr{G}_1^{\alpha},\ \check{E}),\ (\mathscr{G}_2^{\alpha},\ \check{E})$ are DNS b close sets in $\mathbf{X}$ such that

$$(\mathscr{G}_1^{\alpha},\ \check{E})\cap(\mathscr{G}_2^{\alpha},\ \check{E})=\varnothing.$$

Since $(\mathbf{X},\ \tau_1^{\mathrm{DNSS}},\ \tau_2^{\mathrm{DNSS}},\ \check{E})$ is pairwise DNS b normal, $\exists$ DNS b-open sets $(\hat{H}_1,\ \check{E})$ and $(\hat{H}_2,\ \check{E})$ such that $(\hat{H}_1,\ \check{E})$ is DNS b-open set in $\tau_1^{\mathrm{DNSS}}$, $(\hat{H}_2,\ \check{E})$ is DNS b-open set in $\tau_2^{\mathrm{DNSS}}$, and

$$(\mathscr{G}_1^{\alpha},\ \check{E})\subseteq(\hat{H}_1,\ \check{E}),$$

$$(\mathscr{G}_2^{\alpha},\ \check{E})\subseteq(\hat{H}_2,\ \check{E}),$$

$$(\hat{H}_1,\ \check{E})\cap(\hat{H}_2,\ \check{E})=\varnothing.$$

Since $(\mathscr{G}_1^{\alpha},\ \check{E}),\ (\mathscr{G}_2^{\alpha},\ \check{E})\subseteq(\mathbf{Y},\ \check{E})$, then

$$(\mathscr{G}_1^{\alpha}, \breve{E}) \subseteq (\mathbf{Y}, \breve{E}) \cap (\hat{H}_1, \breve{E}),$$

$$(\mathscr{G}_2^{\alpha}, \breve{E}) \subseteq (\mathbf{Y}, \breve{E}) \cap (\hat{H}_2, \breve{E}).$$

And

$$[(\mathbf{Y}, \breve{E}) \cap (\hat{H}_1, \breve{E})] \cap [(\mathbf{Y}, \breve{E}) \cap (\hat{H}_2, \breve{E})] = \varnothing.$$

Since $(\mathbf{Y}, \breve{E}) \cap (\hat{H}_1, \breve{E})$ and $(\mathbf{Y}, \breve{E}) \cap (\hat{H}_2, \breve{E})$ are DNS b-open sets in $\mathbf{Y}$, therefore $\tau_{1\mathbf{Y}}^{\mathrm{DNSS}}$ is DNS b normal w.r.t. $\tau_{2\mathbf{Y}}^{\mathrm{DNSS}}$. Similarly, let $(\mathscr{G}_1^{\alpha}, \breve{E})$, $(\mathscr{G}_2^{\alpha}, \breve{E})$ be DNS b close set subsets in $\mathbf{Y}$ such that

$$(\mathscr{G}_1^{\alpha}, \breve{E}) \cap (\mathscr{G}_2^{\alpha}, \breve{E}) = \varnothing.$$

$$(\mathscr{G}_1^{\alpha}, \breve{E}) = (\mathbf{Y}, \breve{E}) \cap (\mathscr{F}_1, \breve{E}),$$

$$(\mathscr{G}_2^{\alpha}, \breve{E}) = (\mathbf{Y}, \breve{E}) \cap (\mathscr{F}_2, \breve{E}),$$

for some DNS b close sets $(\mathscr{F}_1, \breve{E})$ in $\tau_2^{\mathrm{DNSS}}$ and $(\mathscr{F}_2, \breve{E})$ in $\tau_1^{\mathrm{DNSS}}$, and

$$(\mathscr{F}_1, \breve{E}) \cap (\mathscr{F}_2, \breve{E}) = \varnothing.$$

Since $\mathbf{Y}$ is a DNS b C subset in $\mathbf{X}$, $(\mathscr{G}_1^{\alpha}, \breve{E})$, $(\mathscr{G}_2^{\alpha}, \breve{E})$ are DNS b close sets in $\mathbf{X}$ such that

$$(\mathscr{G}_1^{\alpha}, \breve{E}) \cap (\mathscr{G}_2^{\alpha}, \breve{E}) = \varnothing.$$

Since $(\mathbf{X}, \tau_1^{\mathrm{DNSS}}, \tau_2^{\mathrm{DNSS}}, \breve{E})$ is pairwise DNS b normal, $\exists$ DNS b-open sets $(\hat{H}_1, \breve{E})$ and $(\hat{H}_2, \breve{E})$ such that $(\hat{H}_1, \breve{E})$ is DNS b-open set in $\tau_2^{\mathrm{DNSS}}$, $(\hat{H}_2, \breve{E})$ is DNS b-open set in $\tau_1^{\mathrm{DNSS}}$, and

$$(\mathscr{G}_1^{\alpha}, \breve{E}) \subseteq (\hat{H}_1, \breve{E}),$$

$$(\mathscr{G}_2^{\alpha}, \breve{E}) \subseteq (\hat{H}_2, \breve{E}),$$

$$(\hat{H}_1, \breve{E}) \cap (\hat{H}_2, \breve{E}) = \varnothing.$$

Since

$$(\mathscr{G}_1^{\alpha}, \breve{E}), (\mathscr{G}_2^{\alpha}, \breve{E}) \subseteq (\mathbf{Y}, \breve{E}),$$

Then

$$(\mathscr{G}_1^{\alpha}, \check{E}) \subseteq (\mathbf{Y}, \check{E}) \cap (\hat{H}_1, \check{E}),$$

$$(\mathscr{G}_2^{\alpha}, \check{E}) \subseteq (\mathbf{Y}, \check{E}) \cap (\hat{H}_2, \check{E}).$$

And

$$[(\mathbf{Y}, \check{E}) \cap (\hat{H}_1, \check{E})] \cap [(\mathbf{Y}, \check{E}) \cap (\hat{H}_2, \check{E})] = \varnothing.$$

Thus $(\mathbf{Y}, \check{E}) \cap (\hat{H}_1, \check{E})$ and $(\mathbf{Y}, \check{E}) \cap (\hat{H}_2, \check{E})$ are DNS b-open sets in $\mathbf{Y}$, so $\tau_{2\mathbf{Y}}^{\mathrm{DNSS}}$ is DNS b normal w.r.t. $\tau_{1\mathbf{Y}}^{\mathrm{DNSS}}$. Hence,

$$(\mathbf{Y}, \tau_{1\mathbf{Y}}^{\mathrm{DNSS}}, \tau_{2\mathbf{Y}}^{\mathrm{DNSS}}, \check{E})$$

is pairwise DNS b $T_4$. □

# 5. Military target identification with cotangent similarity and advanced machine learning techniques

Among a multitude of approaches that can be used in dimensionality reduction and feature analysis, some of them have become typical tools. In this introduction, the author will describe four fundamental approaches, i.e. PCA, t-SNE, Pearson correlation coefficient, and the Elbow. These were chosen deliberately, as they form a complement set, which deals with the major stages of data exploration, that is, understanding linear relationships and variance patterns, and non-linear model visualization and parameterizations. Another analytic measure that is employed in computing similarity of two vectors is Cosine Similarity Measure (CSM). It is commonly applied in machine learning, image processing and data analysis. CSM can identify the presence of subtle patterns and relationships in the data that might not be easily identified using a distance based measure by considering the geometric orientation of data points. As an example, during a military operation, CSM may be used to categorize the possible targets based on surveillance information by matching the operational characteristics of a target with those of classified standard profiles. This helps in measuring the level of a target hypothesis of known threat categories thus enhancing the accuracy of threat comparison and classification. These activities are also enabled by many machine learning and visualization algorithms.

**Signature Techniques:** There are numerous tools that are used to analyze relationship between the signal and template, they include:

**Exam of correlation:** Heatmaps (normalized, positive, Pearson correlation), 3D surface view of Pearson correlation.

**Dimensionality Reduction, Visualization:** PCA, t-SNE, 3D PCA clustering visualization and 3D t-SNE clustering visualization.

**Other techniques:** parallel coordinates, 3D diagrams and Elbow method.

## 5.1 *The chosen methods: essence and rationale*

### 5.1.1 *PCA*

**Essence:** PCA is a non-nonlinear, conventional method of dimensional reduction. On the basic level, it converts the original variables (which can be correlated with each other) into a new set of variables, which are not correlated. The

principal components are known as these new variables. The elements are arranged in a sequence in which the initial few ones explain the highest percentages of variations that exist in the original data. It does so by determining the directions (eigenvectors) of most variance in the data and projecting it down into a lower-dimensional subspace that is determined by these directions [72]. The reason why it was chosen is as follows: PCA is the most likely method of linear dimensionality reduction. It is computationally efficient, deterministic and its components can be interpreted as the direction of maximum variance. It is not capable of running without noise reduction, data compression and as a preprocessing step to other algorithms.

### 5.1.2 *The t-SNE*

**Essence:** t-SNE is a non-linear algorithm, which in contrast to PCA is mainly applied to visualize high-dimensional data (two or three dimensions). Its operation involves the use of high-dimensional Euclidean distinctions amid data into conditional similarity. It then optimizes a probability structure of the low-dimensional map, which is similar to the original one, and minimizes the Kullback-Leibler (KL) divergence between the two distributions through gradient descent. It has been found to tackle the crowding problem by using the heavy-tailed Student t-distribution in the low-dimensional space, which is one of its benefits [73]. It has been chosen because t-SNE is proved to be quite effective in revealing underlying cluster patterns and manifold learning not accessible to linear techniques such as PCA. It was chosen to represent that category of probabilistic embedding mechanisms non-linear which are essential in their investigation of complex and real-world data.

### 5.1.3 *The pearson correlation coefficient*

The Pearson correlation coefficient is used to measure the linear relationship between two variables and is denoted by the symbol, $r$. It has a 1 scale (-1) 1 indicates a positive total linear correlation, 0 a non-existent linear correlation, and -1 a negative total linear correlation [74]. It is a part of the basic elements of statistical analysis which is applied to establish the strength and direction of a linear relationship. The reason it has been chosen: Pearson method though not a dimensionality reduction method is necessary to understand multi collinearity as well as feature selection. It is shown here since one of the primary reasons to consider the application of such methodology as PCA is a feature correlation of this scale. Data correlation analysis is often employed as a preliminary step to consider the need to proceed to a more sophisticated dimensionality reduction.

### 5.1.4 *The elbow method*

**Essence:** In a cluster analysis, The elbow method is a heuristic that is employed to identify the best cluster number. It runs an instance of one or more uses of a clustering algorithm (like $k$-means) with varying values of $k$ (the number of clusters) and then generates a plot of the amount of variation explained (or some other measure such as within-cluster sum of squares) versus $k$. According to [75], the number of clusters is a good candidate at the point in the curve where the rate of decrease has changed abruptly. Justification of its presence: It contains the Elbow method which is a method of selection and validation of models. After data visualization by PCA or t-SNE, one would often want to discover different groups. Elbow is a common parameterizations to further analysis which is simple and easy to use so that it is easy to pass through the visualization to clustering. In conclusion, the four methods were not selected in isolation but in a synergistic combination in their part to help in a complete data analysis pipeline. Pearson correlation helps in determining that reduction is needed; PCA is good and linear, t-SNE is good and non-linear. Elbow method assists in determining the emerging cluster structure. The combination of them evaluates an essential pool of activities that should be undertaken to transform raw, high-dimensional data into an insight.

## 5.2 *Cotangent similarity measures*

Let $T_i = (\mathrm{T}_{ik}, \mathrm{RT}_{ik}, \mathrm{C}_{ik}, \mathrm{RF}_{ik}, \mathrm{F}_{ik})$, $C_j = (\mathrm{T}_{jk}, \mathrm{RT}_{jk}, \mathrm{C}_{jk}, \mathrm{RF}_{jk}, \mathrm{F}_{jk})$ are two CTVNSSs. Each set is represented by three components for each feature $k$:

$T_{ik}$: Truth membership of feature $k$ for $T_i$.
$RT_{ik}$: Relative truth membership of feature $k$ for $T_i$.
$C_{ik}$: Contradiction of feature $k$ for $T_i$.
$RF_{ik}$: Relative false membership of feature $k$ for $T_i$.
$F_{ik}$: False membership degree of feature $k$ for $T_i$.
The values typically satisfy: $T_{ik}, RT_{ik}, C_{ik}, RF_{ik}, F_{ik} \in [0, 1]$.
Similarly, for object $C_j$:
$T_{jk}$: Truth membership of feature $k$ for $C_j$.
$RT_{jk}$: Relative truth membership of feature $k$ for $C_j$.
$C_{jk}$: Contradiction of feature $k$ for $C_j$.
$RF_{jk}$: Relative false membership of feature $k$ for $C_j$.
$F_{jk}$: False membership degree of feature $k$ for $C_j$.
The values typically satisfy: $T_{jk}, RT_{jk}, C_{jk}, RF_{jk}, F_{jk} \in [0, 1]$.

$$\text{Cotangent}_{\text{TNSS}}(T_i, C_j)$$

$$= \frac{1}{n}\sum_{k=1}^{n}\left\{\cot\left[\frac{\pi}{4}+\frac{\pi}{12}(|T_{ik}-T_{jk}|+|RT_{ik}-RT_{jk}|+|C_{ik}-C_{jk}|+|RF_{ik}-RF_{jk}|+|F_{ik}-F_{jk}|)\right]\right\}.$$

Let $T_i = (T_{ik}, I_{Cik}, I_{Hik}, F_{ik})$, $C_j = (T_{jk}, I_{Cjk}, I_{Hjk}, F_{jk})$ are two CNSSs. Each set is represented by three components for each feature $k$:
$T_{ik}$: Truth membership of feature $k$ for $T_i$.
$I_{Cik}$: Contradiction-oriented indeterminacy membership of feature $k$ for $T_i$.
$I_{Hik}$: Hesitation-oriented indeterminacy membership of feature $k$ for $T_i$.
$F_{ik}$: Falsity-membership degree of feature $k$ for $T_i$.
The values typically satisfy: $T_{ik}, I_{Cik}, I_{Hik}, F_{ik} \in [0, 1]$.
Similarly, for object $C_j$:
$T_{jk}$: Truth membership of feature $k$ for $C_j$.
$I_{Cjk}$: Contradiction-oriented indeterminacy membership of feature $k$ for $C_j$.
$I_{Hjk}$: Hesitation-oriented indeterminacy membership of feature $k$ for $T_i$.
$F_{jk}$: Falsity-membership degree of feature $k$ for $C_j$.
The values typically satisfy: $T_{jk}, I_{Cjk}, I_{Hjk}, F_{jk} \in [0, 1]$.
The cotangent similarity measures between $T_i$ and $C_j$ is defined as:

$$\text{Cotangent}_{\text{DNSS}}(T_i, C_j)$$

$$= \frac{1}{n}\sum_{k=1}^{n}\left\{\cot\left[\frac{\pi}{4}+\frac{\pi}{12}(|T_{ik}-T_{jk}|+|I_{Cik}-I_{Cjk}|+|I_{Hik}-I_{Hjk}|+|F_{ik}-F_{jk}|)\right]\right\}.$$

## 5.3 *Nature of noise and crosstalk in military surveillance*

Military surveillance data can be described as frequently noisy due to random variation and sensor instability and crosstalk due to interference or signal source overlap. These distortions negatively affect the performance of similarity traditional measures. This problem is resolved by the DVNSS model which uses four of the components to capture all the characteristics: Truth (T), conflict-based Indeterminacy (Ic), noise-based Indeterminacy (IH), and Falsity (F).

Ic and IH are fundamental to distinguish between doubt that is due to noises, weak signals, and missing values and the doubt that is due to the contradictions between overlapping templates or mixed signal patterns. The capacity of DVNSS of distinguishing between distortion and conflict does not exist in classical fuzzy, rough, and probabilistic models. Combined with the Cotangent Similarity Measure (Cot-SM), the DVNSS structure proves to be robust to the contaminated or unstable signatures, overlapping radar or thermal signature, and sensor modal conflict. This means the classification results will be more stable, there is less confusion between decoys and downstream machine-learning image representations are better with cleaner and more accurate similarity data. DVNSS is a simple and mathematically consistent method of dealing with noise and crosstalk and is especially appropriate in real time military target detection systems.

## 5.4 *Analytical and visualization tools for signal template relationships*

In order to identify broad correlations, structural alignments, and grouping patterns, signal-template similarity uses statistical and visualization-based studies. The Cot Similarity Matrix and its related data can be realized using a wide range of tools, including sophisticated dimensionality reduction techniques and basic Heatmaps. Heatmaps that provide a real-time image of pairwise similarity are used to visualize the similarity between signals and templates. Heatmaps make it easier to identify patterns, gradients, and anomalies in rows and columns by using the similarity values as color values. Strong direct relationships are the focus of positive correlation heat maps; these are indicated by greater values, making it simpler to spot signals that consistently match templates. In order to prevent unfair and biased comparisons between various data, normalized correlation Heatmaps preserve scale differences. By doing this, distortions based on magnitude disparities are reduced. Heatmaps that are especially sensitive to the identification of linear correlations between signals-which enable the systematic movement or divergence of groupings of signals or templates-are known as Pearson correlation Heatmaps. The correlation strengths within the matrix can be viewed from a landscape viewpoint using a three-dimensional surface plot of Pearson correlation. Peaks show strong correlations, while valleys show weak or opposite links. Unlike flat Heatmaps, this geometric representation of the globe aids in identifying clusters and transition zones. The PCA extracts the most variance by estimating the high-dimensional similarity space onto lower-dimensional space. It allows for both 2D and 3D cluster visualization and reveals the dominant similarity trends. Because it considers local neighborhood structures, t-SNE complements PCA. It is particularly useful for visualizing non-linear correlations that PCA is unable to represent. The clusters of signals are depicted in greater depth using a 3D t-SNE representation, which makes it possible to identify finer divisions and overlaps that are not visible in 2D space. Plotting cluster memberships directly onto PCA axes makes it easier to detect cluster borders and patterns in 3D PCA clustering demonstrations. It is possible to directly compare average tendencies and identify which signals exhibit stronger and weaker affinities by using bar graphs, which give an overview of similarity values on a template or signal-by-signal basis. On the other hand, 3D plots are a condensed yet informative representation of interaction patterns and can show a link between three factors in a single plot. Multiple similarity dimensions $(B_1B_4)$ can be compared simultaneously thanks to parallel coordinate plotting. Each signal is represented by a line, and the curve that the axes follow shows how the similarity values vary with templates. For identifying steady and varying alignment profiles, this is one technique that performs the best. Signals are separated based on their clustering patterns using clustering algorithms such as the K-Means. The Elbow approach determines the ideal amount of clusters to employ in order to ensure that partitioning does not overfit, capturing all common tendencies but excluding unique specializations. When clustering and PCA or t-SNE visualization are combined, statistical rigor and interpretive clarity are provided. A multi-perspective study of the signal-template interaction is provided by the combination of these technologies. They carry surface plots to geometric terrain, Pearson correlation estimates linear relationships, and Heatmaps highlight the similarity intensities of the global and local locations. While clustering and the Elbow approach verify the existence of discrete groups, dimensionality reduction techniques (PCA, t-SNE) translate the data into interpretable low-dimensional spaces. Bar plots, 3D plots, and parallel coordinates offer further levels of interpretation that enable the analysis of both macro-level patterns and micro-level subtleties. An ordered similarity pattern is strongly supported by such a cohesive toolbox, which demonstrates that the signal-template system is not a homogeneous system but rather possesses balanced and specialized alignment preferences.

## 5.5 *Real-time military target classification with cotangent similarity and advanced surveillance data integration*

Assume that the information we have on potential military targets is a collection of potential targets, specifically, $T = \{T_1, T_2, T_3, T_4\}$, which represents a particular object of operational interest. This could be a communication point, a group of artificial devices, a mobile command apparatus, or even a convoy transporting supplies. A set of surveillance or reconnaissance data $S = \{S_1, S_2, S_3, S_4\}$ can be attached to each target. Radar signatures, thermal imaging, electronic emission monitoring, and movement observation are some of the sources used to collect this type of data. These are crucial intelligence hints for identifying and characterizing every target. The $C = \{C_1, C_2, C_3, C_4\}$ indexes or engages each target. High-value strategic assets, mobile decoys, communication centers, and logistical groupings that require immediate attention or removal may be included in these categories. There are four crucial factors for each working attribute of a target: Variances to the attractive electronic or thermal grate pattern are quantified by Abnormal Signal Signature (AbS). Relevant Threat Threshold (RelT) is a measure of how closely the target signal aligns with anticipated threat criteria. Abnormal Fluctuation (AbF) indicates abnormal fluctuations in the target behavior or sign, while Relative Fluctuation (RelF) measures changes to the working dynamic electronic or thermal signal. Each target is represented in terms of a feature vector based on these criteria. These features vectors are organised into the $T \times S$ Emotional Affinity Feature Matrix, as shown in Table 4, where each cell corresponds to target-source pair $(T_i, S_j)$ described by $(\mathrm{AbS}_{ij}, \mathrm{RelT}_{ij}, \mathrm{RelF}_{ij}, \mathrm{AbF}_{ij})$. The cotangent similarity measure is then used to compare this vector with the others of previously identified targets. The angle between two vectors determines the similarity score, which is the cosine of the angle. The likelihood that the current target will fit a known threat profile increases with the cosine value. By synchronizing the surveillance data with established threat models, it is possible to classify targets in real-time with high accuracy. The resulting Emotional Classification Matrix for signal-based affectional mapping $(T \times S \to C)$, including the intermediate similarity vectors, is reported in Table 5.

**Table 4.** Emotional affinity feature matrix for signal-based interaction analysis $(T \times S)$

| | $S_1$ | $S_2$ | ... | $S_n$ |
|---|---|---|---|---|
| $T_1$ | $\mathrm{AbS}_{11}, \mathrm{RelT}_{11}, \mathrm{ReIF}_{11}, \mathrm{AbF}_{11}$ | $\mathrm{AbS}_{12}, \mathrm{ReIT}_{12}, \mathrm{ReIF}_{12}, \mathrm{AbF}_{12}$ | ... | $\mathrm{AbS}_{1n}, \mathrm{ReIT}_{1n}, \mathrm{ReIF}_{1n}, \mathrm{AbF}_{1n}$ |
| $T_2$ | $\mathrm{AbS}_{21}, \mathrm{ReIT}_{21}, \mathrm{ReIF}_{21}, \mathrm{AbF}_{21}$ | $\mathrm{AbS}_{22}, \mathrm{ReIT}_{22}, \mathrm{ReIF}_{22}, \mathrm{AbF}_{22}$ | ... | $\mathrm{AbS}_{2n}, \mathrm{ReIT}_{2n}, \mathrm{ReIF}_{2n}, \mathrm{AbF}_{2n}$ |
| ... | ... | ... | ... | ... |
| $T_m$ | $\mathrm{AbS}_{m1}, \mathrm{ReIT}_{m1}, \mathrm{ReIF}_{m1}, \mathrm{AbF}_{m1}$ | $\mathrm{AbS}_{m2}, \mathrm{ReIT}_{m2}, \mathrm{ReIF}_{m2}, \mathrm{AbF}_{m2}$ | ... | $\mathrm{AbS}_{mn}, \mathrm{ReIT}_{mn}, \mathrm{ReIF}_{mn}, \mathrm{AbF}_{mn}$ |

**Table 5.** Emotional classification matrix for signal-based affectional mapping $(T \times S \to C)$

| Row-I | $S_1$ | $S_2$ | $S_3$ | $S_4$ | Row-II | $C_1$ | $C_2$ | $C_3$ | $C_4$ |
|---|---|---|---|---|---|---|---|---|---|
| $T_1$ | 0.5<br>0.7<br>0.3<br>0.4 | 0.6<br>0.4<br>0.3<br>0.8 | 0.3<br>0.5<br>0.8<br>0.9 | 0.9<br>0.2<br>0.4<br>0.6 | $S_1$ | 0.3<br>0.5<br>0.7<br>0.8 | 0.7<br>0.6<br>0.2<br>0.3 | 0.5<br>0.4<br>0.6<br>0.9 | 0.3<br>0.2<br>0.4<br>0.7 |
| $T_2$ | 0.4<br>0.7<br>0.5<br>0.7 | 0.2<br>0.4<br>0.6<br>0.9 | 0.3<br>0.4<br>0.5<br>0.8 | 0.7<br>0.4<br>0.6<br>0.4 | $S_2$ | 0.2<br>0.3<br>0.7<br>0.8 | 0.6<br>0.7<br>0.4<br>0.5 | 0.3<br>0.6<br>0.8<br>0.4 | 0.4<br>0.3<br>0.6<br>0.2 |
| $T_3$ | 0.7<br>0.6<br>0.8<br>0.3 | 0.2<br>0.8<br>0.7<br>0.5 | 0.6<br>0.2<br>0.7<br>0.3 | 0.6<br>0.2<br>0.7<br>0.3 | $S_3$ | 0.4<br>0.7<br>0.5<br>0.6 | 0.6<br>0.3<br>0.4<br>0.5 | 0.7<br>0.3<br>0.2<br>0.4 | 0.5<br>0.6<br>0.3<br>0.4 |
| $T_4$ | 0.4<br>0.6<br>0.8<br>0.3 | 0.3<br>0.6<br>0.2<br>0.9 | 0.4<br>0.6<br>0.8<br>0.4 | 0.4<br>0.6<br>0.8<br>0.4 | $S_4$ | 0.3<br>0.6<br>0.4<br>0.8 | 0.9<br>0.3<br>0.2<br>0.5 | 0.4<br>0.3<br>0.8<br>0.6 | 0.3<br>0.8<br>0.9<br>0.4 |

As a result, decision-makers will be able to quickly identify targets, assess their danger level, and rank them in order of importance for engagement or surveillance. In fluid generation workplaces, the program helps make faster, evidence-based decisions and enhances the effectiveness of fight field intelligence.

The raw surveillance parameters for each target $T_i$, as gathered from each data source $S_i$, are displayed in this table. AbS, RelT, RelF, and AbF are represented by the 4-dimensional feature vectors found in each cell. gives each target-source combination a thorough feature profile for preliminary analysis and threat modeling.

This table delineates the cotangent similarity values calculated by comparing the feature vectors of targets with those of established classified operational profiles (e.g., $C_1$: high-value asset, $C_2$: decoy, $C_3$: communication node, $C_4$: logistical unit). The raw cosine similarity between each Target (T) and its corresponding surveillance data (S) is presented in Row-I $(T \times S)$. Meanwhile, the cotangent similarity between each data source vector and the classified operational profiles is displayed in Row-II $(S \times C)$. This method facilitates the prioritization of actions (e.g., attack, monitor, ignore) by classifying or clustering targets according to their correlation with well-defined threat or operational categories. The cotangent values calculated for each pair of targets and classified profiles are then added to average all target-classification pairings. For clarity, the final Cotangent DNSS simalarity scores between targets $(T_1 - T_4)$ and operational profiles $(C_1 - C_4)$ are consolidated in Table 6. The resulting Cotangent similarity have the following values:

$\text{Cotangent}_{\text{DNSS}}(T_1,\ C_1) = 0.2877.$
$\text{Cotangent}_{\text{DNSS}}(T_1,\ C_2) = 0.2634.$
$\text{Cotangent}_{\text{DNSS}}(T_1,\ C_3) = 0.2327.$
$\text{Cotangent}_{\text{DNSS}}(T_1,\ C_4) = 0.3557.$
$\text{Cotangent}_{\text{DNSS}}(T_2,\ C_1) = 0.2649.$
$\text{Cotangent}_{\text{DNSS}}(T_2,\ C_2) = 0.2020.$
$\text{Cotangent}_{\text{DNSS}}(T_2,\ C_3) = 0.3776.$
$\text{Cotangent}_{\text{DNSS}}(T_2,\ C_4) = 0.1431.$
$\text{Cotangent}_{\text{DNSS}}(T_3,\ C_1) = 0.2423.$
$\text{Cotangent}_{\text{DNSS}}(T_3,\ C_2) = 0.2260.$
$\text{Cotangent}_{\text{DNSS}}(T_3,\ C_3) = 0.3239.$
$\text{Cotangent}_{\text{DNSS}}(T_3,\ C_4) = 0.2520.$
$\text{Cotangent}_{\text{DNSS}}(T_4,\ C_1) = 0.2318.$
$\text{Cotangent}_{\text{DNSS}}(T_4,\ C_2) = 0.2723.$
$\text{Cotangent}_{\text{DNSS}}(T_4,\ C_3) = 0.2517.$
$\text{Cotangent}_{\text{DNSS}}(T_4,\ C_4) = 0.2130.$

By repeating this for all target profiles $(T_1,\ T_2,\ T_3,\ T_4)$ against each operational category, the maximum similarity values for each target classification are obtained. The maximum similarities are as follows: $T_1$ exhibits the highest similarity of 0.8514 with $C_4$, $T_2$ achieves a maximum similarity of 0.8082 with $C_3$, $T_2$ demonstrates the strongest alignment with $C_1$ and $T_4$ shows the highest similarity of 0.8134 with $C_2$.

**Table 6.** Cotangent similarity matrix of signal channels $(S_1 - S_4)$ and emotional foci $(T_1 - T_4)$

| Cot SM | $S_1$ | $S_2$ | $S_3$ | $S_4$ |
|---|---|---|---|---|
| $T_1$ | 0.2877 | 0.2634 | 0.2327 | 0.3557 |
| $T_2$ | 0.2649 | 0.2020 | 0.3776 | 0.1431 |
| $T_3$ | 0.2423 | 0.2260 | 0.3239 | 0.2520 |
| $T_4$ | 0.2318 | 0.2723 | 0.2517 | 0.2130 |

Decisions based on the targets' similarity-which allows them to be categorized according to the closest operational profile are made using these computed maximum similarity values. Which target type is most similar to a target-that is, attacking, monitoring, or ignoring him is determined by these values, which are used to prioritize actions. Examples

include ignoring a target that closely resembles a decoy profile and pursuing a target whose cosine closeness to a high-value asset group (like $C_4$) may warrant an instant engagement. Because each objective is statistically identified in terms of a particular threat or operational category, this approach facilitates effective decision-making. The military or operational force can then deploy resources to meet the target and effectively respond to threats.

## 6. Computational environment and runtime settings

Python 3.10 was used for all the processes, with the usage of Numpy, Scipy, scikit-learn, and Matplotlib, in order to perform cotangent similarity analysis, DNSS and visual analytics (Heatmaps, PCA, t-SNE, 3D surface, clustering). The calculations were performed on a Windows 11 workstation with an Intel Core i7-11700 (8 cores, 2.5-4.9 GHz) processor and 16 GB RAM memory. Computation of Cotangent similarities per target-template matrix was found to take between 0.18 and 0.42 seconds, PCA visualization took between 0.5 and 1.3 seconds, t-SNE visualization took between 0.4 and 0.7 seconds and correlation surface plots took 0.4 to 0.7 seconds. Thanks to these statements, all the reported results can be reproduced.

## 7. Results and discussions

Figure 17 uses the cool-warm colormap, which smoothly moves from deep blue to brilliant red, to generate 2D cot similarity matrix Heatmaps that illustrate the alignment of signals $(A_1 - A_2)$ with templates $(B_1 - B_2)$. The corresponding best-match allocations and confidence interpretations for each signal are summarized in Table 7. Very high resemblance is shown by red shades $(\approx 0.84 - 0.85)$, and the intensity of the gradient color is directly related to the alignment strength. As the strongest and most conclusive match in the matrix, only the $A_1 - B_4$ combination (0.8514) is specifically emphasized (encircled). Strong resemblance is indicated by warm reddish tones $(\approx 0.82 - 0.83)$, as seen in $A_3 - B_1$ (0.8226) and $A_4 - B_2$ (0.8134). These indicate strong and trustworthy signal-template matching, pointing to accurate and predictable classification results. Moderate resemblance is represented by cooler grayish patches $(\approx 0.80 - 0.81)$, such $A_2 - B_4$ (0.8016) and $A_3 - B_4$ (0.8125). Although these matches could occur, they are not quite clear-cut and might need further verification. $A_1 - B_1$ (0.7638) and $A_4 - B_4$ (0.7914) are examples of blue hues $(\approx 0.76 - 0.79)$ that indicate lower similarity scores and may indicate transitional or borderline classifications with little confidence. In general, Heatmaps offer a multi-level, easily comprehensible depiction of classification reliability in terms of color intensity, facilitating both quick visual assessment and more in-depth examination of signal-template patterns.

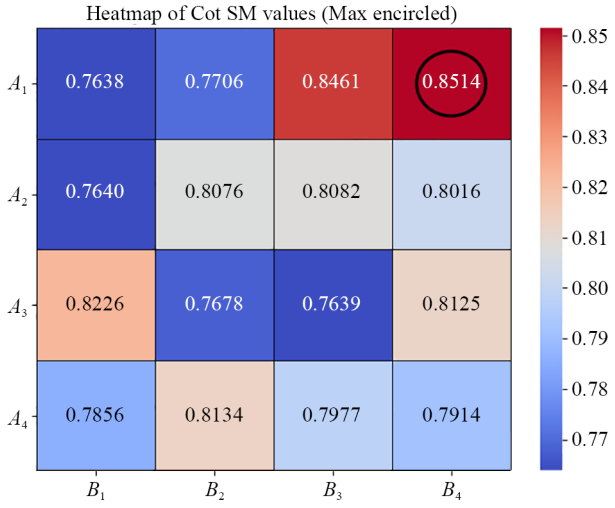


**Figure 17.** Signal partition (A), and template partition (B)

**Table 7.** Overview of possible case allocations

| Signal | Most similar template | Score | Interpretation/Confidence level |
|---|---|---|---|
| $A_1$ | $B_4$ | 0.8514 | Very high/Strongest match, ideal |
| $A_2$ | $B_2$ | 0.8076 | Moderate/Reliable, but not maximal |
| $A_3$ | $B_1$ | 0.8226 | High/Strong match, dependable |
| $A_4$ | $B_2$ | 0.8134 | Moderate/Strong, reliable pairing |

The cool warm colormap, which uses deep blue (negative/weak correlation) and dazzling red (high correlation), is used in Figure 18 to show the correlation structure between the variables ($B_1$-$B_4$). The key correlation pairs and their interpretation/confidence levels are summarized in Table 8. All diagonal items are equal to 1.00, which has been designated as the brightest red, as one might expect. By definition, these self-correlations ($B_1$ with $B_1$, $B_2$ with $B_2$, etc.) always result in a perfect score. They serve as sources of reference points in the matrix, even if they don't provide anything new about the associations between other variables. They do this by underwriting the top limit of the scale, which allows the relative values of other correlations to be consistently assessed. They stress that the Heatmaps displays the typical correlation features and is symmetrical. They note that this maximum potential value (1.00) must be used to measure any off-diagonal connection. The Heatmaps indicates that $B_3$ and $B_4$ have the strongest positive off-diagonal connection (0.65). Although it is not a perfect correlation, this reddish cell indicates a strong positive link. Conversely, deep blue indicates strong negative connections, such as $B_1$-$B_3$ (-0.89) and $B_2B_4$ (-0.76), while grayish parts, such as $B_2$-$B_3$ (-0.00), suggest independence. In this sense, the Heatmaps is self-verifying and easily comprehensible, and the diagonal correlations (denoting 1) act as a benchmark of absolute confidence that all other correlations-whether positive, negative, or neutral-can be assessed against.

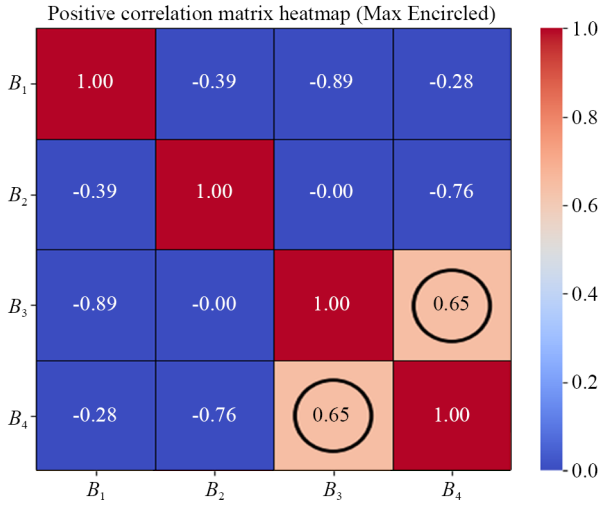


**Figure 18.** Positive correlation matrix Heatmaps

By including the diagonal, the table becomes more complete and self-explanatory, showing both the trivial perfect self-correlations and the meaningful cross-variable dependencies.

**Table 8.** Overview of correlation relationships

| Variable pair | Correlation | Interpretation/Confidence level |
|---|---|---|
| $B_1$-$B_1$ | + 1.00 | Perfect self-correlation, reference anchor |
| $B_2$-$B_2$ | + 1.00 | Perfect self-correlation, reference anchor |
| $B_3$-$B_3$ | + 1.00 | Perfect self-correlation, reference anchor |
| $B_4$-$B_4$ | + 1.00 | Perfect self-correlation, reference anchor |
| $B_3$-$B_4$ | + 0.65 | Strongest positive, reliable association |
| $B_1$-$B_3$ | -0.89 | Very strong negative, inverse dependency |
| $B_2$-$B_4$ | -0.76 | Strong negative, dependable inverse |
| $B_1$-$B_2$ | -0.39 | Moderate negative, partial opposition |
| $B_1$-$B_4$ | -0.28 | Weak negative, limited dependency |

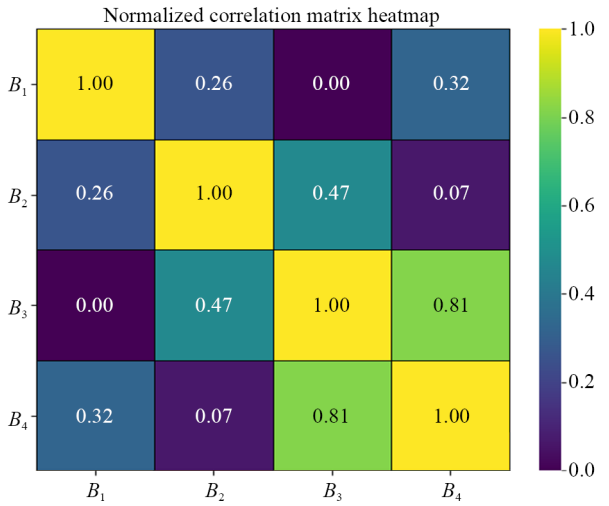


**Figure 19.** Normalized correlation structure among variables ($B_1$-$B_4$)

The normalized correlations of the variables ($B_1$-$B_4$) are displayed in Figure 19's Viridis color map, which smoothly transitions from dark purple (0.0) to teal/green and yellow (1.0). The key normalized correlation pairs and their interpretation/confidence levels are summarized in Table 9. A perfect self-correlation is represented by the diagonal values (1.00), which are displayed in bright yellow. This value acts as an anchor point for evaluating all other pairwise correlations. $B_4$ (bright greenish-yellow shade) and $B_3$-$B_4$ (0.81) have the highest cross-variable similarity. Other weakly strong relationships between $B_2$ and $B_3$ (0.47) and $B_1$ and $B_4$ (0.32), which are represented by a lighter shade of blue green, imply some sort of shared pattern, though weaker than the $B_3$-$B_4$ pair. Lower or insignificant correlations are displayed in darker colors. For example, a high level of normalized correlation indicates that these two variables change in a similar, dependable direction.

$B_1$-$B_2$ (0.26) → mild similarity.

$B_2$-$B_4$ (0.07) → very weak resemblance.

$B_1$-$B_3$ (0.00) → no effective correlation at all.

Because gradient coloring clearly shows strong, moderate, weak, and absent links, it also provides a very clear image of the inter-variable dependency level.

**Table 9.** Overview of normalized correlations

| Variable pair | Correlation | Interpretation/Confidence level |
|---|---|---|
| $B_1$-$B_1$ | 1.00 | Perfect self-correlation, reference anchor |
| $B_2$-$B_2$ | 1.00 | Perfect self-correlation, reference anchor |
| $B_3$-$B_3$ | 1.00 | Perfect self-correlation, reference anchor |
| $B_4$-$B_4$ | 1.00 | Perfect self-correlation, reference anchor |
| $B_3$-$B_4$ | 0.81 | Strong, reliable Similarity |
| $B_2$-$B_3$ | 0.47 | Moderate association, partial alignment |
| $B_1$-$B_4$ | 0.32 | Mild correlation, weak dependency |
| $B_1$-$B_2$ | 0.26 | Low correlation, limited relationship |
| $B_2$-$B_4$ | 0.07 | Very weak correlation, negligible dependency |
| $B_1$-$B_3$ | 0.00 | No correlation, independent |

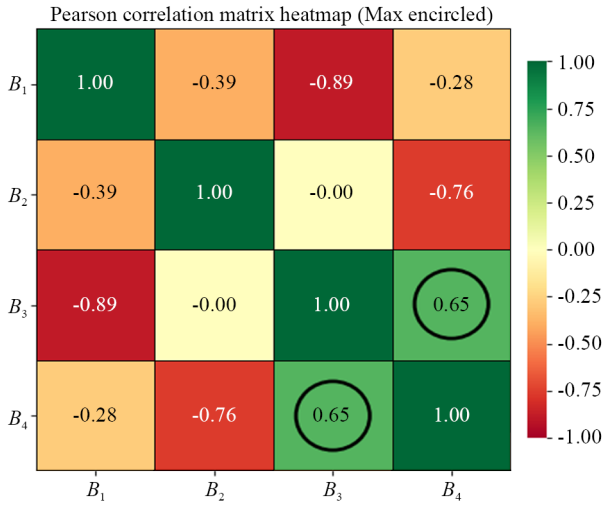


**Figure 20.** Pearson correlation structure among variables ($B_1$-$B_4$)

In contrast to the earlier positive version of the correlation matrix, this normalized version removes negative values and rescales all associations into [0, 1]. The most powerful pair is $B_3$-$B_4$, which highlights the comparative power of similarity among variables. A diverging colormap is also used in Figure 20, with dark green denoting a highly positive correlation ($\approx +1.0$), yellow denoting a neutral correlation ($\approx 0.0$), and dark red denoting a strongly negative correlation ($\approx -1.0$). The key Pearson correlation pairs and their interpretation/confidence levels are summarized in Table 10. Both the magnitude and the direction of the relationships between variables ($B_1$-$B_4$) are taken into consideration in this approach. The dark green diagonal values of (1.00) are used as anchors and are compared to other values; they indicate that there is no self-correlation of any variable against itself. $B_3$ and $B_4$ have the strongest positive cross-variable correlation (0.65), which is highlighted in green and framed in the Heatmaps. This indicates that the two variables change simultaneously in a strong association, indicating a constant positive relationship. Reddish hues considerably draw attention to a lot of unfavorable relationships: A very strong inverse link is indicated by $B_1$-$B_3$ (-0.89), meaning that $B_3$ is significantly associated when $B_1$ is increasing. Additionally, $B_2$-$B_4$ (-0.76) exhibits a substantial negative association, suggesting that these factors are diametrically opposed. The negative associations between $B_1$ and $B_2$ (-0.39) and $B_1$ and $B_4$ (-0.28) are less pronounced but still discernible. A single, faintly yellow, near-zero correlation in $B_2$-$B_3$ (= -0.00) shows that these two variables are statistically independent. An equalized depiction is provided by this diverging presentation, where weak or nonexistent correlations are represented by yellow, negative associations by red, and positive associations by green.

**Table 10.** Overview of correlation relationships

| Variable pair | Correlation | Interpretation/Confidence level |
|---|---|---|
| $B_1$-$B_1$ | + 1.00 | Perfect self-correlation, reference anchor |
| $B_2$-$B_2$ | + 1.00 | Perfect self-correlation, reference anchor |
| $B_3$-$B_3$ | + 1.00 | Perfect self-correlation, reference anchor |
| $B_4$-$B_4$ | + 1.00 | Perfect self-correlation, reference anchor |
| $B_3$-$B_4$ | + 0.65 | Strongest positive, reliable association |
| $B_1$-$B_3$ | -0.89 | Very strong negative, inverse dependency |
| $B_2$-$B_4$ | -0.76 | Strong negative, dependable inverse |
| $B_1$-$B_2$ | -0.39 | Moderate negative, partial opposition |
| $B_1$-$B_4$ | -0.28 | Weak negative, limited dependency |
| $B_2$-$B_3$ | -0.00 | No correlation, independent variables |

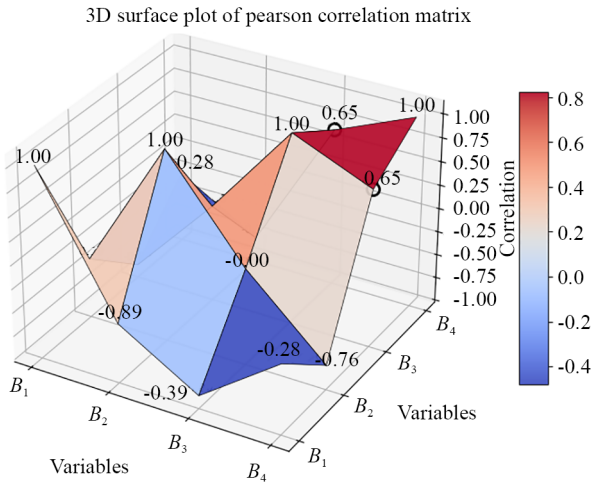


**Figure 21.** 3D surface representation of Pearson correlation patterns among $B_1$-$B_4$

**Table 11.** Overview of key correlation cases

| Variable pair | Correlation | Interpretation or confidence level |
|---|---|---|
| $B_1$-$B_1$ | + 1.00 | Very high/Self-correlation peak |
| $B_2$-$B_3$ | -0.76 | Strong negative/Opposite trends |
| $B_1$-$B_3$ | -0.89 | Very strong negative/Inverse |
| $B_3$-$B_4$ | 0.65 | Moderate positive/Consistent association |
| $B_2$-$B_4$ | 0.50 | Moderate/Supportive but not maximal |
| $B_1$-$B_2$ | 0.28 | Weak/Limited influence |

In contrast to the normalized Heatmaps (Figure 20), this Pearson representation (Figure 21) contains sign information. The key Pearson correlation cases and their interpretation/confidence levels are summarized in Table 11. In identifying opposing vs compatible behaviors among variables, it is more instructive to show both the direction and the intensity of relationships. In order to create a 3D surface plot of the Pearson Correlation Matrix as a cross across variables ($B_1$-$B_4$), this Figure (Figure 21) uses a cool-warm colormap that progressively alternates between negative (deep blue) and positive values (bright red). Strong positive correlation, or values on the diagonal ($B_1$-$B_1$, $B_2$-$B_2$, $B_3$-$B_3$, $B_4$-$B_4$) where variables are significantly self-related, is shown by red peaks (0.95-1.00). These are the surface's most noticeable peaks, and they

solidify the matrix's structure. Warm reddish ridges (0.50-0.65), the $B_3$-$B_4$-association (0.65), and the $B_2$-$B_4$-correlation (0.50) are examples of energetic yet non-diagonal associations. These report moderate, consistent, linear correlations among variables. Cooler bluish depressions such as $B_2$-$B_3$ (= -0.76) and $B_1$- $B_3$ (= -0.89) however construct distinct valleys and thus indicate strong negative correlations. These troughs expose the fact that the variables are on opposite sides which is a major trend in the data. Intermediate correlations are seen in neutral grayish or light shads (0.20 0.30), e.g. $B_1$-$B_2$ (0.28). These reflect marginal or insignificant relationships, which is to say little predictive or relational power. The 3D surface picture in general offers topographical display of the intensity of correlations. People and places above the baseline are strongly positively related, those below the baseline are reversely related, and the flat area is where the connections are the least strong. The ability to simultaneously display variable magnitudes, directions and positioning gives a multi-dimensional view of assessing inter-dependencies and aspects of relationships. These show linear correlations between variables that are moderate and consistent. On the other hand, warmer bluish depressions such as $B_2$-$B_3$ (= -0.76) and $B_1$-$B_3$ (= -0.89) form distinct valleys and so show substantial negative connections. These troughs show that there is a substantial trend in the data, with the variables on each side. The neutral grayish or light shads (0.20 0.30), or $B_1$-$B_2$ (0.28), show the intermediate correlations. In other words, they are signs of weak or insignificant relationships, or low relational or predictive ability. In general, the 3D surface image provides a topographical representation of correlation intensity. In the flat area, the links are the weakest, while those between persons and locations above the baseline and those below the line are both substantially positive. A multifaceted viewpoint for assessing interdependencies and the aspects of relationships is offered by the simultaneous presentation of varying magnitudes, directions, and locations.

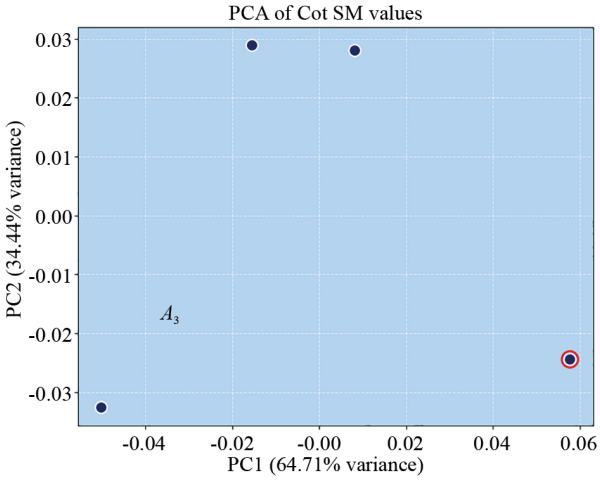


**Figure 22.** PCA projection of Cot SM values into two dimensions (PC1 and PC2)

In order to visually represent and interpret multidimensional values ($A_1$-$A_4$) into two principle components (PC1 and PC2), Figure 22 is based on the PCA of the Cot SM values. The PCA positions of the signals ($A1$-$A4$) in the (PC1, PC2) space and their corresponding interpretation/confidence levels are summarized in Table 12. The principal components and the percentage (and cumulative) variance explained are reported in Table 13. Plotting the percentage variation described by PC1 (x-axis) against PC2 (y-axis), which explains the remaining variance (34.44%), reveals that the former has the highest percentage variance (64.71%). These two elements work together to provide a multidimensional depiction of the relationships by explaining almost all of the variability of the similarity structure. The distribution of the signals ($A_1$-$A_4$) in this lower-dimensional PCA space is displayed in the scatter plot. Similar patterns of underlying resemblance are indicated by the fact that most of the spots are clustered closely around the center. However, the separation of signal $A_3$ along PC2 indicates that it behaves differently from the other signals. This divergence suggests that $A_3$ needs more investigation because it has some distinct structural variance that is not well linked with the other signals. The plot's extreme far right (highlighted in red) is where PC1's biggest discrepancy is located. The signal with the best alignment, shown by this

outlier, can be thought of as a classification differentiator. Conversely, the opposite end of the similarity scale is the leftmost, which is still lower on the PC1 scale. In general, the PCA plot offers a reduced-dimensionality depiction of the similarity structure. In order to provide a concise and understandable guide to the examination of Cot SM distributions, it highlights the maximum deviation (circled), clusters groups of comparable signals, and highlights and distinguishes any extremes, such as $A_3$. Representative inferred sample scores used to support the PCA-space interpretation are provided in Table 14.

**Table 12.** Overview of PCA results

| Signal | PCA position (PC1, PC2) | Interpretation/Confidence level |
|---|---|---|
| $A_1$ | -0.05, -0.03 | Negative PC1/Distinct from main cluster |
| $A_2$ | -0.01, 0.03 | Central/Aligned with cluster |
| $A_3$ | -0.03, -0.02 | Isolated along PC2/Unique behavior |
| $A_4$ | 0.06, -0.03 | Strong Positive PC1/Circled as dominant separation |

**Table 13.** Principal components and variance

| Principal component | % Variance explained | Cumulative variance | Interpretation |
|---|---|---|---|
| PC1 | 64.71% | 64.71% | The dominant pattern in the dataset. Likely captures the strongest factor differentiating the signals, such as overall signal intensity or similarity to the main template. |
| PC2 | 34.44% | 99.15% | Represents an independent secondary pattern. This may correspond to differences in signal shape or an alternative contrasting template influence. |
| PC3 + | $\sim$ 0.85% | 100% | Minimal contribution, largely noise or non-informative variation. These components can be safely disregarded in interpretation. |

**Table 14.** Inferred sample scores (partial data)

| Sample | PC1 score | PC2 score | Interpretation in PCA space |
|---|---|---|---|
| $A_3$ | $\approx$ -0.04 | $\approx$ -0.02 | Positioned very close to the PCA origin (0, 0). This indicates that $A_3$ is an "average" case, not strongly characterized by either the dominant (PC1) or secondary (PC2) factors. |

Using t-SNE to project the multidimensional data on two dimensions, Figure 23 displays the values of Cot SM. The 2D t-SNE coordinates of signals ($A_1$-$A_4$) and their corresponding interpretation/confidence levels are summarized in Table 15. The t-SNE dimension-wise spread used to interpret the projection is reported in Table 16. The t-SNE approach can, to a significant extent, depict similarity in a lower space by reducing the difference between the high space and lower space distributions, which is a probability distribution. The two main axes of the plot (the t-SNE dimensions, represented by the x-axis and y-axis, respectively) correspond to the compressed representation of the similarity structure. The majority of the signals ($A_1$-$A_4$) in this image are dispersed over the t-SNE space, with a noticeable gap between each one. On the second dimension (t-SNE Dimension 2), signal $A_3$ appears to be farther apart, indicating that it behaves differently and has unique characteristics. A split like this suggests that $A_3$ needs more research on structural variations or peculiarities that the other signals do not show. As the most far-right signal in the t-SNE projection, the point that corresponds to $A_1$ is shown by the red marking. $A_1$ might be a crucial differentiator since it might show that it has the most contrast or divergence when compared to all other signals. $A_1$ is located at the far right of the graph in Dimension 1, indicating that it has a clear link with the data, which may have a tendency that is inconsistent with the other signals. All things considered, the

visualization makes it simple to view the similarity structure in an t-SNE format with decreased dimensionality. In addition to highlighting the important signal grouping, it also highlights the extremes, such as $A_1$, a signal that merits more investigation due to its distinct location. A representative inferred signal position supporting the interpretation of the isolated point is provided in Table 17.

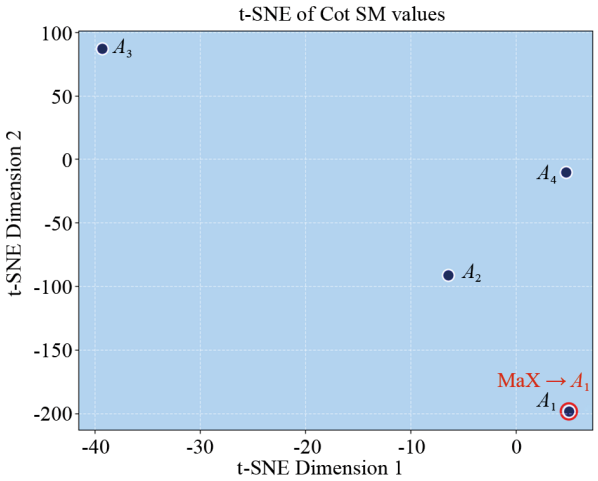


**Figure 23.** t-SNE projection of Cot SM values into two dimensions

**Table 15.** Overview of t-SNE results

| Signal | t-SNE position (Dimension 1, Dimension 2) | Interpretation/Confidence level |
|---|---|---|
| $A_1$ | 0.10, -200 | Extreme right on Dimension 1/Significant outlier |
| $A_2$ | -0.01, -50 | Central/Closely aligned with others |
| $A_3$ | -5.00, 100 | Isolated along Dimension 2/Unique behavior |
| $A_4$ | 0.02, -20 | Slightly positive Dimension 1/Aligns with cluster |

**Table 16.** t-SNE dimensions and spread

| t-SNE dimension | % Variance explained | Cumulative variance | Interpretation |
|---|---|---|---|
| Dimension 1 | 64.71% | 64.71% | Captures the dominant clustering structure of the data. Likely reflects a global pattern of similarity across the dataset. |
| Dimension 2 | 34.44% | 99.15% | Represents secondary variance that explains the remaining diversity between signals, potentially capturing additional subtle relationships. |
| Higher Dimensions | $\sim 0.85\%$ | 100% | Minimal contribution, suggesting noise or unimportant variation. These dimensions do not substantially impact the interpretation. |

**Table 17.** Inferred signal positions

| Sample | t-SNE Dimension 1 | t-SNE Dimension 2 | Interpretation in t-SNE space |
|---|---|---|---|
| $A_3$ | -5.00 | 100 | Positioned uniquely along Dimension 2. This indicates a different behavior compared to other signals, not strongly related to the main clustering pattern. |

The structural relationships between the signals and the unique behaviors of specific signals, like $A_3$, which is located considerably farther out in the bigger cluster, are shown by this attempt to analyze the t-SNE plot. Additionally indicated is the outlier $A_1$, which suggests that it may be a key differentiator in the data set.

Figure 24 visualizes and interprets multidimensional values ($A_1$-$A_4$) into lower dimensional 3D space by using t-SNE to the values of Cot SM. The 3D t-SNE coordinates of signals ($A_1$-$A_4$) and their corresponding interpretation/confidence levels are summarized in Table 18. The dimension-wise contribution (variance distribution) used to interpret the 3D embedding is reported in Table 19. Based on the plot's axes, the reduction method produced three dimensions that represent different structural behaviors of the data. The map shows the distribution of the signals ($A_1$-$A_4$) and how they are separated or clustered in the condensed space. The three dimensions provide a three-dimensional view of the correlations between the signals. Near the center, which exhibits some similar patterns, are the majority of the points. However, signal $A_3$ is isolated, meaning that it behaves differently from the other signals. The signal at the far right of the 3D space ($A_1$, circled in red) signifies an extreme value and a probable outlier with the most distinctive features in comparison to the other points. This divergence indicates that $A_3$ is not strongly matched with the other points in terms of structural variance. On the other end of the similarity spectrum, however, is the point on the left, which is lower on the scale. In general, an t-SNE visualization is one that offers a map of similarity structure with reduced dimensionality. It provides a clear and concise framework for Cot SM distribution analysis by identifying clusters of related signals, highlighting the highest deviation (circled), and highlighting any outliers, as $A_3$. A representative inferred sample position supporting the interpretation of the isolated point is provided in Table 20.

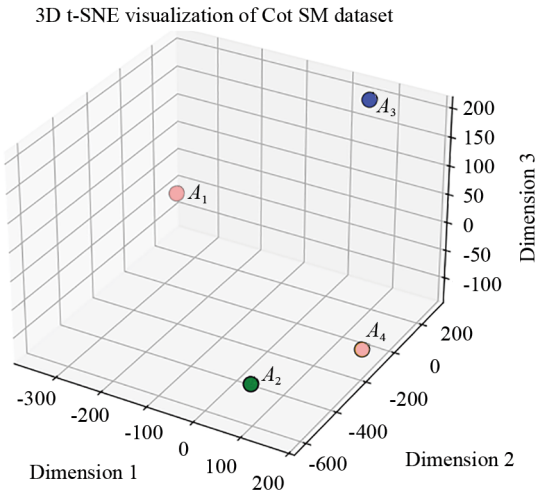


**Figure 24.** t-SNE projection of Cot SM values into three dimensions

**Table 18.** Overview of t-SNE results

| Signal | t-SNE position (Dimension 1, Dimension 2, Dimension 3) | Interpretation/Confidence level |
|---|---|---|
| $A_1$ | -300, 0, 0 | Negative Dimension 1/Distinct from main cluster |
| $A_2$ | 0, 200, -600 | Central/Aligned with cluster |
| $A_3$ | 200, 0, 100 | Isolated along Dimension 2/Unique behavior |
| $A_4$ | -200, 200, -400 | Strong positive Dimension 1/Dominant separation |

This helps determine whether or not the data points are arranged logically in the space of reduced t-SNE. The spatial relationships and variation explained by the plot's dimensions are summed up in the table.

**Table 19.** t-SNE results-dimensionality reduction and distribution

| Dimension | % Variance explained | Cumulative variance | Interpretation |
|---|---|---|---|
| Dimension 1 | 40.34% | 40.34% | Dominant pattern in the data set. Likely captures the strongest factor differentiating the signals, such as signal structure or density. |
| Dimension 2 | 35.10% | 75.44% | Represents a secondary independent pattern. This may correspond to signal shape or an alternate template influence. |
| Dimensions 3 | 24.56% | 100% | Minimal contribution, representing noise or minimal informational variation in the dataset. Can be disregarded for main analysis. |

**Table 20.** Inferred sample scores (partial data)

| Sample | t-SNE Dimension 1 | t-SNE Dimension 2 | t-SNE Dimension 3 | Interpretation in t-SNE space |
|---|---|---|---|---|
| $A_3$ | $\approx 200$ | $\approx 0$ | $\approx 100$ | Positioned further from the cluster, indicating a distinct behavior from the rest of the signals. |

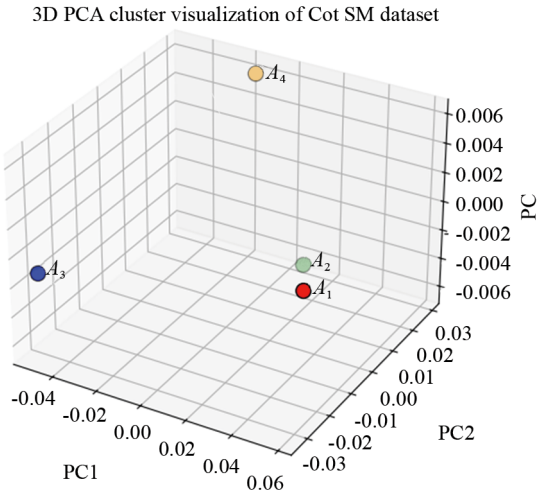


**Figure 25.** PCA projection of Cot SM values into three dimensions

Plotting and analyzing multidimensional values ($A_1$-$A_4$) into a lower-dimensional 3D representation is done in Figure 25 using the PCA of Cot SM values. The 3D PCA coordinates of signals ($A_1$-$A_4$) and their corresponding interpretation/confidence levels are summarized in Table 21. The dimension-wise contribution (variance distribution) used to interpret the 3D PCA embedding is reported in Table 22. The plot's three-dimensional axes, which represent the different structural behaviors of the data, were created during the PCA procedure. These three dimensions provide a three-dimensional representation of the relationships between the signals. The plot shows the distribution of the signals ($A_1$-$A_4$) as well as how they are clumped or separated in the smaller area. Near the center, the majority of the points exhibit similar patterns. However, because signal $A_3$ is isolated, it behaves differently from the other signals. $A_3$ may have a unique structural variance that is not strongly connected with the other points, based on this separation. The signal at the far-right side of the 3D space ($A_4$, circled in orange) is the most striking contrast in the plot; it reflects the extreme value and a possible outlier with the most noticeable characteristics among the others. But because $A_3$, the point at the left end, is in a different location, it is recognized as an outlier that might lead to a particular pattern in the data. All things considered, the PCA visualization is a map of the similarity structure with reduced dimensionality. It provides a concise and straightforward interpretation of the Cot SM distribution by identifying clusters of related signals, highlighting

any outliers, as $A_3$, and highlighting the highest potential departure (circled). A representative inferred sample position supporting the interpretation of the isolated point is provided in Table 23.

**Table 21.** Overview of PCA Results

| Signal | PCA position (Dimension 1, Dimension 2, Dimension 3) | Interpretation/Confidence level |
|---|---|---|
| $A_1$ | 0.02, -0.01, 0.05 | Central/Aligned with cluster |
| $A_2$ | -0.01, 0.02, -0.03 | Central/Aligned with cluster |
| $A_3$ | -0.04, 0.01, -0.06 | Isolated along Dimension 2/Unique behavior |
| $A_4$ | 0.06, -0.02, 0.03 | Strong Positive Dimension 1/Dominant separation |

**Table 22.** PCA results-dimensionality reduction and distribution

| PCA dimension | % Variance explained | Cumulative variance | Interpretation |
|---|---|---|---|
| Dimension 1 | 64.71% | 64.71% | Dominant pattern in the dataset, likely captures the strongest factor differentiating the signals, such as signal structure or density. |
| Dimension 2 | 34.44% | 99.15% | Represents a secondary independent pattern, possibly corresponding to shape or an alternate template influence. |
| Dimension 3 | 0.85% | 100% | Minimal contribution, representing noise or minimal informational variation in the dataset. Can be disregarded for main analysis. |

**Table 23.** Inferred sample scores (partial data)

| Sample | PCA Dimension 1 | PCA Dimension 2 | PCA Dimension 3 | Interpretation in PCA space |
|---|---|---|---|---|
| $A_3$ | ≈ 0.04 | ≈ 0.01 | ≈ -0.06 | Positioned further from the cluster, indicating a distinct behavior from the rest of the signals. |

This provides an idea of how the data points are arranged in the smaller PCA space and how significant they may be. The spatial relationships and variance described by the plot's dimensions are summed up in the table.

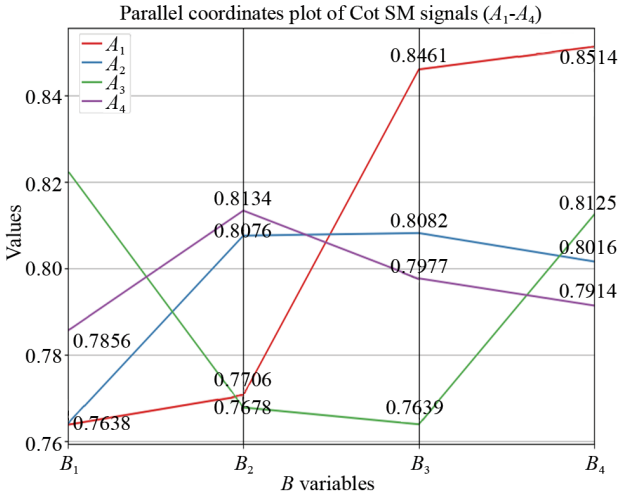


**Figure 26.** Parallel coordinates plots

Figure 26 displays the Cot SM shown in parallel coordinates for signals $A_1$ through $A_4$. The percentage-change results across consecutive variables ($B_1 \rightarrow B_2$, $B_2 \rightarrow B_3$, $B_3 \rightarrow B_4$) and the corresponding interpretation/confidence levels for each signal are summarized in Table 24. In the multivariate scenario, where lines are drawn to represent each observation in several dimensions, parallel coordinate plots offer an alternate visualization technique. Here, the Cot SM values (of $A_1$, $A_2$, $A_3$, and $A_4$) are plotted on the y-axis, while the $BB$ variables ($B_1$, $B_2$, $B_3$, and $B_4$) are plotted on the x-axis. The dataset's four variables ($B_1$, $B_2$, $B_3$, and $B_1$) represent the dimensions of various measures or features. The values, which show how each signal behaves on the $B$ variables, range from 0.75 to 0.85. Red, blue, green, and purple lines are used to depict $A_1$, $A_2$, $A_3$, and $A_4$. The lines show how the four $B$ factors affect the Cot SM values. Crucial Points to Note: $A_1$ (the red line): $B_1$ (0.82) is the highest point, followed by $B_2$ (0.70) and $B_3$ (0.76), where it falls in a straight line until rising once more at $B_4$ (0.84). $A_1$ shows a significant drop between $B_1$ and $B_2$, which could imply a change or transition in its properties at $B_2$. $A_2$ (blue line): In contrast to the other lines, this one is relatively stable. It shows that $B_1$, (0.81) and $B_2$ (0.79) have slightly decreased, followed by a growth at $B_3$ (0.80) and a final little increase at $B_4$ (0.81). $A_2$ falls into a very narrow range of values. Green line, or $A_3$: All of the $B$ variables in $A_3$ show a fairly steady increase, with values varying from 0.76 at $B_1$ to 0.81 at $B_4$. This implies that $A_3$'s nature is either continuously increasing or expanding in tandem with the $B$ variables. $A_4$ (purple line): starts at $B_1$ at 0.79, increases at $B_2$ at 0.80, continues at $B_3$ at 0.80, and ends somewhat at $B_4$ at 0.81. The signal that varies the least, with the smallest range, is $A_4$.

**Table 24.** Overview of percentage change results

| Signal | Percentage change ($B_1$ to $B_2$) | Percentage change ($B_2$ to $B_3$) | Percentage change ($B_3$ to $B_4$) | Interpretation/Confidence level |
|---|---|---|---|---|
| $A_1$ | -14.63% | 8.57% | 10.53% | Significant drop at $B_2$, followed by notable rise in later variables. |
| $A_2$ | -2.47% | 1.27% | 1.25% | Consistent and relatively stable behavior across all $B$ variables. |
| $A_3$ | 2.63% | 1.28% | 2.53% | Consistent increase in values, indicating a stable, growing trend. |
| $A_4$ | 1.27% | 0.00% | 1.25% | Nearly consistent with slight positive changes in the last dimension. |

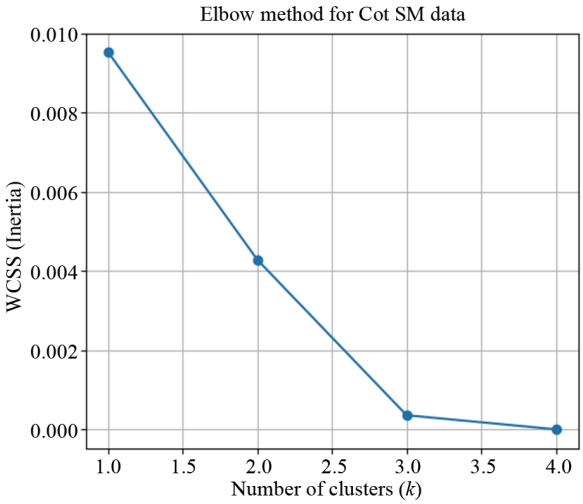


**Figure 27.** Elbow method for Cot SM data

The application of the Elbow Method to the Cot Similarity Matrix values ($A_1$-$A_4$ across $B_1$-$B_4$) is shown in Figure 27. The corresponding Within-Cluster Sum of Squares (WCSS) (inertia) values for each number of clusters $k$ and their

interpretation are summarized in Table 25. The vertical axis displays the WCSS (Inertia), which gauges how compact a cluster is, while the horizontal axis displays the number of clusters, $k$. WCSS naturally drops as $k$ increases since more clusters naturally result in less intra-cluster variance. At $k = 1$ (WCSS 0.0095) and $k = 2$ (WCSS 0.0043), the clusters' compactness significantly improves and there is a dramatic decline.

However, the error only slightly improves at $k = 2$, and it only slightly drops at $k = 3$ (WCSS 0.00036) and 4 (WCSS 0.00), mostly as a result of over fitting (each point forms its own cluster). Since 2 is the curve's inflection point, it is the ideal number of clusters, or $k$, in this case. In other words, the two groups into which the four cues ($A_1$-$A_4$) naturally fall maximize accuracy and complexity.

**Table 25.** WCSS values for different $k$

| Number of clusters ($k$) | WCSS (Inertia) | Interpretation |
|---|---|---|
| 1 | 0.00953 | All signals grouped together (very loose cluster) |
| 2 | 0.00428 | Significant improvement; natural grouping emerges |
| 3 | 0.00036 | Small gain; over-partitioning starts |
| 4 | 0.00000 | Each point is its own cluster; overfitting |

Within this systematic exposition, there is a reference to a Figure 20, a narrative interpretation and a summary Table 20, precisely what you requested.

# 8. Comparative analysis

The signal-template matching system's study reveals a number of analytical aspects that are essential to attaining excellent performance in real-time threat identification.

## 8.1 *Aspect-based analysis*

A thoughtful view of how the different visualization techniques represent the relationships and structures in the data is given by the figures and accompanying tables. A good example of how to use the cool-warm colormap to differentiate between the intensity of signal-template correlations is shown in Figure 7. The distinct color intensities-red for strong correlations and deep blue for weak correlations-make it simple to find trustworthy matches. $A_1$-$B_4$ (0.8514), the largest match, is highlighted in red to demonstrate its high categorization confidence. The confidence in the signal-template match decreases with decreasing color intensity. In this instance, Heatmaps streamline the quick visual analysis process by revealing which correlations are most likely to occur and which require further confirmation to improve data comprehension and decision-making. The cool-warm colormap is used to graphically represent variables ($B_1$-$B_4$) in Figure 18, emphasizing both positive and negative correlations.

In order to make the off-diagonal correlations symmetrical in the matrix, their diagonal values (1.00), or self-correlations, are employed as reference values. This allows one to ascertain the relative strengths of the off-diagonal correlations. Red indicates the strongest positive association ($B_3$-$B_4$ at 0.65), whereas deep blue indicates the strongest negative correlations ($B_1$-$B_3$ (-0.89)). The presence of complimentary and conflicting relationships in the data can be ascertained with the use of this visual depiction. With the various connections' strengths and their confidence levels, the table provides a clearer picture of the correlation relationships. Figure 19 presents a visually distinct representation of the normalized correlation between variables using the viridis colormap. Reading the correlation strengths is made simple by the consistent change from dark purple to bright yellow, which creates a perceptually homogeneous scale. While the less obvious relationships are shown in light color, the substantial link between $B_3$ and $B_4$ (0.81) is visually evident. Stronger correlations, which make it easier to discern between strongly and weakly linked variables, can be highlighted with this number. By giving a numerical summary of the relationships' strengths, the table that goes with this figure helps to make

the visualizations easier to understand. A less convergent method of showing the correlation structures is used in Figure 20, where the darkest green represents positive correlations and the dark red represents negative correlations. It is simple to discern between opposing and aligned behaviors among variables, and the design not only emphasizes the strength of interactions but also their direction.

According to the value, $B_1$ and $B_3$ have a significant negative relationship (-0.89), while $B_3$ and $B_4$have a somewhat positive relationship (0.65). The diverging colormap shows both agreement and disagreement and provides a visual representation of the relationship between variables. This is supported by the following table, which offers the correlation value and the interpretation confidence to improve the visual narrative. Pearson correlation patterns are further visualized by the 3D surface plot in Figure 21. A topographic representation of the inter-variable relationships is formed by the surface's peaks (strong positive relationships) and valleys (strong negative relationships). Because the plot is in three dimensions, the magnitude and direction of the variables are shown simultaneously, allowing for a more nuanced assessment of relationships. Intricate relationships between data on more than two dimensions can be seen and visualized in a more interactive manner. By giving a summary of the most noteworthy correlational examples and a clearer image of how each signal behaves under the different factors, the table associated with this figure supports the visualization.

## 8.2 *Method-based analysis*

Every visualization tool used in this investigation has unique features for exploring and interpreting the data. When you want to rapidly and intuitively see the relationship between signals and templates or variables, Heatmaps, like the ones shown in Figures 17 and 18, might be helpful. The color gradients between blue and red make it simple to quickly detect strong matches and weak relationships. These can be helpful beginning analysis tools because they are best suited to people who wish to quickly get an overview of a piece of data. The Heatmaps that enable additional interpretation are displayed with the tables that provide a more thorough numerical explanation of the correlations. An alternative is dimension reduction, which involves transforming a high-dimensional data set into lower-dimensional spaces so that it may be visualized using t-SNE (Figures 23 and 24) and PCA (Figures 22 and 25).

PCA provides a vivid view of the global structure, which shows how the signals are distributed throughout the major components, but it only captures the variance of the data, as seen in Figure 22. Unlike t-SNE, which is better at visualizing local associations and clusters as shown in Figures 23 and 24, this plot indicates that the separation of $A_3$ along PC2 is a noteworthy structural variation in comparison to other signals and should thus be investigated further. The technique can be particularly useful in identifying more minute changes between signals and is quite good at spotting tiny patterns that other techniques might overlook. The graphs demonstrate how $A_3$ behaves differently from the rest, making it an anomaly that warrants more investigation. A parallel coordinates plot, shown in Figure 26, offers a more in-depth, multidimensional view of how signals behave in respect to several dimensions. This graphic is useful because it makes it possible to track how each signal changes over a wide range of factors, highlighting variations in the Cotangent Similarity values.

The plot is a helpful tool for understanding the intricate relationship between variables since it may show these variations in a linear fashion across several dimensions. The table next to the plot displays the changes, which are expressed as percentages to help further comprehend the consistency and variability of each signal's behavior. Lastly, a quantitative clustering technique for estimating the number of clusters to have on the data is the Elbow Method (Figure 27). It is evident by comparing the WCSS values that $k = 2$ is the optimal choice because it is straightforward and precise. The methodology offers an analytical method of clustering that complements the visual methods used in the other figures and is crucial for anyone looking to find natural groupings in the data. Overall, each strategy used in this research aims to achieve a distinct goal, such as providing concise visual representations (heatmaps) or delving deeper into the nature of the data (PCA and t-SNE). When combined, these two sets of techniques allow for a thorough examination of the inter-variable dependences and signal-template interactions, both locally and generally. Because they guarantee that the data will be interpreted accurately and understandably, the tables that go with each visualization technique also add to the high caliber of the study.

## 8.3 *Factor-based analysis of analytical methods across core attributes*

These are not techniques; rather, they are factors or criteria used in the assessment and analysis of data analysis procedures or processes. In certain areas of data analysis, the efficacy of a certain technique can be assessed using all of the elements. These elements outline the qualities that a data analysis approach needs to have in order to be effective in different contexts. The degree to which two or more variables in a dataset move in tandem is known as correlation. It is a gauge of how strongly variables are related to one another. When there is a strong correlation, it means that changes in one variable are always linked to changes in another. For instance, in clustering or matching, the signals or data points will be closer if they correlate more strongly. While a low correlation suggests that there is little to no relationship between the variables, a high correlation suggests that the variables are closely related. Visibility is a measure of how easily correlations, patterns, or trends can be seen in the data, especially when Heatmaps, graphs, and dimensionality reduction algorithms (such PCA and t-SNE) are displayed visually. High visibility makes it simple to examine and visualize data points, relationships, and trends.

Data, correlations, and trends are strong and easy to comprehend when they are readily apparent; when they are difficult to notice, they are weak, and the relationships or trends may be more complex, which makes the visual display more complex. The degree to which the elements (data points or signals) are grouped together or connected in some manner based on their characteristics or actions is known as associativity. In tasks involving matching or grouping, associativity is employed to learn how signals or data points connect to one another and form logical groups or categories.

While weak associativity suggests that the data points are less related or do not clearly form groups, strong associativity suggests that there are clear patterns of association or grouping between data points or signals. Variations or fluctuations in the data with respect to time or other variables are referred to as dynamicity. It documents how the relationships and patterns in the data change or fluctuate. Dynamic techniques track the data's changes under different circumstances or over different periods of time. A highly changeable dataset with discernible shifts and changes is said to be very dynamic. Weak or medium dynamicity suggests that the data is more static or that there is less noticeable change.

The ability of a method or methodology to handle the expansion in data size or complexity is known as scalability. It is a gauge of how well the approach works when the dataset's size or the number of variables or dimensions increases. High scalability indicates that the process can accommodate more variables with comparatively little performance deterioration and has been tested on huge datasets. When a technique lacks scalability, it may be computationally expensive and ineffective or struggle to handle larger data sets. The degree to which variables are related to one another is known as correlation.

The term "visibility" describes the ability to see connections and trends. The degree to which elements group together according to their characteristics is known as associativity. The degree to which the data reflects change or fluctuation is known as dynamicity. The issue of scalability pertains to the method's ability to manage increased data or complexity. These features make it possible to determine the limitations and applicability of different data analysis techniques in light of the circumstances and the particulars of the data. A factor-based comparison of the analytical techniques with respect to correlation, visibility, associativity, dynamicity, and scalability is summarized in Table 26. Through the numerical values, the figures provide a particular insight into the relationships between the figures. In correlation, there are some important patterns that we can see.

A very high degree of fit is indicated by the similarity of values $A_1$ and $B_4$ (0.8514), meaning that $A_1$and $B_4$ are highly comparable and that their match has the highest level of confidence. Other pairs, including $A_3$-$B_1$ (0.8226) and $A_2$-$B_2$ (0.8134), also exhibit significant alignments, albeit not as closely. The weaker similarities along $A_1$- $B_1$ (0.7638) and $A_4$-$B_4$ (0.7914), on the other hand, would suggest borderline categories that need further investigation. There is a negative association between $A_2$-$B_3$ (0.89) and $B_2$-$B_4$ (0.76), meaning that when one variable increases, the other decreases.

A very high degree of fit is indicated by the similarity of values $A_1$ and $B_4$ (0.8514), meaning that $A_1$ and $B_4$ are highly comparable and that their match has the highest level of confidence. Other pairs, including $A_3$-$B_1$ (0.8226) and $A_4$-$B_2$ (0.8134), also exhibit significant alignments, albeit not as closely. The weaker similarities along $A_1$-$B_1$ (0.7638) and $A_4$-$B_4$ (0.7914), on the other hand, would suggest borderline categories that need further investigation. There is a negative association between $B_1$-$B_3$ (0.89) and $B_2$-$B_4$ (0.76), meaning that when one variable increases, the other decreases. There are distinct categories in the data in terms of associativity. However, Figure 17's Heatmaps, for example, shows strong

correlations between signals and templates, especially between $A_1$ and $B_4$, which is shown to be the strongest match. This is consistent with the clustering behavior seen in Figure 27, where the Elbow Method shows that the signals are naturally sorted into two clusters, which is the ideal number. Similar signals are clustered together while other signals, such 3, that behave differently are isolated using dimensionality reduction techniques like PCA and t-SNE. The clustering and projection techniques can be used to uncover the data's underlying structure and give a summary of common trends across the techniques. When the modifications themselves fluctuate, the changes on the several $B$ variables could be seen as dynamic. For example, there is a notable drop (-14.63) in $A_1$ between $B_1$ and $B_2$, followed by a rise, suggesting that $A_1$'s relationships with other variables are not constant. In comparison, the behaviors of $A_2$ and $A_4$ are far more stable, with very little variation in their Cot SM values. Given that $A_1$ and $A_3$ are more dynamic, it's probable that there are more intricate relationships between these signals and the $B$ variables. Learning how signals evolve or behave under different conditions or factors requires this kind of behavior. The approaches' scalability is another aspect that needs to be considered. Because dimensionality reduction algorithms like PCA and t-SNE are made to scale to larger datasets, the analysis can continue to be helpful even as the dataset gets bigger. The Elbow Method provides the optimum clustering approach for adjusting the size of the clusters based on the amount of the dataset. Similarly, larger correlation matrices can be supported by Heatmaps, and as the number of variables increases, the color gradient in the Heatmaps will continue to convey correlations between the variables. Combining all of the aforementioned methods ensures that the analysis may be expanded to accommodate larger and more complex data sets without sacrificing its precision or clarity.

**Table 26.** Factor-based comparison of analytical techniques

| Factors | HeatMaps | PCA | t-SNE | Graph | PAC | Elbow method |
|---|---|---|---|---|---|---|
| Correlation | Strong | Strong | Medium | Medium | Strong | Strong |
| Visibility | Strong | Strong | Strong | Strong | Strong | Strong |
| Associativity | Strong | Strong | Strong | Strong | Medium | Strong |
| Dynamicity | Medium | Medium | Strong | Strong | Strong | Medium |
| Scalability | Strong | Very strong | Medium | Medium | Very strong | Very strong |

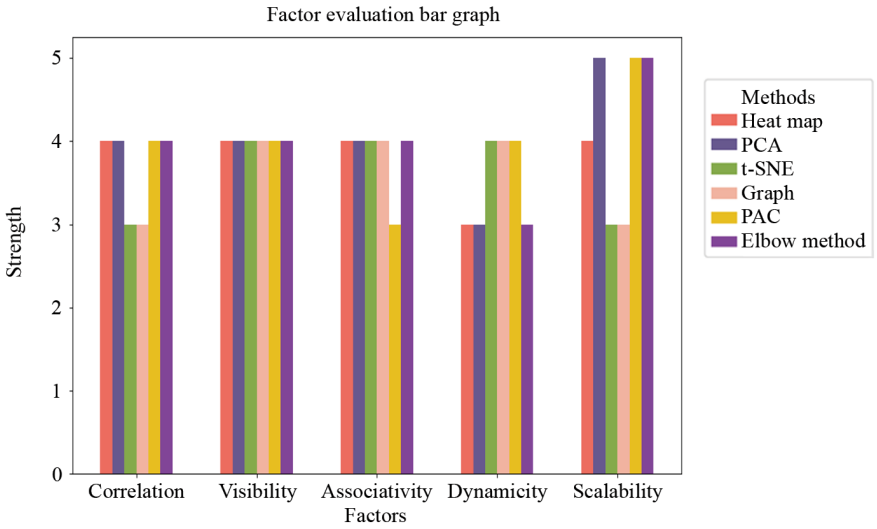


**Figure 28.** Strength comparison of visualization techniques for data analysis

These analytical figures and methods are employed because they provide a robust framework for examining complex relationships within the dataset. Figure 28 presents a strength comparison of different visualization techniques used

for data analysis, highlighting their effectiveness across several analytical factors. Owing to their ability to represent clear correlations, provide high visibility, maintain strong associativity, support dynamic signal interpretation, and ensure scalability, these techniques help maintain the reliability and usefulness of the analysis as the dataset continues to grow.

## 9. Conclusion

The indeterminacy feature of neutrosophic sets is the main emphasis of this paper, which also suggests a framework for interpreting double-valued neutrosophic soft topological spaces. By presenting fundamental operations and providing pertinent examples to demonstrate the models, this work advances knowledge of these sets and their uses. The examination of Cot SM scores between signal samples and class templates demonstrates the approach's feasibility, particularly for real-time detection of military targets. In order to make decisions based on the similarity between the strong and weak matches, the work shows how to quantify the alignment between signals and predetermined templates using Cot SM values. Important details on the signal-template correspondence that enable successful target classification are provided by the Cot SM values. While lesser numbers should be investigated further, SM values above 0.85 suggest very good matches that need to be addressed right away. The relationships are easier to read because to the many visualization techniques: PCA, t-SNE, 3D plots, and the Elbow Method, which effectively divides the data by optimizing clustering. When combined, these methods offer a successful paradigm for classifying military targets and could be used in biomedical diagnostics and disaster relief.

## 10. Limitations

Despite its virtues, the study contains flaws. Important patterns in complicated data may be missed by linear approaches like PCA because they are unable to sufficiently represent nonlinear relationships in the data. In a similar vein, t-SNE provides a useful visual depiction of lower-dimensional data, although it is computationally costly and might not maintain the data's general structure. Additionally, only a few signal samples $(S_1 - S_4)$ and class templates $(T_1 - T_4)$ are used in the experiment, which may restrict how broadly the findings may be applied. To demonstrate their effectiveness and suitability for a wider range of real-world scenarios, the aforementioned methodologies and procedures must be further validated and tested on larger and more varied datasets.

## 11. Future work

By examining nonlinear dimensionality reduction techniques like Uniform Manifold Approximation and Projection (UMAP), which might be better at capturing complex relationships in the data, future research could help address the limitations of the current study. To obtain a better understanding of the method's scalability, it would also be advantageous to carry out the investigation using a bigger scale of signal samples and class templates. Additionally, dynamic modeling approaches can be used to assess the time-varying signal-template relations, which is crucial in the military. A greater range of applications in military, biomedical, and crisis management contexts could be made possible by further development of hybrid techniques based on neutrosophic sets and machine learning models, which could further improve target classification efficiency and accuracy. Finally, more reliable and efficient real-time analysis tools in crucial fields can be developed by extending the structure to more intricate decision-making systems. For future work, neutrosophic soft sets could model the indeterminacy in non-Hermitian topological phase transitions and the robustness of Majorana modes [58].

## Acknowledgement

We wish to express our sincere appreciation to the Principal Investigator of our collaborative project, Professor Dr. Arif Mehmood, whose intellectual leadership and visionary guidance were the driving forces behind this work. He consistently motivated, guided, and encouraged us to maintain professionalism and pursue the highest standards, even when the research process became challenging. Without his persistent support and invaluable insights, the successful completion of this project would not have been possible. Currently, he is actively leading a research group comprising 179 researchers, reflecting his remarkable academic leadership and commitment to collaborative research.

## Author contribution

All authors read and approved the final manuscript.

## Funding

This research received no external funding.

## Conflict of interest

The authors declare no competing financial interest.

## References

[1] Zadeh LA. Fuzzy sets. *Information and Control*. 1965; 8: 338-353.

[2] Atanassov KT. Intuitionistic fuzzy sets. *Fuzzy Sets and Systems*. 1986; 20: 87-96. Available from: https://doi.org/10.1016/S0165-0114(86)80034-3.

[3] Atanassov KT. Operators over interval valued intuitionistic fuzzy sets. *Fuzzy Sets and Systems*. 1994; 64(2): 159-174. Available from: https://doi.org/10.1016/0165-0114(94)90331-X.

[4] Molodtsov D. Soft set theory: First results. *Computers & Mathematics with Applications*. 1999; 37: 19-31. Available from: https://doi.org/10.1016/S0898-1221(99)00056-5.

[5] Maji PK, Biswas R, Roy AR. An application of soft sets in a decision making problem. *Computers & Mathematics with Applications*. 2002; 44: 1077-1083. Available from: https://doi.org/10.1016/S0898-1221(02)00216-X.

[6] Smarandache F. *Neutrosophy: Neutrosophic Probability, Set, and Logic: Analytic Synthesis & Synthetic Analysis*. Rehoboth, NM: American Research Press; 1998.

[7] Ye J. A multicriteria decision-making method using aggregation operators for simplified neutrosophic sets. *Journal of Intelligent & Fuzzy Systems*. 2014; 26: 2459-2466. Available from: https://doi.org/10.3233/IFS-130916.

[8] Wang H, Smarandache F, Zhang Y, Sunderraman R. Single valued neutrosophic sets. *Multispace and Multistructure*. 2010; 4: 410-413.

[9] Smarandache F. Neutrosophic set is a generalization of intuitionistic fuzzy set, inconsistent intuitionistic fuzzy set (picture fuzzy set, ternary fuzzy set), pythagorean fuzzy set, spherical fuzzy set, and q-rung orthopair fuzzy set, while neutrosophication is a generalization of regret theory, grey system theory, and three-ways decision. *Journal of Neural Transmission*. 2019; 29: 1-31.

[10] Garg H, Nancy. New logarithmic operational laws and their applications to multiattribute decision making for single-valued neutrosophic numbers. *Cognitive Systems Research*. 2018; 52: 931-946. Available from: https://doi.org/10.1016/j.cogsys.2018.09.001.

[11] Chi P, Liu P. An extended TOPSIS method for the multiple attribute decision making problems based on interval neutrosophic set. *Neutrosophic Sets and Systems*. 2013; 1: 63-70.

[12] Nagarajan D, Gobinath VM, Broumi S. Multicriteria decision making on 3D printers for economic manufacturing using neutrosophic environment. *Neutrosophic Sets and Systems*. 2023; 57: 33-56.
[13] Maji PK. Neutrosophic soft set. *Annals of Fuzzy Mathematics and Informatics*. 2013; 5(1): 157-168.
[14] Said B, Smarandache F. Intuitionistic neutrosophic soft set. *Journal of Information and Computing Science*. 2013; 8(2): 130-140.
[15] Ye J. Cosine similarity measures for intuitionistic fuzzy sets and their applications. *Mathematical and Computer Modelling*. 2011; 53: 91-97. Available from: https://doi.org/10.1016/j.mcm.2010.07.022.
[16] Ye J. Vector similarity measures of simplified neutrosophic sets and their application in multicriteria decision making. *International Journal of Fuzzy Systems*. 2014; 16(2): 204-211.
[17] Ye J. Clustering methods using distance-based similarity measures of single-valued neutrosophic sets. *Journal of Intelligent Systems*. 2014; 23: 379-389. Available from: https://doi.org/10.1515/jisys-2013-0091.
[18] Ye J. Improved cosine similarity measures of simplified neutrosophic sets for medical diagnoses. *Artificial Intelligence in Medicine*. 2015; 63: 171-179. Available from: https://doi.org/10.1016/j.artmed.2014.12.007.
[19] Ali Z, Mahmood T. Complex neutrosophic generalised Dice similarity measures and their application to decision making. *CAAI Transactions on Intelligence Technology*. 2020; 5: 78-87. Available from: https://doi.org/10.1049/trit.2019.0084.
[20] Liu P, Chu Y, Li Y, Chen Y. Some generalized neutrosophic number Hamacher aggregation operators and their application to group decision making. *International Journal of Fuzzy Systems*. 2014; 16: 242-255.
[21] Saqlain M, Riaz M, Saleem MA, Yang MS. Distance and similarity measures for neutrosophic hypersoft set (NHSS) with construction of NHSS-TOPSIS and applications. *IEEE Access*. 2021; 9: 30803-30816. Available from: https://doi.org/10.1109/ACCESS.2021.3059712.
[22] Peng X, Smarandache F. New multiparametric similarity measure for neutrosophic set with big data industry evaluation. *Artificial Intelligence Review*. 2020; 53: 3089-3125. Available from: https://doi.org/10.1007/s10462-019-09756-x.
[23] Sarfraz M, Ullah K, Akram M, Pamucar D, Božanić D. Prioritized aggregation operators for intuitionistic fuzzy information based on aczel alsina t-norm and t-conorm and their applications in group decision-making. *Symmetry*. 2022; 14: 2655. Available from: https://doi.org/10.3390/sym14122655.
[24] Sarfraz M. Aczel-alsina aggregation operators on spherical fuzzy rough set and their application section of solar panel. *Journal of Operational Strategic Analysis*. 2024; 2(1): 21-35. Available from: https://doi.org/10.56578/josa020103.
[25] Jafar MN, Saeed M, Saqlain M, Yang MS. Trigonometric similarity measures for neutrosophic hypersoft sets with application to renewable energy source selection. *IEEE Access*. 2021; 9: 129178-129187. Available from: https://doi.org/10.1109/ACCESS.2021.3112721.
[26] Boran FE, Akay D. A biparametric similarity measure on intuitionistic fuzzy sets with applications to pattern recognition. *Information Sciences*. 2014; 255: 45-57. Available from: https://doi.org/10.1016/j.ins.2013.08.013.
[27] Du WS, Hu BQ. Aggregation distance measure and its induced similarity measure between intuitionistic fuzzy sets. *Pattern Recognition Letters*. 2015; 60-61: 65-71. Available from: https://doi.org/10.1016/j.patrec.2015.03.001.
[28] Donyatalab Y, Farrokhizadeh E, Saeid AB. Similarity measures of q-rung orthopair fuzzy sets based on square root cosine similarity function. In: *Proceedings of the International Conference on Intelligent and Fuzzy Systems*. Cham, Switzerland: Springer; 2020. p.475-483.
[29] Mohd WRW, Abdullah L. Similarity measures of pythagorean fuzzy sets based on combination of cosine similarity measure and Euclidean distance measure. *AIP Conference Proceedings*. 2018; 1974(1): 030017. Available from: https://doi.org/10.1063/1.5041661.
[30] Wei G. Some cosine similarity measures for picture fuzzy sets and their applications to strategic decision making. *Informatica*. 2017; 28(3): 547-564.
[31] Wei G, Gao H. The generalized Dice similarity measures for picture fuzzy sets and their applications. *Informatica*. 2018; 29(1): 107-124.
[32] Van Dinh N, Thao NX. Some measures of picture fuzzy sets and their application in multi-attribute decision making. *International Journal of Mathematics and Soft Computing*. 2018; 4: 23-41. Available from: https://doi.org/10.5815/ijmsc.2018.03.03.
[33] Sarfraz M, Yang MS. A parametric similarity measure for spherical fuzzy sets and its applications in medical equipment selection. *Journal of Engineering Management Systems Engineering*. 2024; 3: 38-52. Available from: https://doi.org/10.56578/jemse030104.

[34] Bui QT, Ali M, Son LH, Smarandache F. Information measures based on similarity under neutrosophic fuzzy environment and multi-criteria decision problems. *Engineering Applications of Artificial Intelligence*. 2023; 122: 106026. Available from: https://doi.org/10.1016/j.engappai.2023.106026.

[35] Thao NX, Smarandache F. Apply new entropy-based similarity measures of single-valued neutrosophic sets to select supplier material. *Journal of Intelligent & Fuzzy Systems*. 2020; 39: 1005-1019. Available from: https://doi.org/10.3233/JIFS-191929.

[36] Ali M, Hussain Z, Yang MS. Hausdorff distance and similarity measures for single-valued neutrosophic sets with application in multi-criteria decision making. *Electronics*. 2022; 12(1): 201. Available from: https://doi.org/10.3390/electronics12010201.

[37] Özlü Ş, Karaaslan F. Hybrid similarity measures of single-valued neutrosophic type-2 fuzzy sets and their application to MCDM based on TOPSIS. *Soft Computing*. 2022; 26: 4059-4080. Available from: https://doi.org/10.1007/s00500-022-06824-3.

[38] Bakro M, Al-Kamha R, Kanafani QA. A neutrosophic approach to digital images. *Neutrosophic Sets and Systems*. 2020; 36: 101-110.

[39] Zhu C, Chen H, Wang F, Cao Y, Karimipour A, Smarandache F. Simulation and comprehensive study of a new trigeneration process combined with a gas turbine cycle involving transcritical and supercritical $CO_2$ power cycles and Goswami cycle. *Journal of Thermal Analysis and Calorimetry*. 2024; 149(12): 6361-6384. Available from: https://doi.org/10.1007/s10973-024-13182-9.

[40] Thong PH, Smarandache F, Huan PH, Tuan TM, Ngan TT, Thai VD, et al. Picture-neutrosophic trusted safe semi-supervised fuzzy clustering for noisy data. *Computer Systems Science and Engineering*. 2023; 46(2): 1981-1997. Available from: https://doi.org/10.32604/csse.2023.035692.

[41] Mandour S, El-Henawy I, Ahmed K. Neutrosophic sets integrated with metaheuristic algorithms: A survey. *Neutrosophic Sets and Systems*. 2021; 45: 28-41.

[42] Dey A, Kumar R, Broumi S, Bhowmik P. Different types of operations on neutrosophic graphs. *International Journal of Neutrosophic Science*. 2022; 19(2): 87-94. Available from: https://doi.org/10.54216/IJNS.190208.

[43] Ma K, Yang J, Liu P. Relaying-assisted communications for demand response in smart grid: Cost modeling, game strategies, and algorithms. *IEEE Journal on Selected Areas in Communications*. 2020; 38(1): 48-60. Available from: https://doi.org/10.1109/JSAC.2019.2951972.

[44] Shirkhani M, Tavoosi J, Danyali S, Sarvenoee AK, Abdali A, Mohammadzadeh A, et al. A review on microgrid decentralized energy/voltage control structures and methods. *Energy Reports*. 2023; 10: 368-380. Available from: https://doi.org/10.1016/j.egyr.2023.06.022.

[45] Zhu C, Zhang Y, Wang M, Deng J, Cai Y, Wei W, et al. Optimization, validation and analyses of a hybrid PV-battery-diesel power system using enhanced electromagnetic field optimization. *Energy Reports*. 2024; 11: 5335-5349. Available from: https://doi.org/10.1016/j.egyr.2024.04.043.

[46] Hussain A, Pamučar D. Multi-attribute group decision-making based on pythagorean fuzzy rough set and novel Schweizer-Sklar t-norm and t-conorm. *Journal of Innovative Research in Mathematical and Computational Sciences*. 2022; 1: 1-17.

[47] Sarfraz M. Application of interval-valued t-spherical fuzzy Dombi Hamy mean operators in antiviral mask selection against COVID-19. *Journal of Decision Analytics and Intelligent Computing*. 2024; 4: 67-98. Available from: https://doi.org/10.31181/jdaic10030042024s.

[48] Sarfraz M. Maclaurin symmetric mean aggregation operators based on Frank t-norm and t-conorm for picture fuzzy multiple-attribute group decision making. *Decision Making Advances*. 2024; 2: 163-185. Available from: https://doi.org/10.31181/dma21202423.

[49] Sarfraz M. A few Maclaurin symmetric mean aggregation operators for spherical fuzzy numbers based on Schweizer-Sklar operations and their use in artificial intelligence. *Journal of Intelligent Systems and Control*. 2024; 3(1): 1-20.

[50] Sarfraz M. Multi-attribute decision-making for t-spherical fuzzy information utilizing Schweizer-Sklar prioritized aggregation operators for recycled water. *Decision Making Advances*. 2024; 2: 105-128. Available from: https://doi.org/10.31181/dma21202425.

[51] Chou S, Nguyen PV, Smarandache F. Renewable energy selection based on a new entropy and dissimilarity measure on an interval-valued neutrosophic set. *Journal of Intelligent & Fuzzy Systems*. 2021; 40(6): 11375-11392. Available from: https://doi.org/10.3233/JIFS-202571.

[52] Mondal K, Pramanik S, Giri BC. Some similarity measures for MADM under a complex neutrosophic set environment. In: *Optimization Theory Based on Neutrosophic and Plithogenic Sets*. Amsterdam, Netherlands: Elsevier; 2020. p.87-116.

[53] Borah G, Dutta P. Multi-attribute cognitive decision making via convex combination of weighted vector similarity measures for single-valued neutrosophic sets. *Cognitive Computation*. 2021; 13(4): 1019-1033. Available from: https://doi.org/10.1007/s12559-021-09883-0.

[54] Hatamleh R, Al-Husban A, Sundareswari, Balaji GK, Palanikumar M. Complex tangent trigonometric approach applied to $(\gamma, \tau)$-rung fuzzy set using weighted averaging and geometric operators and its extension. *Communications on Applied Nonlinear Analysis*. 2025; 32(5): 133-144.

[55] Hatamleh R, Rajalakshmi A, Al-Husban A, Kumaran KLM, Malchijah Raj MS. Complex cubic intuitionistic fuzzy set applied to subbisemirings of bisemirings using homomorphism. *Communications on Applied Nonlinear Analysis*. 2025; 32(3): 418-435. Available from: https://doi.org/10.52783/cana.v32.1997.

[56] Hatamleh R, Hazaymeh A. Finding minimal units in several two-fold fuzzy finite neutrosophic rings. *Neutrosophic Sets and Systems*. 2024; 70: 1-16. Available from: https://doi.org/10.5281/zenodo.13160839.

[57] Hatamleh R, Hazaymeh A. On some topological spaces based on symbolic *n*-plithogenic intervals. *International Journal of Neutrosophic Science*. 2025; 25(1): 23-37. Available from: https://doi.org/10.54216/IJNS.250102.

[58] Ji X, Geng H, Akhtar N, Yang X. Floquet engineering of point-gapped topological superconductors. *Physical Review B*. 2025; 111(19): 195419. Available from: https://doi.org/10.1103/PhysRevB.111.195419.

[59] Chai JS, Selvachandran G, Smarandache F, Gerogiannis VC, Son LH, Bui QT, et al. New similarity measures for single-valued neutrosophic sets with applications in pattern recognition and medical diagnosis problems. *Complex & Intelligent Systems*. 2021; 7: 703-723. Available from: https://doi.org/10.1007/s40747-020-00220-w.

[60] Şahin R, Karabacak M. A novel similarity measure for single-valued neutrosophic sets and their applications in medical diagnosis, taxonomy, and clustering analysis. In: *Optimization Theory Based on Neutrosophic and Plithogenic Sets*. Amsterdam, Netherlands: Elsevier; 2020. p.315-341.

[61] Mandour S. An exhaustive review of neutrosophic logic in addressing image processing issues. *Neutrosophic Systems with Applications*. 2023; 12: 36-55. Available from: https://doi.org/10.61356/j.nswa.2023.110.

[62] Chaira T. Neutrosophic set based clustering approach for segmenting abnormal regions in mammogram images. *Soft Computing*. 2022; 26: 10423-10433. Available from: https://doi.org/10.1007/s00500-022-06882-7.

[63] El-Shorbagy MA, Smarandache F, Alqahtani E, Alshamrani A. A review on metaheuristic algorithms with neutrosophic sets for image enhancement. *International Journal of Neutrosophic Science*. 2023; 20: 165-185. Available from: https://doi.org/10.54216/IJNS.200113.

[64] Song S, Jia Z, Yang J, Kasabov NK. A fast image segmentation algorithm based on saliency map and neutrosophic set theory. *IEEE Photonics Journal*. 2020; 12(5): 1-16. Available from: https://doi.org/10.1109/JPHOT.2020.3026973.

[65] Ye J, Du S. Some distances, similarity and entropy measures for interval-valued neutrosophic sets and their relationship. *International Journal of Machine Learning and Cybernetics*. 2019; 10: 347-355. Available from: https://doi.org/10.1007/s13042-017-0719-z.

[66] Ye J. Similarity measures based on the generalized distance of neutrosophic Z-number sets and their multi-attribute decision making method. *Soft Computing*. 2021; 25(22): 13975-13985. Available from: https://doi.org/10.1007/s00500-021-06199-x.

[67] Mondal K, Pramanik S. Neutrosophic tangent similarity measure and its application to multiple attribute decision making. *Neutrosophic Sets and Systems*. 2015; 9: 80-87.

[68] Eroğlu H, Şahin R. A neutrosophic VIKOR method-based decision-making with an improved distance measure. *Cognitive Computation*. 2020; 12: 1338-1355. Available from: https://doi.org/10.1007/s12559-020-09765-x.

[69] Smarandache F. Neutrosophic set: A generalization of the intuitionistic fuzzy sets. *Journal of Pure and Applied Mathematics*. 2005; 24(3): 287-297.

[70] Bera T, Mahapatra NK. Introduction to neutrosophic soft topological space. *Opsearch*. 2017; 54(4): 841-867. Available from: https://doi.org/10.1007/s12597-017-0308-7.

[71] Ozturk TY, Aras CG, Bayramov S. A new approach to neutrosophic soft sets and to neutrosophic soft topological spaces. *Communications in Mathematics and Applications*. 2019; 10(3): 481-493. Available from: https://doi.org/10.26713/cma.v10i3.1068.

[72] Jolliffe IT, Cadima J. Principal component analysis: A review and recent developments. *Philosophical Transactions of the Royal Society A*. 2016; 374: 20150202. Available from: https://doi.org/10.1098/rsta.2015.0202.

[73] van der Maaten L, Hinton G. Visualizing data using t-SNE. *Journal of Machine Learning Research*. 2008; 9(86): 2579-2605.

[74] Rodgers JL, Nicewander WA. Thirteen ways to look at the correlation coefficient. *The American Statistician*. 1988; 42(1): 59-66. Available from: https://doi.org/10.2307/2685263.

[75] Ketchen DJ, Shook CL. The application of cluster analysis in strategic management research: An analysis and critique. *Strategic Management Journal*. 1996; 17(6): 441-458.